UNICA

UNIVERSITÀ
DEGLI STUDI
DI CAGLIARI

Ph.D. DEGREE IN

Life, Environmental and Drug Sciences

Cycle XXXV

INNOVATIVE FORMULATIONS FOR THE TREATMENT OF *PLASMODIUM* INFECTIONS

Scientific Disciplinary Sector

CHIM/09

Ph.D. Student: ***Federica Fulgheri***

Supervisor: ***Prof. Maria Manconi***

Final exam. Academic Year 2021/2022

Thesis defence: July 2023 Session

Alla mia famiglia

Table of contents

Abstract……4
Introduction……..5
Analysis of complementarities between nanomedicine and phytodrugs for the treatment of malarial infection
Aim of the Thesis……...17
Chapter I……18
Formulation of nutriosomes loading curcumin or quercetin, alone or in association with artemisinin, as a potential adjunctive oral treatment of malaria infections
Chapter II……37
Nanoemulsions loading artemisinin and quercetin as a promising nanosystem for the oral treatment of malaria: in vitro and in vivo evaluation
Chapter III……..51
Improvement of oral therapy of malaria by designing an advanced natural adjuvant based on apigenin loaded in silica doped nutriosomes
References……..72

Abstract

Nanomedicine is one of the most innovative strategies to target drugs at the action site and increase their activity index. Phytomedicine is the most traditional method used to treat human diseases and solve health problems. Their combination represents the future prospective to a better care of human health. Considering the importance of nanomedicine and the natural origin of many current malaria therapies, in this thesis, three innovative lipid-based formulations have been developed loading natural bioactives. For each formulation, physico-chemical characteristics, biocompatibility, and biological activity were evaluated.

Introduction

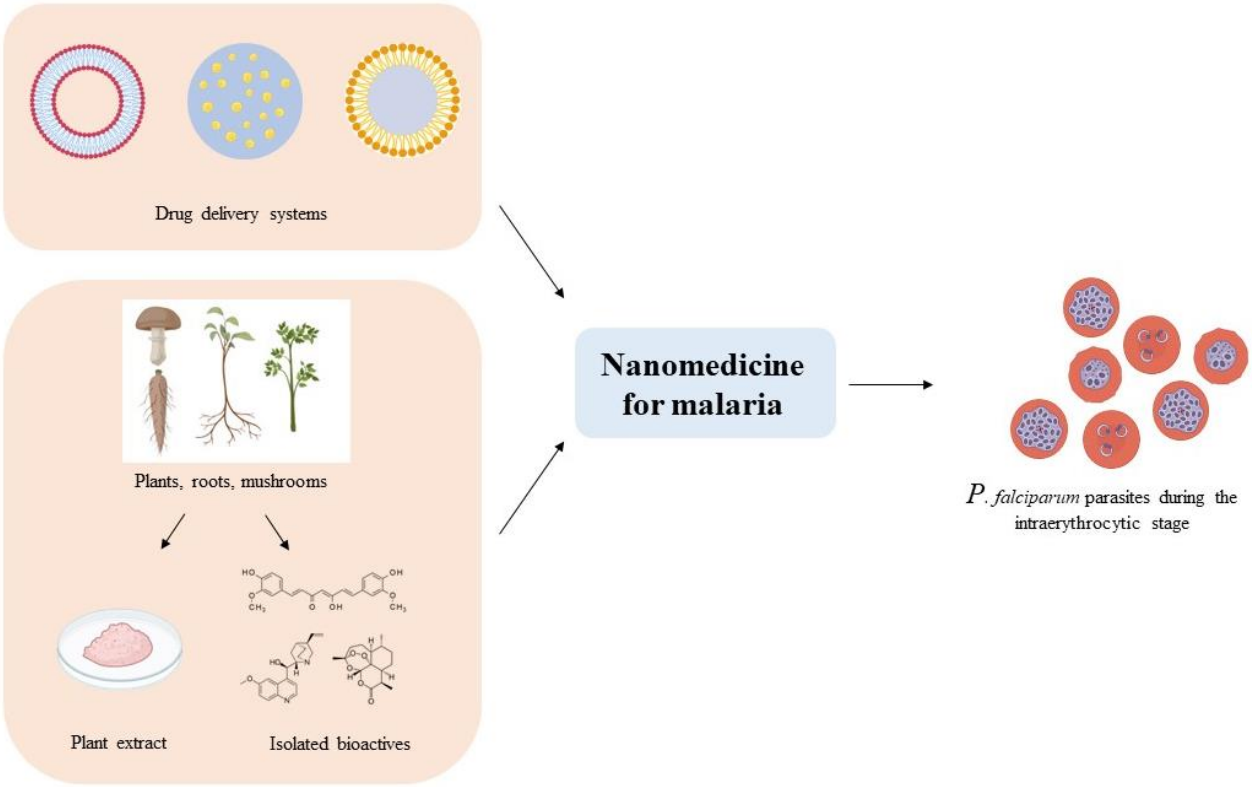

Analysis of complementarities between nanomedicine and phytodrugs for the treatment of malarial infection

Federica Fulgheri[1], Maria Letizia Manca[1*], Xavier Fernàndez-Busquets[2,3,4], and Maria Manconi[1]

[1]Dept. of Life and Environmental Sciences, University of Cagliari, University Campus, S.P. Monserrato-Sestu Km 0.700, Monserrato, 09042, CA, Italy

[2]Barcelona Institute for Global Health (ISGlobal), Hospital Clínic-Universitat de Barcelona, Rosselló 149-153, 08036 Barcelona, Spain

[3]Nanomalaria Group, Institute for Bioengineering of Catalonia (IBEC), The Barcelona Institute of Science and Technology, Baldiri Reixac 10-12, 08028 Barcelona, Spain

[4]Nanoscience and Nanotechnology Institute (IN2UB), University of Barcelona, Martí i Franquès 1, 08028 Barcelona, Spain

1. Introduction

Malaria, a life-threatening infectious disease caused by parasites of the genus *Plasmodium*, is transmitted to the human host by mosquitoes of the genus *Anopheles*. The estimated number of malaria cases in 2021 amounted to 247 million in 84 endemic countries [1]. Over the last two decades, malaria mortality rate (deaths per 100,000 population at risk) was reduced from 30 to 15. However, 2021 accounted for about 619,000 deaths, increasing by 12% compared with 2019 [1]. Despite the progress made in the fight against the global burden represented by this disease, malaria is still one of the most prevalent infectious diseases and the main cause of morbidity in the tropical regions and subtropical areas and there is still a long way to go towards its eradication. 95% of cases in 2021 were reported in Africa, where drug resistance, weather conditions, and poor infrastructure are only some of the factors that affect negatively on malaria control [2]. *Anopheles* mosquitoes can grow and multiply in tropical and subtropical areas, where the climate permits their survival and the growth cycle of parasites. In some countries, malaria is transmitted throughout the entire year and area, but in other regions its transmission is limited by colder periods, high altitudes, or arid conditions [3]. Among them, Africa south of the Sahara has the highest transmission, and other areas where malaria is endemic are South-East Asia and Central America [4,5]. Europe has been malaria free since 2015 because improved healthcare facilities and life conditions can drastically reduce the infection propagation [3]. Indeed, as reported above, climate factors, such as temperature, humidity and rainfall can modulate malaria's transmission intensity by influencing the rate of parasite growth and the number, quality and egg-laying of vectors [6]. Malaria is propagated by Anopheles mosquitoes, which host Plasmodium during its sexual phase [7]. During a blood meal, parasitized female Anopheles inoculate through the skin of the vertebrate host Plasmodium sporozoites present in the

salivary glands. In the human host, Plasmodium transits to the asexual phase [8]. About 20% of sporozoites move to the lymphatic system, while the remaining ca. 80% of them reach the liver [9]. Within hepatocytes, sporozoites grow into merozoites which, after developing to a mature form, are released into the blood circulation to infect red blood cells and start the intraerythrocytic cycle. Inside the red blood cells, parasites replicate asexually, developing from ring stages into early trophozoites, mature trophozoites and schizonts [10]. The latter forms consist of many daughter merozoites that are finally released from the parasitized erythrocyte. Each one of them can infect a new red blood cell to start the blood-stage cycle, which takes approximately 48 hours to complete in *Plasmodium falciparum* (*P. falciparum*). The intraerythrocytic stage of the infection is responsible for the symptoms of the disease, and in *falciparum* malaria is associated with periodic fever episodes every 48 hours [9]. In each cycle, a small percentage of parasites can differentiate to a sexual form, which consists in the development of male and female gametocytes. This stage is crucial for malaria transmission, and if gametocytes are ingested by a female Anopheles mosquito during a blood feed, a zygote can be formed in the mosquito midgut, which develops into an oocyst, from where new sporozoites egress that can be injected into a new host to start a new cycle [11]. Uncomplicated malaria has symptoms such as periodic fevers, chills, headaches and nausea, and the infection can be eradicated with a prompt and complete therapy. However, in the case of Plasmodium vivax and Plasmodium ovale, a dormant liver-resident hypnozoite stage can reactivate and cause further infections, unless a prolonged drug treatment is administered to the patient [11]. An incomplete, delayed, or inappropriate therapy can lead to severe malaria, with a 10-20% case fatality [12]. Hence, the primary objective of antimalarial therapies is to eliminate all parasites, thus avoiding the progression from uncomplicated to severe malaria and the transmission of the infection [12].

Medicinal plants were traditionally used in the treatment of malaria as drugs and adjuvants. The first antimalarial drug historically and extensively used was quinine, exctracted from the *Cinchona* tree bark, and imported in Europe by Spanish missionaries in the 1660s [13]. The quinine derivative chloroquine was synthesized in the 1940s and became the drug of choice for malaria treatment. Its massive use led to widespread parasite resistance emergence, and it has been currently substituted as a first-line treatment by artemisinin, another natural-occurring drug obtained from the weed *Artemisia annua*, traditionally used in Chinese medicine [14]. Nowadays, the recommended treatment for uncomplicated *P. falciparum* malaria is artemisinin-based combination therapy (ACT), which is a combination of a derivative of artemisinin with a second antimalarial compound [16]. The different registered artemisinin-based combination therapies involve the use of artemether-lumefantrine, artesunate-amodiaquine, artesunate-mefloquine, artesunate-sulfadoxine, artesunate-pyrimethamine and dihydroartemisinin-piperaquine. The artemisinin derivatives rapidly act against asexual stages of

all Plasmodium species, which are quickly eliminated from the blood circulation, whereas the second, longer-acting partner drugs, wipe off the remaining parasites [15].

In most malaria-endemic regions, due to the difficulty in accessing to expensive drugs and the lack of healthcare facilities, other traditional remedies from medicinal plants are often used to treat malaria, reducing its severity [16]. Often, their actual effectiveness has not been scientifically evaluated but they may provide an alternative solution permitting self-administration and low-cost therapies. Additionally, several natural molecules used in association with conventional drugs may act as adjuvants improving the general health conditions of the patient and potentiating its immune response [17,18]. Previous studies underlined the importance of folklore knowledge of traditional anti-malarial plants as a crucial source to develop new therapies [19]. An innovative alternative to improve the pharmacokinetics of these natural bioactive molecules and achieve the desired pharmacological response at the target tissue is the use of suitable delivery nanosystems [20]. The loading of natural molecules in ad-hoc formulated systems can offer solutions to malaria challenges such as improving and prolonging therapeutic efficacy and simplifying the treatment or reducing the pathogen's resistance to them. Their size, shape, physico-chemical characteristics, and surface properties positively affect the biological performance of payloads, increasing their therapeutic index and the desired outcomes [21].

The aim of the present review is to examine the available literature on synergies and complementarities obtained combining nanomedicine and natural drugs for the treatment of malaria. Attention has been devoted to the beneficial complementary effects provided by nano-delivered phytochemicals, which do not always ensure a complete efficacy but, as adjuvants, usually improve the efficacy of drugs. The review focuses on the importance of nanomedicine to strengthen the efficacy of phytochemicals and their potential clinical transferability.

2. Evolution of clinical therapy using natural molecules and their derivatives

Cinchona bark was extensively used in the 18th century as remedy for the treatment of malaria. From it, quinine with other alkaloids were separated in the early part of the 19th century [22]. Subsequently, quinine was accidently synthetized for the first time by William H. Perkin's in 1856 and for a long time had been the only available antimalarial drug [23,24]. Its use was a strategic asset during the wars occurred in the 20th century due to the massive malaria infections, which stimulated the search for synthetic replacements such as plasmochin, primaquine, mepacrine, quinacrine, resochin and finally chloroquine in 1946. Quinine and its derivatives were the drugs of choice for the treatment and prevention of malaria until the late 1980s [25]. In the 1970s, the resistance of *P. falciparum* to chloroquine increased especially in Southeast Asia, where malaria infection became critical. Once

again, a war, in this case in Vietnam, accounted for a large number of malaria victims and triggered the Asian efforts to discover new antimalarial drugs, which led to the discovery of artemisinin by Youyou Tu [26]. Artemisinin, artemether and artesunate, as well as other artemisinin derivatives, have brought the global anti-malarial treatment to a new era, saving millions of lives [27]. These fast-acting antimalarials were later combined with mefloquine, lumefantrine and piperaquine, which are slowly removed from the body, ensuring a better elimination of malaria infection. Artemisinin-based combination therapies are extensively used to avoid the spread of parasite strains that were resistant to previous antimalarial drugs and caused increased morbidity and mortality in many malaria-endemic countries [28]. Artemisinin resistance, defined as delayed parasite clearance after a 3-day course of artemisinin-based combination therapy, has been already observed in different endemic areas such as Eastern India, South America and Papua New Guinea and is associated with the presence of *pfKelch13* mutations [29,30]. Identifying new partner drugs or adjuvants to be associated with artemisinin derivatives is mandatory along with reducing their high costs, ensuring their local efficacy, and facilitating their affordable use [31].

A modern strategy to improve antimalarial treatments is the preventive or synergic supplementation of special foods, like plants or mushrooms that are traditionally used in the ethnomedicine; their diffusion as nutraceuticals in poor countries could help to reduce the transmission and severity of malaria infections [32]. Firstly, they can positively affect the gut microbiota directly linked to human health, reducing the severity of many diseases [33]. Additionally, plants and mushrooms are usually rich in antioxidants, and often contain antiplasmodial molecules like sesquiterpenes, for which a good activity against *P. falciparum* has been observed, with IC50s between ~2.3 μg/mL and ~3.10 μg/mL [34][35]. Literature points out that a large number of plants also have antimalarial activity, especially *in vitro*. Muregi et al. obtained extracts from 11 plant species traditionally used in Kenya for the treatment of malaria and 93% of them had *in vitro* antiplasmodial activity, justifying their ethnopharmacological use [36]. *Glycyrrhiza glabra* L. is traditionally used in Iran for the treatment of malaria and its efficacy was confirmed by an *in vivo* study performed using different fractions of its root extract [37]. Bankole et al. evaluated the *in vivo* antimalarial activity of the aqueous extracts obtained from three plants used in traditional medicine of Nigeria [38]. The result of the study disclosed the potent antimalarial activity of the leaf extract of *Markhamia tomentosa*, supporting its traditional use in malaria treatment and underlining the importance of this knowledge on improving future medicine. Kumar et al. prepared a methanolic extract from *Dissotis rotundifolia* and docked the phytochemicals against the *P. falciparum* dihydrofolate reductase. Twentynine phytochemicals were identified as potential antifolates, of which dimethylmatairesinol, flavodic acid, sakuranetin, and sesartemin were those with higher affinity [39]. Following a literature review, Sharma et al. found

that 86 plants of the Annonaceae family are reported to have antimalarial activity. They are of the genera Xylopia (11 species), Uvaria (10 species), Polyalthia (9 species), and Annona (6 species). Leaves, stem bark, and root bark are the most commonly used plant parts in antimalarial screening [40].

Besides plant extracts, the antimalarial efficacy of separate phytochemicals has been also evaluated. Two well-known triterpenoids ursolic acid and lupeol were isolated from the unsaponified fraction of petroleum ether extract of *Ficus benjamina* leaves. They were able to significantly inhibit the activity of the 3D7 strain of *P. falciparum* as the IC50 was 18 μg/ml and 3.8 μg/ml [41]. Roseoflavin, analogue of riboflavin, had *in vitro* antimalarial activity in the low nanomolar range against *P. falciparum* in the presence of extracellular riboflavin at different concentrations within the human plasma levels, while it increased the survival and reduced the parasitemia of mice infected with *Plasmodium vinckei vinckei,* when intraperitoneally administered (20 mg/kg/day) [42]. Annang et al. discovered a novel family of four macrolides isolated from an extract of the fungus *Strasseria geniculata* CF-247251, with potent antiplasmodial activity at low micromolar concentrations against *P. falciparum* 3D7 and Dd2 lines [43]. Ezenyi et al. reported the *in vitro* and *in vivo* antiplasmodial activity of *Chromolaena odorata* leaf extract, which was fractionated in different gradient fractions to identify the most effective components [44]. Quercetin-4'-methyl ether was the most active component, which, administered at 2.5–5 mg/kg in mice, significantly suppressed malaria, with effects similar to those of chloroquine and artemisinin. The effectiveness of quercetin and other similar flavonoids traditionally used in ethnomedicine against *P. falciparum* was confirmed by *in vitro* studies [45].

Considering these promising findings, certain phytocomplexes or phytochemicals, if preventively used or associated to a therapeutic regimen with artemisinin, are expected to provide favourable outcomes in malaria treatment but more studies are needed to confirm their effectiveness.

3. Delivery of quinine and its derivatives in nanosystems

An advanced strategy to improve antimalarial therapy is the use of nanosystems, which has the potential to increase the therapeutic effectiveness of existing drugs and reduce the pathogen resistance by the improvement of their stability, adsorption, and distribution, and control of their metabolism, excretion, and reduced toxicity profiles [46]. Nanocarriers are ideal tools to implement the strategies for the prevention and cure of malaria, overcoming some problems associated to conventional therapies [47,48]. In a previous study, two antimalarial drugs derived from quinine, chloroquine and primaquine have been encapsulated in four different dendritic derivatives, which clearly improved the *in vitro* IC50 of the drugs and the *in vivo* bioavailability [49]. Additionally, the used systems could

be manufactured with reduced costs, thus permitting their commercialization in the low per-capita income regions where malaria is endemic. It has also been reported that the delivery of quinine in polymeric nanocapsules coated with polysorbate and sized around 200 nm decreased the deleterious *in vitro* effects induced by this drug on ovaries and partially on testicles [50]. Quinine was later co-encapsulated with curcumin in polysorbate-coated nanocapsules, and in this form was able to decrease *P. falciparum* parasitemia more efficiently than an equimolar mixture of quinine and curcumin [51]. The prepared nanocapsules also protected the payloads from degradation caused by UV light. Bajerski et al. tested the stability of quinine and curcumin co-loaded in nanoemulsion in comparison with the solutions of the two antimalarial compounds isolated or associated, and the results obtained demonstrated that they were successfully protected from degradation by the nanosystem [52].

Amolege et al. loaded quinine in mesoporous silica nanoparticles due to their promising properties, such as large surface area, tuneable pore size or volume, high thermal property, nontoxicity, and biocompatibility [53]. Drug was delivered in particles functionalized with 3-phenylpropyl silane and unfunctionalized ones, the latter were the most effective carriers as offered a higher inhibition of parasite growth and increased animal survival compared to those obtained using the drug in free form or loaded in functionalized nanoparticles. Scheuer et al. loaded quinine in nanocapsules with a curcuma oil core and a polycaprolactone or Eudragit® RS100 membrane, coated with polysorbate 80 [54]. Drug-containing nanocapsules significantly improved the survival of animals, confirming the optimal performances of the delivery system and the synergic effect provided by the association of quinine with curcumin. Michels et al. studied the effects of the surface characteristics of nanocapsules loading quinine and coated with polysorbate 80 or Eudragit® RS100 by interfacial deposition. Free quinine or quinine loaded in the two kinds of nanocapsules was administered intravenously to *Plasmodium berghei*-infected rats and both nanocapsules were able to increase the intra-erythrocytic concentration and the plasma half-life time of quinine, while only quinine loaded in nanocapsules coated with Eudragit® RS100 increased the survival of animals compared to non-treated animals up to values similar to those provided by chloroquine, used as positive control [55]. In another study, chloroquine and fosmidomycin co-loaded in immunoliposomes targeted to *P. falciparum*-infected red blood cells improved by tenfold the antiplasmodial efficacy of the free compounds [56]. Magnetic composite nanoparticles of ferric oxide and ferrous oxides coated with heparin were used for the delivery of quinine, improving the *in vitro* and *in vivo* antimalarial activity of the drug without significant associated hemolysis or cytotoxicity but ensuring the suppression of parasitemia in *P. berghei*-infected mice [57]. Alternatively, quinine was loaded into nanocapsules prepared with poly(ε-caprolactone) and polysorbate 80, which were intravenously administered to Wistar rats

infected with *P. berghei* [58]. Dose-depending parasitemia suppression was observed (29%, 86% and 100% after the administration of 30, 60 and 75 mg quinine/kg/day, respectively). When free quinine was administered, 105 mg of free quinine/kg/day was required to reach a complete parasitemia elimination.

Studies, performed to *in vitro* and *in vivo* deliver quinine and its derivatives using ad hoc formulated nanosystems, underline their key role played in improving the drug efficacy, reducing side effects, and minimizing drug resistance. Unfortunately, most of the studies were carried out using animals and, as far as we're aware, no clinical trials with these nanosystems were done, to confirm their better performances.

4. Delivery of artemisinin and its derivatives in nanosystems

Despite the effectiveness of artemisinin and its derivatives in the treatment of malaria, their bioavailability, efficacy, toxicity and patient compliance can be improved [59]. Their loading in affordable delivery systems represents a strategy to simplify the protocols and potentiate the therapeutic effect. According to this challenge, several studies have been performed loading artemisinin and its derivatives in different nanosystems and testing their efficacy *in vitro* and *in vivo*. Isacchi et al. designed liposomes and polyethylene glycol (PEG)-coated (PEGylated) liposomes loaded with artemisinin, which were evaluated *in vivo* for their pharmacokinetic properties on male CD1 mice in comparison with free artemisinin at the same concentration (10 mg/kg) after a single intraperitoneal administration. While free artemisinin was quickly eliminated from plasma, the incorporation of artemisinin in liposomes enhanced its half-life, especially in the presence of the PEG, which increased it by 5 times [60]. Wang et al. designed hollow mesoporous ferrite nanoparticles, an innovative delivery system that contained artemisinin in the inner magnetite shell and heparin on the outer mesoporous shell. Their magnetic properties were exploited for their targeting to parasite-infected red blood cells, thanks to the attraction between the magnetic nanoparticles and paramagnetic hemozoin, which accumulates in the parasite during the erythrocytic stage [61].

Artesunate is the artemisinin derivative approved for intravenous clinical treatment of malaria. *In vivo* it is rapidly metabolized to dihydroartemisinin, which has a short half-life (~30–45 min) and fast action. Dimeric artesunate-loaded liposomes, developed by Ismail et al., offered good *in vitro* antimalarial activities with an IC50 (0.39 nM) lower than the that of free artemisinin (IC50 5.17 nM) and similar to that of artemisinin-loaded liposomes (IC50 3.13 nM) [62]. *In vivo* antimalarial studies demonstrated an anti-recrudescence effect (around 40%) provided by these novel liposomal formulations when injected at 60 mg/kg to mice infected by *P. berghei*. Their antimalarial effect at low dosage (15 mg/kg) was 2.3-fold higher than that of free artemisinin. Dimeric artesunate was

obtained by esterification of two artesunate molecules with 3-(dimethylamino)-1,2-propanediol followed by quaternization, following its loading in choline conjugate micelles coated with hyaluronic acid [63]. The obtained nanosystem did not lead to hemolysis or cytotoxicity and possessed superior antimalarial efficacy compared to that of the free drug. Artemether-loaded solid lipid nanoparticles, intraperitonially administered to mice infected with *P. berghei* (5 mg/kg body weight), provided a significant enhancement of the bioavailability of this poorly water-soluble drug, and positively affected the animal survival, which was significantly increased in comparison with that of mice treated with free artemether or with a marketed formulation containing artemether [64]. In another study, arteether was formulated in nanoemulsions prepared by a high-pressure homogenization technique with an incorporation efficiency ranging between 82 and 93% and size ranging between 125 and 268 nm. Free arteether was intramuscularly administered while arteether nanoemulsions and arteether dispersed in nut oil were orally administered to mice infected with *Plasmodium yoelii*. Free arteether intramuscularly administered at 12.5 mg/kg x 5 days had a curative rate of 100%, arteether nanoemulsion orally administered had 80% of curative rate and arteether oil dispersion orally administered only 30% [65]. New promising nanosystems to deliver the artemether are zein nanoparticles, tailored to prolong the half-life of this drug after intravenous administration [66]. These nanoparticles prolonged (80%) the residence time of drug in the circulation in comparison to that of the free drug (~83 min versus ~46 min, $p < 0.01$), confirming their ability to prolong the therapeutic effect and reduce the dosing frequency in a clinical treatment. Alternatively, dihydroartemisinin was loaded into surface modified lipid nanoemulsions made of soybean oil and PEG 4000, leading to droplet sizes ranging between 26 and 56 nm. When administered to *P. berghei*-infected mice, dihydroartemisinin-loaded nanoemulsions displayed a higher inhibition of parasite growth in comparison to the empty nanoemulsion, or the commercially available dihydroartemisinin formulation P-Alaxin® [67].

In the available literature, some clinical studies on the efficacy of artemisinin or its derivatives, alone or in combination with a partner drug, are reported; however, to the best of our knowledge, no clinical studies are available on the evaluation of the antimalarial performances of artemisinin, or its derivatives delivered in nanosystems. On the contrary, the promising results obtained *in vivo* in animals, delivering these molecules in ad hoc formulated nanosystems, underlined the important achievements, which could be addressed and the need to improve the studies to reach the possibility to perform clinical trials as promising strategy to ameliorate the malaria therapy and patient compliance, especially when orally administered.

5. Delivery of alternative natural molecules in nanosystems

Being malaria infections a serious problem in tropical and subtropical regions of the world, traditional medicinal herbs are widely used to treat the disease [68]. Some of them, when tested *in vivo*, suppressed parasitemia, thus being a potential source of new antimalarial compounds. However, many natural bioactives have poor oral bioavailability because of their low water solubility, chemical instability and/or poor permeability and they can be hard to formulate by traditional methods [69]. Loading them in nanosystems could overcome these issues and their association with other antimalarials could help improving the current therapy [70].

The antimalarial activity of quercetin-loaded phytosomes was tested *in vitro* in *P. falciparum*, showing anti-parasitic activity at a drug concentration of 400 µg/mL [71]. Curcumin was loaded in phospholipid vesicles containing Eudragit® S100 and hyaluronan (hyalurosomes) or the water-soluble dextrin Nutriose® FM06 (nutriosomes). To facilitate their storage, the vesicles were freeze-dried and rehydrated before their use. Upon oral administration, only Eudragit-nutriosomes improved the *in vivo* antimalarial activity of curcumin in a dose-dependent manner, enhancing the survival of *P. yoelii*-infected mice up to 11 days [72,73]. Curcumin, due to its weak bioavailability, rapid metabolism, and limited chemical stability, has a restricted application in clinical usages. To overcome these limits, it was loaded into nanostructured lipid carriers, which permitted to control drug release, it improved its *in vivo* antiplasmodial activity against *P. berghei*. The nanoformulation significantly increased the survival of malaria-infected mice when compared to the controls treated with free curcumin [74]. Instead of pure curcumin, a mixture of curcuminoids was loaded in lipid nanoparticles tailored for parenteral administration using trimyristin, tristerin and glyceryl monostearate as solid lipids and medium chain triglyceride as liquid lipid [75]. Prepared particles were spheric, sized between 120 and 250 nm, and negatively charged as the zeta potential ranged from −28 mV to −45 mV as a function of the nature of the used lipid matrix, which also affected the entrapment efficiency of drug. Nanoparticles were sterilized by filtration and intraperitoneally administered to albino mice being two-fold more effective in antimalarial treatment than free curcuminoids at the same dosage. Poly(butyl methacrylate-co-morpholinoethyl sulfobetaine methacrylate)-based nanoparticles loaded with curcumin had *in vitro* and *in vivo* antimalarial efficacy similar to that of the free drug. However, they presented specific targeting to parasitized red blood cells in comparison with parasite-free red blood cells (74.8%/0.8% respectively), which was maintained upon loading of curcumin (82.6%/0.3%) [76]. Alternatively, curcumin was loaded in hydrogel nanoparticles prepared with hydroxyl propyl methyl cellulose combined with polyvinyl pyrrolidone to enhance absorption and prolong its rapid elimination thanks to the evasion of the reticulo-endothelial system [77]. Nanoparticles sized around 100 nm, were highly monodispersed

and after freeze-drying and rehydration with distilled water loaded around 99% of drug in amorphous state. Curcumin-loaded nanoparticles were safe by oral administration and had a superior antimalaria effect over free curcumin. Further genotoxicity studies confirmed their possible use for a prolonged duration, and the overall results suggested their possible use as an adjunct in malarial therapy along with standard therapy. Liposomal formulations of monensin, with or without free artemisinin, were more effective than free monensin on reducing the growth of *P. falciparum* 3D7 in culture and increasing animal survival when tested *in vivo* on *P. berghei* NK65 and *P. berghei* ANKA infected mice [78].

Terpenes were also delivered in nanosystems to improve their antimalaria efficacy and, among these, lupeol was loaded in special nanoemulsion [79]. It is a monohydroxylated pentacyclic triterpenoid, which has antimalarial potential, but its therapeutic potential is still under-exploited due to their low intestinal absorption. Nanoemulsion was prepared with caprylic acid, oleic acid as oil phase and tween 20 and transcutol as surfactant and co-surfactant. The formulation allowed an improved efficacy with a half dose of phytochemical, which seem to be related to a significant increase in blood glucose and haemoglobin level.

The search for new antimalarials must never stop but the need for low-cost therapeutic agents represents a huge challenge. New natural products as antimalarial drugs, together with the great potential of drug delivery systems, could play an important role in the fight against malaria.

6. Future challenges for malaria eradication

Despite the recent achievements, eradication of malaria is far from being envisaged and the disease continues causing hundreds of thousands of deaths annually and generates significant economic costs for endemic regions. In these areas, it is necessary to implement the access to affordable, quality, people-centred healthcare and services, which are strongly correlated with malaria control [80]. At the same time, safe, effective, and low-cost drugs are needed along with affordable and self-administrable therapies, permitting a prompt and complete treatment. Plant metabolites represent an opportunity as source of innumerable medicinal compounds with a diversity of chemical structures and therapeutic effects. Some have already been reported as promising alternatives in inhibiting or reducing malaria infection and progression and might potentially be developed into new future treatments [81]. When designing their formulations, it is important to consider that the parasite is hosted in the parasitophorous vacuole of red blood cells and, therefore, the drugs must cross multiple lipid bilayers to access their intraparasitic targets [82]. Additionally, an increased residence time in the blood circulation may facilitate interactions with parasitized red blood cells [82]. Then, the delivery of future antimalarial drugs in appropriate nanosystems represents a valuable approach to reach important therapeutic benefits and ameliorate the effectiveness of phytochemicals by protecting them from degradation, improving efficacy on the target parasite, ameliorating biopharmaceutic and pharmacological properties, facilitating oral administration, reducing dose frequency and concentration, and overcoming potential side effects [83]. In

addition to the administration of conventional drugs, nanosystems are useful for the delivery of phytochemicals, which are usually poorly soluble in water, easily degradable and have low bioavailability, thus these advanced systems could improve their biopharmaceutic and pharmacokinetic profile and reduce the toxicity. Additionally, as a function of the structure, composition, and surface properties, they can address cell-adhesion and retained release. These advantages are crucial for malaria therapy, which need to massive target infected red blood cells and parasite membranes while remaining to permanence in the blood stream for a long period of time [82]. Other important aspects, which may be improved by the delivery in nanosystems to facilitate the malaria therapy, is the route of administration and patient compliance as their application could permit to use the oral route as the first choice for clinical treatment of malaria limiting the parenteral and intravenous administration to the most severe cases.

The main drawbacks limiting the clinical uses of delivery nanosystems is their high cost and complex administration that hamper the development of commercial nanotechnology-based malaria medicines economically affordable in endemic areas [48]. To overcome this problem, easy and affordable nanosystems must be designed and tested for the delivery of natural phytochemicals. After detailed *in vivo* antimalarial evaluation and thorough toxicological studies, these formulations may be recommended as antimalarials especially in rural communities where the conventional drugs are unaffordable or unavailable and the health facilities are inaccessible.

Aim of the thesis

To prepare new formulations tailored for the oral administration loading natural antimalarial compounds, such as curcumin, quercetin and apigenin, which may act as adjuvants and enhancers of the well-known antimalarial effect of artemisinin.

Chapter I

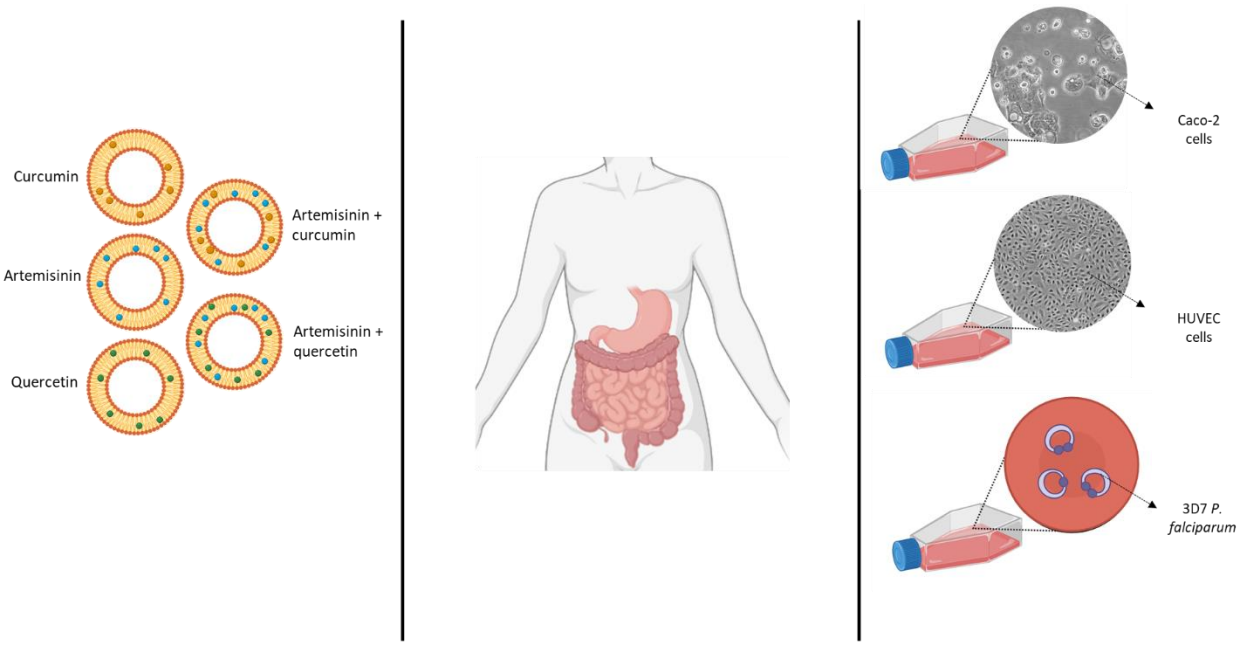

Nutriosomes design

Stability in gastro and intestinal simulated fluids

In vitro test

Formulation of nutriosomes loading curcumin or quercetin, alone or in association with artemisinin, as a potential adjunctive oral treatment of malaria infections

Federica Fulgheri[1], Matteo Aroffu[1], Miriam Ramírez[2,3,4], Lucía Román-Álamo[2,3,4], José Esteban Peris[5], Iris Usach[5], Amparo Nacher[5,6], Maria Manconi[1*], Xavier Fernàndez-Busquets[2,3,4] and Maria Letizia Manca[1]

[1]Dept. of Scienze della Vita e dell'Ambiente, University of Cagliari, via Ospedale 72, 09124 Cagliari, Italy

[2]Nanomalaria Group, Institute for Bioengineering of Catalonia (IBEC), The Barcelona Institute of Science and Technology, Baldiri Reixac 10-12, ES-08028 Barcelona, Spain

[3]Barcelona Institute for Global Health (ISGlobal, Hospital Clínic-Universitat de Barcelona), Rosselló 149-153, ES-08036 Barcelona, Spain

[4]Nanoscience and Nanotechnology Institute (IN2UB), University of Barcelona, Martí i Franquès 1, 08028 Barcelona, Spain

[5]Department of Pharmacy and Pharmaceutical Technology and Parasitology, University of Valencia, 46100 Valencia, Spain

[6]Instituto Interuniversitario de Investigación de Reconocimiento Molecular y Desarrollo Tecnológico (IDM), Universitat Politècnica de València, Universitat de València, Av. Vicent Andrés Estellés s/n, 46100, Burjassot, Valencia, Spain

1. Introduction

Malaria is an old parasitic disease that, despite being preventable and curable, remains a worrisome disease [84]. It caused around 247 million cases worldwide in 2021, most of them in Africa [1]. It mostly occurs in tropical and subtropical areas, and the causes of illness and death are directly related to poverty and economic inequality in low-income regions with poor access to medication, treatment, and healthcare [85]. Malaria is a life-threatening disease caused by *Plasmodium* parasites; although the most severe malaria is caused by *Plasmodium falciparum*, *Plasmodium vivax*, *Plasmodium ovale*, *Plasmodium malariae* and *Plasmodium knowlesi* that can also cause moderate or severe symptomatology, although with a lower mortality rate [86].

Chloroquine was used as first line antimalarial for many years and continued to be an effective drug nearly 80 years later [87], but the problem of resistance, along with the multiple side effects, has led researchers to look for alternative molecules. Artemisinin, a natural sesquiterpene lactone isolated from *Artemisia annua L.* (Asteraceae family), was found to exsert strong antimalarial effect without parasite resistance. Indeed, artemisinin and its derivatives are currently used as first-choice treatment in endemic countries [88]. It is effective against the blood phase of parasites, preventing their development to more pathological mature stages, thus providing rapid clinical response in severe malaria [89]. Current treatments combine artemisinin or its more potent derivative,

dihydroartemisinin, with a second antimalarial drug that has a different mechanism of action and longer half-life [90,91]. The combined treatments have continuously gained importance for their high efficacy level against malaria parasites, however, reports on the failure of this combination strategy underline the need to improve the performances of current treatments, especially by increasing their poor bioavailability and short half-life and reducing drug resistance [88].

According to this purpose, in a previous study, curcumin was co-loaded in liposomes with artemisinin to ameliorate the efficacy of antimalaria treatment [92]. Curcumin is a polyphenol traditionally used in the Chinese medicine and obtained from the rhizomes of turmeric. In the last few decades, it gained interest due to its promising beneficial activities especially when delivered in nanocarriers [93]. In addition to its antioxidant and anti-inflammatory effects, it can exert anti-microbial activity as well, and inhibits the growth of a variety of pathogens, including *P. falciparum*, *Leishmania* and *Trypanosoma* [94–96]. Quercetin is another polyphenol belonging to the class of flavonoids, having antioxidant, antiaging, anti-inflammatory, and antibacterial activities [97], whose ability to inhibit the growth of *Plasmodium* has been previously confirmed [98]. The combination of artemisinin with curcumin or quercetin appears promising especially if they are opportunely formulated in nanosystems, which can improve stability, bioavailability and biodistribution of the payloads facilitating the target to the parasite [48]. Among the different nanosystems, liposomes have been tested as carriers of different antimalaria drugs especially for parental administration [92,99]. Recently, special phospholipid vesicles, called nutriosomes and enriched with a dextrin (Nutriose® FM06), have been tailored for oral administration, as they are more resistant than liposomes under the harsh conditions of the gastro-intestinal tract [100,101]. In a previous work, they were used to deliver curcumin and they were orally administered at 25 or 75 $mg \cdot kg^{-1} \cdot day^{-1}$ to mice infected with the lethal murine malaria parasite *Plasmodium yoelii* 17XL [102]. The polyphenol was used in dispersion or loaded in eudragit-hyaluronan liposomes or eudragit-nutriosomes and only when it was loaded in eudragit-nutriosomes, its viability in mouse was significantly increased. Similarly, in a further work, curcumin-loaded eudragit-nutriosomes were able to extend the life expectancy of *P. yoelii*-infected mice relative to that of animals treated with free curcumin and to the untreated controls [103]. The addition of Nutriose® FM06 to phospholipid vesicles permits the formation of gastrointestinal-resistant carriers more efficient than the corresponding liposomes in protecting the loaded molecules and improving their bioavailability and biodistribution [104]. Indeed, orally administered nutriosomes loaded with Nasco grape-pomace delivered the load phytochemicals to the central nervous system and protected against neurotoxicity of the dopaminergic system [100]. The dextrin used in nutriosomes acted also as a cryo-protector, preventing their breakage during a freeze-drying process [101].

Despite the different studies performed using nutriosomes as oral carriers, they have never been tested for the delivery of first-choice antimalarial drugs alone or in combination with other phytochemicals. According to this, the aim of this study was to design a new oral formulation for malaria treatment loading artemisinin (as first-choice antimalarial drug), curcumin, or quercetin, alone or in association, in nutriosomes. Curcumin or quercetin were added since their previously confirmed effect against malaria and are expected to enhance the well-known efficacy of artemisinin. The physico-chemical and technological properties of the prepared vesicles were investigated along with their *in vitro* biocompatibility using two different cell lines (human colon adenocarcinoma epithelial cells and human umbilical vein endothelial cells). Moreover, the antiparasitic activity has been evaluated *in vitro* against 3D7 *P. falciparum*.

2. Material and methods

2.1 Materials

Soy phosphatidylcholine (Lipoid S75, S75) was purchased from Lipoid GmbH (Ludwigshafen, Germany). Artemisinin was purchased from Carbosynth Ltd (London, United Kingdom). Nutriose® FM06, a soluble dextrin obtained from maize, was gently provided by Roquette (Lestrem, France). Curcumin, quercetin and other reagents and solvents of analytical grade were purchased from Sigma-Aldrich (Milan, Italy). Glycerol was purchased from Carlo Erba (Milan, Italy). Water was purified through a Milli-Q system from Millipore (Milford, MA). All plastics and reagents for cells have been purchased from Sigma-Aldrich (Milan, Italy).

2.2 Quantification of artemisinin, curcumin, and quercetin

The phytochemicals were quantified using a high-performance liquid chromatograph (HPLC) Agilent equipped with a G1379A degasser, a G1310A pump, a G1329A 94 automatic injector and a G1314A variable wavelength spectrophotometric detector. The column was a Waters “Nova-Pack” C18 (4 µm, 3.9 mm × 150 mm) and the composition of the mobile phase was slightly different depending on the molecule to be analysed: acetonitrile, water, 60:40, v/v for artemisinin, acetonitrile, water, acetic acid, 49:50:1, v/v/v for curcumin, acetonitrile, water, acetic acid, 29:70:1, v/v/v for quercetin. Detection of artemisinin was performed at 216 nm, that of curcumin at 425 nm and that of quercetin at 380 nm. The injection volume was 25 µl, and the flow rate was 1 ml/min. Stock solutions (5 mg/mL) of each phytochemical were prepared using the mobile phase as solvent. From these, other working solutions at different concentrations (artemisinin from 5 to 500 µg/mL; curcumin from 0.05 to 20 µg/mL; quercetin from 0.1 to 100 µg/mL) were prepared by dilution. The calibration curve of

each molecule was obtained plotting peak areas versus concentrations. The regression analysis gave a correlation coefficient value (R2) of 1 for artemisinin, 0.9998 for curcumin and 1 for quercetin (Figure 2 SM).

Vesicles loading artemisinin, curcumin or quercetin or combinations of artemisinin and curcumin or artemisinin and quercetin were analysed after disrupting them with methanol (dilution 1/100). Alternatively, in the *in vitro* release assay, quantification was done measuring absorbance of artemisinin at 216 nm, that of curcumin at 425 nm and that of quercetin at 380 nm, as described in paragraph 2.6.

2.3 Vesicle preparation

Artemisinin (10 mg/ml) or curcumin (10 mg/ml each) or quercetin (10 mg/ml) or association of artemisinin and curcumin (10 mg/ml each) or association of artemisinin and quercetin (10 mg/ml each), were weighted in a glass vial together with Nutriose® FM06 (200 mg/ml) and S75 (260 mg/ml) and hydrated with an aqueous blend of phosphate buffered solution (PBS, pH 7.4) and glycerol (80:20) at 25 °C. The obtained dispersions were sonicated (10 cycles, 5 s on and 2 s off, 14 μ of probe amplitude) with a high intensity ultrasonic disintegrator (Soniprep 150, MSE Crowley, London, UK). Empty vesicles (without artemisinin, curcumin or quercetin) were prepared as well, to evaluate the effect of these phytodrugs on vesicle assembling and characteristics. The dispersions were frozen at –80 °C and freeze-dried for 48 hours, at -80 °C and 0.08 mbar, using a FDU-8606 freeze-dryer (Operon, Gimpo, South Korea). Freeze-dried samples were then rehydrated with bi-distilled water at room temperature (25 °C) up to the initial volume (2 ml) by manually shaking them for 2 minutes.

The non-entrapped phytodrugs were separated from the vesicle dispersions by dialysis using water (4 l) as release medium. Each dispersion (1 ml) was transferred to a Spectra/Por® dialysis tube (12-14 kDa MW cut-off, 3 nm pore size; Spectrum Laboratories Inc., DG Breda, The Netherlands) and purified for 2 hours at 25 °C under constant stirring, refreshing the medium after 1 hour, aiming at ensuring the complete removal of the unentrapped molecules. The entrapment efficiency of payloads in vesicles was calculated as the percentage of their concentration found after dialysis versus that initially measured. The amount of artemisinin, curcumin and quercetin in each sample was determined as reported in paragraph 2.2.

2.4 Characterization of vesicles

Formation and morphology of vesicles were evaluated by cryogenic transmission electron microscopy (cryo-TEM). Sample (5 μl) was applied on a grid Lacey carbon film (Electron Microscopy Science, Hatfield, PA, USA). The grid was mounted on an automatic plunge freezing apparatus (Vitrobot FEI, Eindhoven, The Netherlands) to control humidity and temperature,

immersed in liquid ethane, fast cooled from outside by liquid nitrogen, avoiding the formation of ice crystals. Observation was made at ~–170 °C in a Tecnai F20 microscope (FEI, Eindhoven, The Netherlands) operating at 200 kV, equipped with a cryo-specimen holder Gatan 626 (Warrendale, PA, US). Digital images were recorded with an Eagle FEI camera, 4098×4098 pixels. Magnification between 20,000-30,000× and a de-focus range of 2-3 μm was used [105,106].

Mean diameter and polydispersity index (a measure of the size distribution width) were evaluated by dynamic light-scattering measurements with a Zetasizer Ultra from Malvern Instruments (Worcestershire, UK). Samples were backscattered by a helium-neon laser (633 nm) at an angle of 173° and a constant temperature of 25 °C. Zeta potential was determined using the Zetasizer Ultra by using the M3-PALS (Mixed Mode Measurement-Phase Analysis Light Scattering) technique, which measures the particle electrophoretic mobility. Before the analysis, each sample was diluted 100-folds with PBS to be optically clear and avoid the attenuation of the laser beam by the particles along with the reduction of the scattered light that can be detected [107]. Mean diameter, polydispersity index and zeta potential were evaluated before and after freeze-drying and rehydration with bi-distilled water.

2.5 Vesicle behaviour at pH 1.2 and pH 7.0, simulating the gastro-intestinal environment

A solution at pH 1.2 and high ionic strength was prepared dissolving 1.75 g of sodium chloride in 94 ml of distilled water and adding hydrochloric acid (0.1 M) up to 100 ml. A solution at pH 7.0 and high ionic strength was prepared by dissolving 0.726 g of disodium hydrogen phosphate, 0.356 g of sodium dihydrogen phosphate and 1.754 g of sodium chloride in distilled water and bringing the volume up to 100 ml. The pH was adjusted to 7.0 with a diluted solution of phosphoric acid.

To evaluate stability under the harsh conditions mimicking the gastro-intestinal environment, each vesicle dispersion was diluted 100-fold either with the solution at pH 1.2 and incubated at 37 °C for 2 hours, or with the solution at pH 7.0 and incubated at 37 °C for 6 hours. After incubation, the mean diameter, the polydispersity index, and the zeta potential were immediately measured, to detect possible variations connected with destabilization phenomena. Further, the amount of payloads still entrapped in the vesicles has been measured before and after dilution and incubation with the two different media to estimate their leakage.

2.6 *In vitro* release assay

A solution of either artemisinin, curcumin or quercetin was prepared by diluting 10 mg of the compound in a 100 ml flask with a mixture of methanol and water (50:50 v/v). Drug-loaded vesicles were diluted 1/100 using saline solution. Spectra/Por® dialysis membranes (12-14 kDa MW cut-off,

3 nm pore size; Spectrum Laboratories Inc) were placed between the donor and receptor compartments of Franz vertical cells. The receptor compartment was filled with saline solution (~ 6 ml), which was continuously stirred with a small magnetic bar and maintained at a constant temperature of 37 ± 1 °C. 100 µl of either the free drug in solution or loaded in nutriosomes opportunely diluted were placed in the donor compartment above the dialysis membrane. Every 12 hours and up to 48 hours, the receptor compartment's solution was replaced with an equal volume of a fresh solution. At the end of the experiment, the dialysis membrane was washed with 2 ml of methanol to recover the total amount of compound and, in the case of the nutriosomes, to break the vesicles and consequently release the eventual payload. Subsequently, the obtained solutions were assayed for curcumin and quercetin content using a plate reader and disposable 96-well plates by means of UV detection (425 for curcumin and 380 for quercetin). Artemisinin content was assayed by HPLC as reported in paragraph 2.2.

2.7 Cell viability assay

Cell viability was evaluated using two different cell lines: human colon adenocarcinoma epithelial cells (Caco-2) and human umbilical vein endothelial cells (HUVECs). Caco-2 cells were cultured in high glucose Dulbecco's Modified Eagle's Medium, supplemented with 10% of foetal bovine serum and 1% of penicillin and streptomycin. HUVECs were cultured in Medium 199 supplemented with 10% of foetal bovine serum and 1% of penicillin and streptomycin. Both Caco-2 and HUVEC cells were maintained at 37 °C with 5% carbon dioxide. Cells were subcultured every two days. For the viability test, cells were seeded in 96-well plates at a density of 10000 cells/well for Caco-2 and 5000 cells/well for HUVECs. After a 24-h incubation, medium was removed, and cells were then exposed to different concentrations (40, 20, 10, 5, 2.5 µg/ml of each bioactive molecule) of either the drugs in dimethyl sulfoxide or loaded in vesicles. After 48 hours, medium was renewed and 10 µl of resazurin solution (0.125 mg/ml) was added to each well [108]. After 6 hours, the fluorescent signal generated from the resorufin, proportional to the number of living cells in the sample, was measured at 530 nm excitation wavelength and 590 nm emission wavelength using a Tecan Infinity 200 Pro microplate reader (Tecan Group Ltd., Männedorf, Switzerland). The viability was calculated as percentage of living cells in comparison to the untreated control cells (100% viability).

2.8 *In vitro P. falciparum* growth inhibition assay

P. falciparum 3D7 parasites were cultured in human B^+ erythrocytes at 37 °C under a gas mixture of 92.5% nitrogen, 5.5% carbon dioxide, and 2% oxygen, using complete Roswell Park Memorial Institute (RPMI) 1640 medium (supplemented with 2 mM l-glutamine, 50 µM hypoxanthine, 5 g/l

Albumax II, 25 mM HEPES, pH 7.2). The medium was changed every two days maintaining 1% parasitaemia and 3% haematocrit. Parasitaemia was determined by observing under the microscope blood smears of the culture previously fixed with methanol and stained with Giemsa diluted 1:10 in Sorenson's buffer (pH 7.2) for 10 minutes. For the growth inhibition assay, sorbitol synchronization was performed to obtain ring forms, parasitaemia adjusted to 1.5% and haematocrit to 6% [109]. 75 µl of the culture were seeded in 96-well plates with 75 µl of the vesicle dispersions or free drug solutions at different concentrations obtained by serial 1:2 dilutions (artemisinin solution and artemisinin nutriosomes from 0.250 to 0.002 µg/ml; artemisinin-curcumin and artemisinin-quercetin nutriosomes from 2.500 to 0.020 µg/ml; quercetin solution from 25 to 1.195 µg/ml; curcumin solution and quercetin nutriosomes from 50 to 0.391 µg/ml; curcumin nutriosomes from 75 to 0.586 µg/ml). Plates were incubated for 48 hours as described above. The percentage of parasitaemia was calculated as the value found in erythrocytes treated with vesicle formulations or free drug solutions compared to that of untreated control erythrocytes. The growth inhibition graphs and IC50 values were obtained through sigmoidal fitting of growth data at different drug concentrations, analysed with the GraphPad Prism 8 software (GraphPad Software, San Diego, CA, USA).

2.9 Ethical issues

The human blood used in this work was from voluntary donors and commercially obtained from the Banc de Sang i Teixits (www.bancsang.net). Blood was not collected specifically for this research; the purchased units had been discarded for transfusion, usually because of an excess of blood relative to anticoagulant solution. Prior to their use, blood units underwent the analytical checks according to the current legislation. Before being delivered to us, unit data were anonymized and irreversibly dissociated, and any identification tag or label had been removed to guarantee the non-identification of the blood donor. No blood data were or will be supplied, in accordance with the current Spanish Ley Orgánica de Protección de Datos and Ley de Investigacion Biomédica. The blood samples will not be used for studies other than those made explicit in this research.

2.10 Statistical analysis of data

Results are expressed as the means ± standard deviations. Multiple comparisons of means (ANOVA) were used to substantiate statistical differences between groups, while Student's t-test was used to compare two samples. Significance was tested at the 0.05 level of probability (p). Data analysis was carried out with the software package XLStatistic for Excel.

3 Results

3.1 Vesicle preparation and characterization

Vesicles have been prepared by direct sonication, which is a one-step easy method specifically used to produce small vesicles avoiding the use of organic solvents. Artemisinin (10 mg/ml), curcumin (10 mg/ml) or quercetin (10 mg/ml), alone or in association, were loaded in nutriosomes, which have previously demonstrated to be ideal phospholipid vesicles for oral administration of natural bioactive molecules [110]. To effectively load the phytochemicals, a preformulation study was performed aiming at finding the most appropriate type and amount of phospholipid, the ideal amount of payloads to be entrapped and the type and amount of additives capable of ensuring a better stability of the final dispersions (Table 1-2SM). In the simplest cases, using phospholipid at lower concentration, the payloads, alone or combined, were not entrapped, and quickly precipitated forming two-phase dispersions. Due to the formation of large aggregates, it was not possible to measure mean diameter and polydispersity of these samples. The addition of Nutriose® FM06 among the solid components and glycerol in the aqueous phase as structuring and thickening agents, permitted the formation of more homogenous dispersions, but even with these additives the formation of a precipitate was observed as well, nevertheless in a longer time (after 2 weeks). To avoid these phenomena, especially the loss of playloads and improve the stability of the dispersions, vesicles were freeze-dried and rehydrated just before the use, simply adding the correct amount of water (2 ml), and gently shaking them manually (for 2 minutes). Nutriose® FM06 acted as cryoprotectant, which avoided the break of vesicles during the freeze-drying process and allowed the immediate and simple rehydration. The effective formation of the vesicles and their morphology were confirmed by direct observation by means of cryo-TEM, which revealed the formation of uni- and oligolamellar spherical vesicles (Figure 1).

Mean diameter, polydispersity index and zeta potential of vesicles were measured immediately after sonication and after freeze-drying and rehydration (Table 1 and Table 2SM).

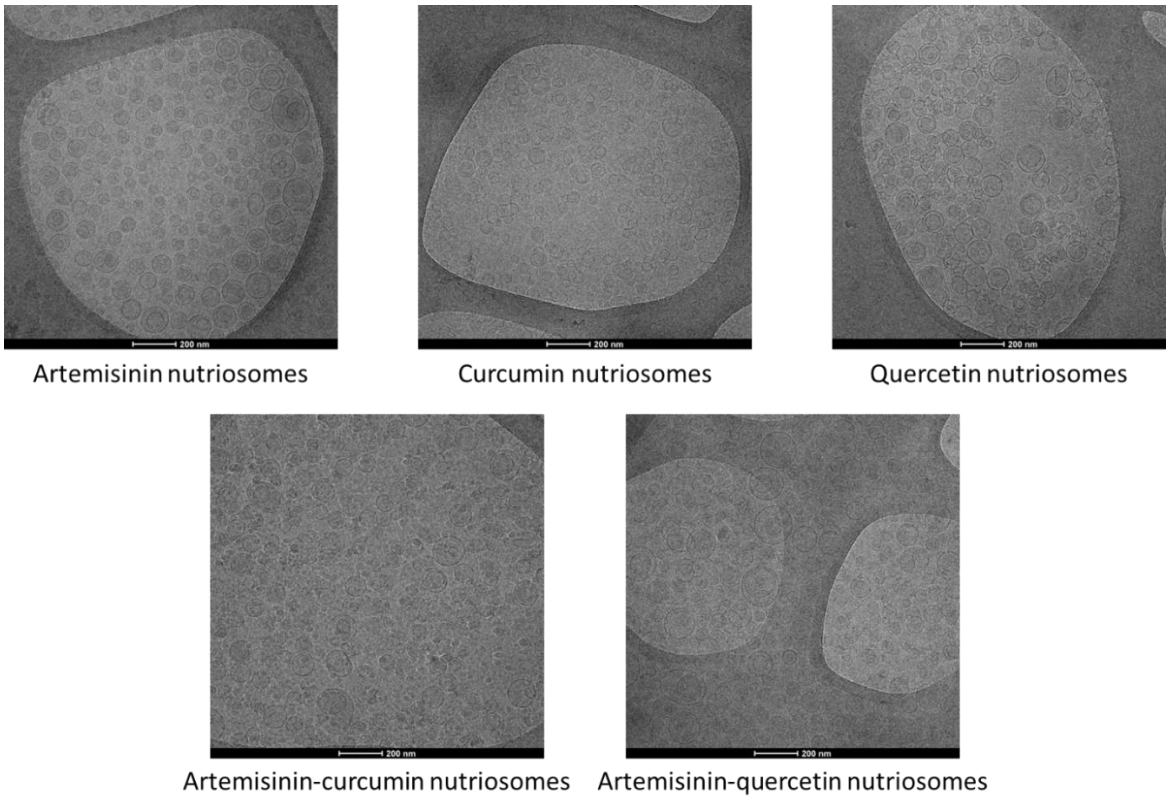

Figure 1. Representative cryo-TEM images of freshly prepared artemisinin nutriosomes, curcumin nutriosomes, quercetin nutriosomes, artemisinin-curcumin nutriosomes and artemisinin-quercetin nutriosomes.

Table 1. Mean diameter (MD), polydispersity index (PI) and zeta potential (ZP) of nutriosomes before and after freeze-drying. Entrapment efficiency (EE) of the samples before and after freeze-drying. Mean values ± standard deviations obtained from at least 3 samples are reported. The same symbols ($^{\circ}$, $^{\#}$, *, $^{+}$, §, $^{\&}$, $^{\$}$) indicate values that are not statistically different ($p>0.05$).

	Before freeze-drying				After freeze-drying			
Sample	MD (nm)	PI	ZP (mV)	EE (%)	MD (nm)	PI	ZP (mV)	EE (%)
Artemisinin nutriosomes	$95^{*} \pm 3$	0.18	$-10^{*+} \pm 1$	$22^{\S} \pm 10$	$93^{*} \pm 2$	0.17	$-8^{+} \pm 1$	$16^{\S} \pm 14$
Curcumin nutriosomes	$152^{\#} \pm 48$	0.34	$-10^{*+} \pm 1$	$65^{\&} \pm 10$	$108^{\circ\#} \pm 4$	0.25	$-8^{+} \pm 1$	$62^{\&} \pm 21$
Quercetin nutriosomes	$125^{\circ\#} \pm 2$	0.15	$-11^{*} \pm 1$	$51^{\$} \pm 10$	$121^{\circ\#} \pm 2$	0.17	$-8^{+} \pm 1$	$45^{\$} \pm 8$
Artemisinin-curcumin nutriosomes	$111^{\circ\#} \pm 1$	0.26	$-8^{+} \pm 1$	$22^{\S} \pm 7$ $60^{\$} \pm 10$	$121^{\circ\#} \pm 21$	0.24	$-7^{+} \pm 2$	$20^{\S} \pm 17$ $48^{\$} \pm 15$
Artemisinin-quercetin nutriosomes	$119^{\circ\#} \pm 4$	0.13	$-8^{+} \pm 1$	$21^{\S} \pm 5$ $67^{\&} \pm 13$	$128^{\circ\#} \pm 16$	0.18	$-8^{+} \pm 1$	$21^{\S} \pm 18$ $70^{\&} \pm 25$
Empty nutriosomes	$114^{\circ\#} \pm 8$	0.16	$-10^{*+} \pm 1$	-	$146^{\circ\#} \pm 40$	0.24	$-10^{*+} \pm 1$	-

Nutriosomes loading artemisinin were the smallest (~95 nm) and had a low polydispersity index (0.18); the lyophilization and rehydration process did not significantly modify the values (~93 nm).

Before freeze-drying, curcumin loading nutriosomes were larger (~152 nm) than those loading artemisinin (~95 nm) and had the highest polydispersity index (~0.34), indicating a polydisperse and unstable dispersion. Freeze-dried and rehydrated curcumin nutriosomes were similar to those measured after sonication, and to all the other samples, as their size was ~108 nm. The simultaneous loading of curcumin and artemisinin did not affect the size of the vesicles (~111 nm) and the polydispersity index remained high (0.26) but slightly lower than that of curcumin loaded nutriosomes (~0.34). The rehydration of freeze-dried artemisinin-curcumin nutriosomes led to the formation of vesicles with a size (~121 nm) not statistically different to the others and with a similar polydispersity index (0.24). Before and after freeze-drying, quercetin loaded nutriosomes had the same size (~123) and a low polydispersity index (0.15 before and 0.17 after freeze-drying), indicating a monodispersed sample. The co-loading of quercetin with artemisinin did not affect the vesicle size (~119 nm) and the sample remained monodispersed (polydispersity index was 0.13). Empty nutriosomes after sonication were sized ~114 nm. The mean diameter of empty nutriosomes did not statistically increase after lyophilization and rehydration processes (~130 nm), while the polydispersity index increased from 0.16 to 0.24.

Before and after freeze-drying, the zeta potential was not affected by the payloads (~-9 mV) and the negative values were mostly due to the negative groups of phosphatidylcholines facing the inter-vesicle medium [111].

The entrapment efficiency of artemisinin with or without curcumin or quercetin was the lowest (~19%). Entrapment efficiency of quercetin nutriosomes was ~45% and increased when it was co-loaded with artemisinin (~70%). Differently, the entrapment efficiency of curcumin nutriosomes was ~62%, which was the highest value among nutriosomes loading a single compound. The entrapment efficiency of curcumin decreased when it was co-loaded with artemisinin (~48%). There was no significant difference between the entrapment efficiency of each sample before and after freeze-drying (Table 1).

To evaluate the stability on storage, freeze-dried samples were stored at 25 °C, manually rehydrated by gentle shaking, at scheduled time points (3, 6 and 12 months) and analysed to measure their mean diameter, polydispersity index and zeta potential (Figure 2). Parameters of quercetin and artemisinin-quercetin loaded nutriosomes remained constant for 12 months confirming their good stability probably related to a positive effect of quercetin on vesicle assembling and stability. In the case of artemisinin nutriosomes size remained constant (~106 nm) but the polydispersity index increased up to 0.24 and 0.22 at 6 and 12 months. At 6 and 12 months, the size and polydispersity index of curcumin loaded nutriosomes significantly increased up to ~183 nm and 0.27. Artemisinin-curcumin nutriosomes followed the same path, but the increase of size was particularly evident at 12 months

(~205 nm) while the polydispersity index reached higher values starting from 6 months (~0.27). Overall, quercetin and artemisinin-quercetin nutriosomes were the most stable formulations, being able to maintain low mean diameter and polydispersity index values over 12 months storage.

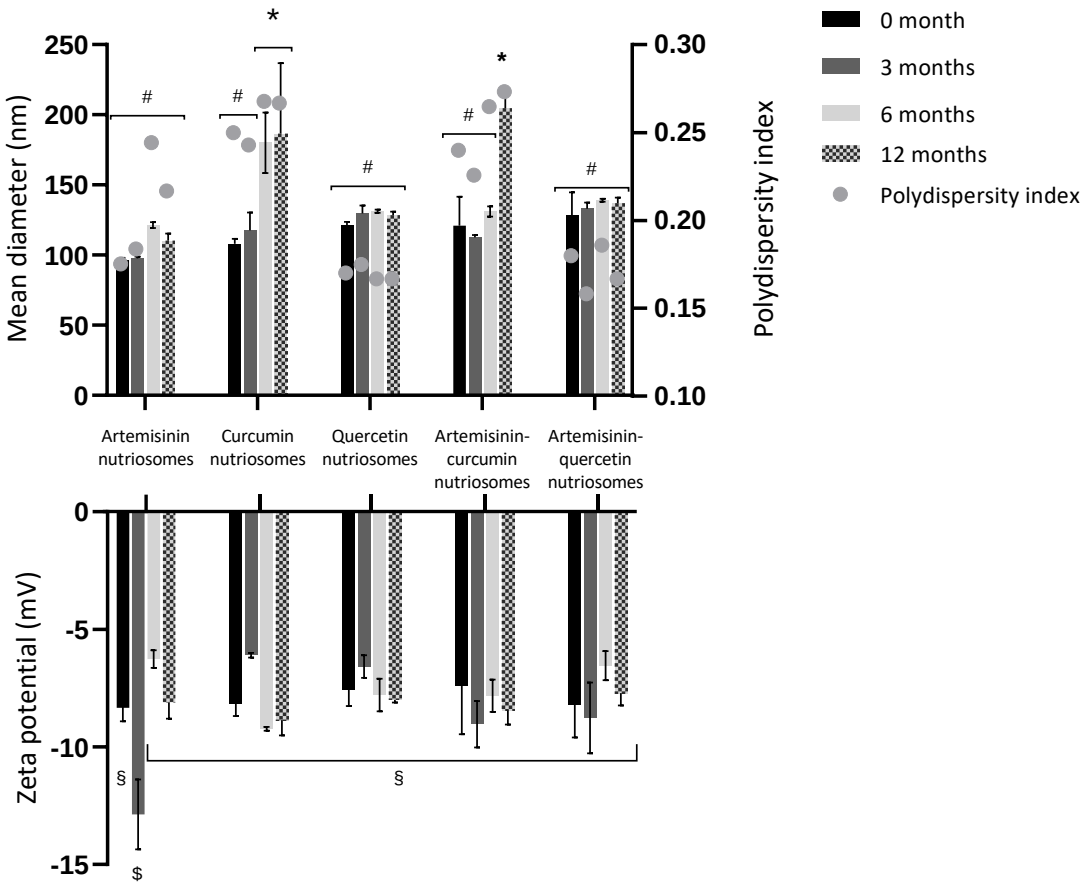

Figure 2. Mean diameter, polydispersity index and zeta potential of nutriosomes stored for 3, 6 and 12 months at 25 °C and rehydrated before the analysis. Mean values (bars) ± standard deviations are reported (n = 3). The same symbols (*, #, §, $) indicate values that are not statistically different (p>0.05).

3.2 Nutriosome stability at pH 1.2 and 7.0

Nutriosomes were diluted with solution at pH 1.2 or 7.0 and high ionic strength and incubated at 37 °C to evaluate their possible behaviour in the stomach and intestine after oral administration. Indeed, a strong change in vesicle parameter indicates a possible break or aggregation of vesicles, which in turn is generally associated with the leakage of payloads. Artemisinin-curcumin nutriosomes were able to resist under these harsh conditions without breaking, since their size remained unvaried at 2 hours in acidic solution or 6 hours in neutral solution (~129 nm), confirming their potential stability in gastrointestinal fluids (Table 2). The other samples underwent a small increase in size at 2 and 6

hours, but they remained homogenously dispersed, as the polydispersity index remained lower than 0.24.

At 2 hours and pH 1.2, an inversion of zeta potential was observed for each formulation, due to the presence of H^+ in the acidic medium, which coated the vesicle surface, while the zeta potential remained unchanged at 6 hours and pH 7.0 [112]. Nutriosomes were able to retain the payloads during the incubation period, at pH 1.2 and 7.0, as the entrapment efficiency of each sample after incubation was not statistically different from that of the corresponding freshly prepared sample (Table 2).

Table 2. Mean diameter (MD), polydispersity index (PI), zeta potential (ZP) and entrapment efficiency (EE) of the vesicles diluted and incubated at 37 °C, at pH 1.2 for 2 hours (t_{2h}) and at pH 7.0 for 6 hours (t_{6h}). Mean values ± standard deviation obtained from at least 3 replicates are reported. The same symbols (*, °, $, +, §, @, #, &) indicate values that are not statistically different (p>0.05)

Sample	Time	MD (nm)		PI		ZP (mV)		EE (%)	
		pH 1.2	pH 7	pH 1.2	pH 7	pH 1.2	pH 7	pH 1.2	pH 7
Artemisinin nutriosomes	$t_{2h/6h}$	118* ± 5	123*$ ± 8	0.15	0.19	+5# ± 4	–5& ± 1	19 ± 10	19 ± 12
Curcumin nutriosomes	$t_{2h/6h}$	122*° ± 3	122*$+ ± 2	0.20	0.18	+7# ± 3	–5& ± 2	65 ± 13	65 ± 18
Quercetin nutriosomes	$t_{2h/6h}$	149§ ± 3	159§ ± 4	0.20	0.17	+6# ± 3	–6& ± 2	49 ± 8	49 ± 10
Artemisinin-curcumin nutriosomes	$t_{2h/6h}$	132°$ ± 5	134°$+ ± 5	0.17	0.18	+3# ± 3	–4& ± 3	18 ± 6 61 ± 11	18 ± 10 64 ± 10
Artemisinin-quercetin nutriosomes	$t_{2h/6h}$	187@ ± 8	195@ ± 8	0.24	0.17	+5# ± 4	–5& ± 2	19 ± 4 63 ± 14	19 ± 8 63 ± 14

3.3. *In vitro* release assay

The amount of payloads released from nutriosomes was measured and compared with that released through the same membrane filled with the solutions of curcumin, quercetin or artemisinin at the same concentration (Figure 3). Using the solution, the three bioactive molecules were almost completely released at 48 hours (curcumin ~90%, quercetin ~95% and artemisinin ~100%). Using artemisinin-loaded nutriosomes, artemisinin was also completely released at 48 hours ~100%). Artemisinin was already mostly released at 24 hours using solution and nutriosomes (~86%). Differently, when curcumin and quercetin were loaded in nutriosomes, the release was significantly slowed as only ~53% of each bioactive molecule was released at 48 hours, confirming the carrier

ability to control the release of the loaded molecules. Using curcumin or quercetin nutriosomes, the first amount of payload was quickly released because it was not actually entrapped inside the vesicles, while the release of entrapped payload was retarded (curcumin ~62% and quercetin ~45%). Differently, the entrapment efficiency of artemisinin was very low (~19%) and its release was equal to that obtained with the drug in solution. Results indicates that nutriosomes seem to be optimal carriers for curcumin and quercetin but not for artemisinin.

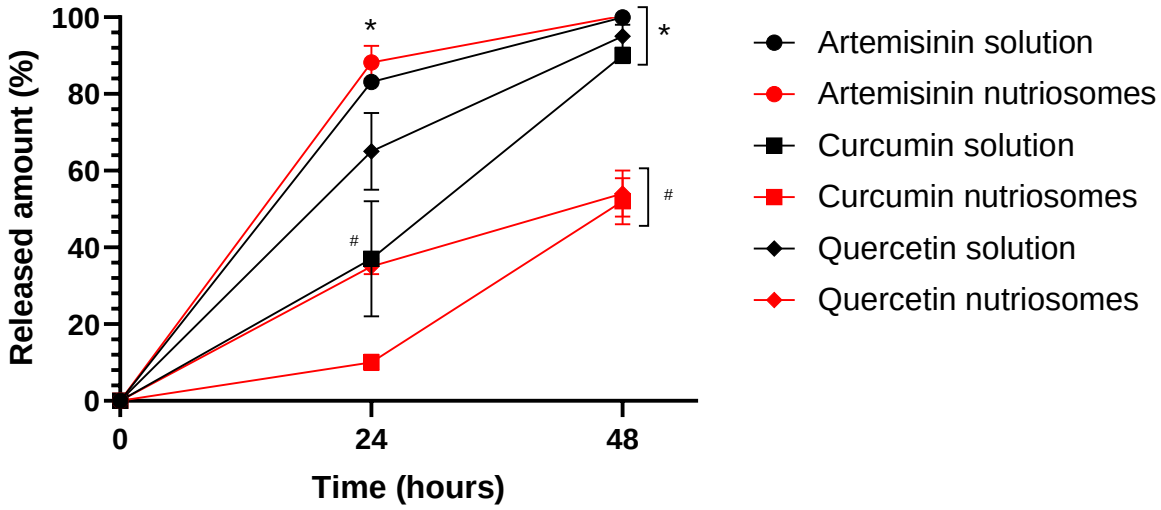

Figure 3. Released amount (%) of artemisinin, curcumin, and quercetin through a dialysis membrane filled with these phytodrugs in water solutions or in nutriosomes dispersions over 48 hours. Mean values ± standard deviations are reported (n = 3). The same symbols (*, #) indicate values that are not statistically different ($p>0.05$).

3.4. Cell viability assay

Cell viability was evaluated using the resazurin assay, which is a simple, fast, and sensitive test [108]. It permits to measure the cell viability through the reduction, live cell mediated, of resazurin to the fluorescent product resorufin. Being the formulations designed for oral administration, Caco-2 cells were selected as a model of the intestinal epithelial barrier. HUVECs are very sensitive cells that are widely used for cytotoxicity assay and therefore were used as well for this assay. No significant toxicity has been observed neither treating Caco-2 nor HUVECs with curcumin-, quercetin- and artemisinin-loaded nutriosomes. Artemisinin solution at the highest concentration used (40 μg/ml) was highly biocompatible as the viability of Caco-2 cells was ~89% and that of HUVECs was ~99%. Using the lower concentrations, the viability was ≥ 100%. Treating Caco-2 cells with quercetin solution, at the highest concentration (40 μg/ml), the viability was lower (~73%) and increased up to ~100% using lower concentrations. When quercetin (alone or in combination with artemisinin) was

loaded in the vesicles at the highest concentration (40 µg/ml) the viability was higher than 100%, probably because of the carrier ability to reduce the payload toxicity. On the other hand, when Caco-2 cells were treated with curcumin solution at 40 and 20 µg/ml, a high cytotoxicity was observed (viability ~1%); in contrast, when the cells were treated with curcumin and artemisinin-curcumin (40 and 20 µg/ml) loaded in nutriosomes, the viability was higher than 80%. The viability of HUVECs treated with quercetin solution at 40 µg/ml was ~46%, at 20 µg/ml was ~84%, and at lower concentrations was higher than 100%. When quercetin was loaded in nutriosomes, alone or with artemisinin, the viability was higher than 85%, irrespective of the used concentration. Similarly to Caco-2, treatment of HUVECs with curcumin solution provided the lowest cell viability values, which were lower than 20% using 40, 20, 10, 5 µg/ml and ~80% using 2.5 µg/ml. In a similar manner, HUVEC viability increased treating them with curcumin loaded in nutriosomes, with or without artemisinin, as the viability was ~68% using 40 µg/ml, ~93% using 20 µg/ml and higher than 100% at lower concentrations. Results underline that curcumin was toxic in solution at the highest concentrations, quercetin was less toxic, and artemisinin did not cause any toxicity, using the same concentrations. Anyways, their loading in nutriosomes reduced the toxicity of curcumin and quercetin also at highest concentrations.

Figure 4. Viability of Caco-2 (left panel) and HUVEC (right panel) cells, incubated with artemisinin, curcumin, or quercetin in solution or loaded in nutriosomes and diluted to reach 40, 20, 10, 5 and 2.5

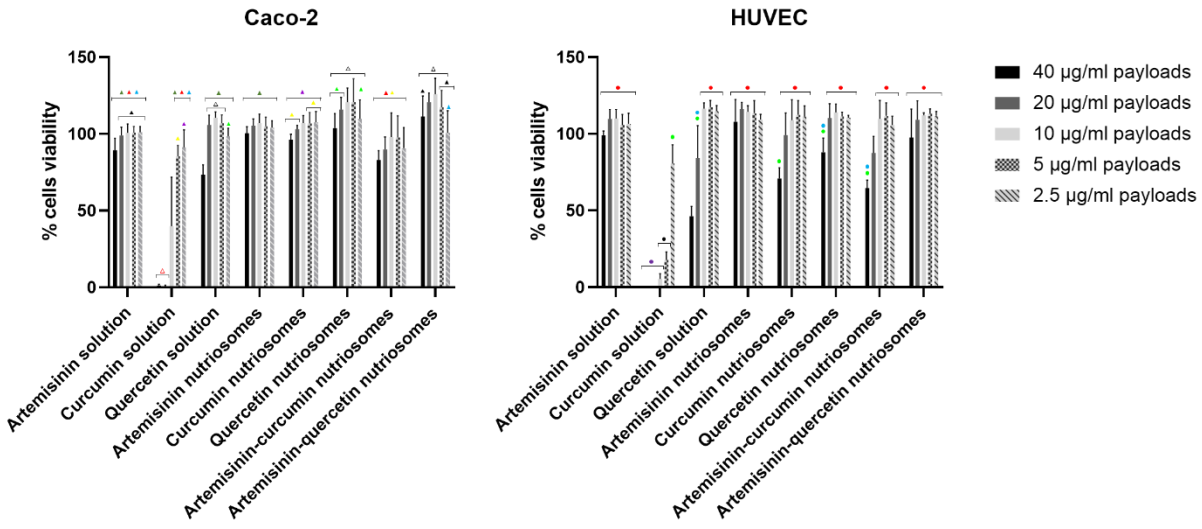

µg/ml of each payload. Mean values (bars) ± standard deviations are reported. In each panel, the same symbols indicate values that are not statistically different ($p>0.05$).

3.5. *P. falciparum* growth inhibition assay

The ability of formulations to inhibit the growth of *P. falciparum* cultured in human B+ erythrocytes was evaluated (Table 3). As expected, the *in vitro* antimalarial activity of artemisinin was the highest and there was no statistical differences among the solution and the nutriosomes loading artemisinin alone or in combination with curcumin or quercetin, their IC50 ranged from 0.006 to 0.149 µg/ml ($p>0.05$ among these values). The IC50 of curcumin solution was ~3.949 µg/ml and that of quercetin solution was ~7.258 µg/ml ($p>0.05$ between the two values), confirming that their efficacy was lower than that of artemisinin, which is a potent antimalaria drug. The effect of quercetin was not affected by its loading in nutriosomes (IC50 ~7.020 µg/ml) while that of curcumin was slightly affected. Indeed, when curcumin was loaded in nutriosomes the IC50 was higher (~8.777 µg/ml, $p<0.05$ versus the IC50 of curcumin and quercetin solutions) than that of free curcumin. The co-loading of curcumin or quercetin with artemisinin in nutriosomes had a negligible effect on parasite growth compared to that of artemisinin loaded nutriosomes, as their IC50 was ~0.149 and 0.062 µg/ml ($p>0.05$ between the two values), since their effect was masked, thus unmeasurable, by that of the most potent artemisinin (Table 3).

Table 3. IC50 values (µg/ml) of artemisinin, curcumin and quercetin in solution or loaded in nutriosomes against *in vitro P. falciparum* 3D7 cultures. Mean values ± standard deviations are reported (n = 3). The same symbols (*, $^{\#, \S}$) indicate values that are not statistically different ($p>0.05$).

Samples	IC50 (µg/ml)
Artemisinin solution	0.006* ± 0.004
Curcumin solution	3.949$^{\#}$ ± 1.277
Quercetin solution	7.258$^{\#\S}$ ± 2.613
Artemisinin nutriosomes	0.070* ± 0.036
Curcumin nutriosomes	8.777§ ± 0.649
Quercetin nutriosomes	7.020$^{\#\S}$ ± 2.664
Artemisinin-curcumin nutriosomes	0.149* ± 0.057
Artemisinin-quercetin nutriosomes	0.062* ± 0.024

4. Discussion

Curcumin, quercetin and artemisinin (10 mg/ml) were successfully loaded in nutriosomes alone or alternatively artemisinin was co-loaded with curcumin or quercetin. Nutriosomes are special and effective phospholipid vesicles enriched with Nutriose® FM06 and specifically tailored for oral

administration, which have demonstrated to be ideal for the delivery of curcumin and other natural molecules or extracts [101,104]. Nutriose® FM06 is a water-soluble branched dextrin with high levels of fibre content, which did not form gelled dispersions in water. However, its addition to the lamellar vesicles exerts a triple function since improves the vesicle resistance during their passage through the gastro-intestinal environment, increases the loading of lipophilic payloads and facilitates the vesicle reforming after freezer-drying, acting as cryoprotectant [113]. Actually, nutriosomes were stable, small and monodispersed, except those loading curcumin (alone or in association with artemisinin), which were bigger and slightly polydispersed probably due to the impossibility to intercalate all the used payload (10 mg/ml) inside the bilayer. Indeed, curcumin is generally loaded at lower concentrations (10-100 folds lower) in phospholipid vesicles as it is a large molecule with a complex structure [114,115]. Artemisinin is also very difficult to be loaded in liposomes in high amount and when loaded in liposomes, it was usually tested for parental administration at lower concentrations [116,117]. Nutriosomes were able to load a small amount of artemisinin (~19%), while curcumin and quercetin were loaded in higher amount, ~62 and ~45% when loaded alone, and ~48 and ~70% when loaded with artemisinin. The freeze-drying process did not lead to payload leakage, as there was no significance difference in terms of entrapment efficiency between each sample before and after freeze-drying.

Due to the lower amount of artemisinin entrapped in nutriosomes, these vesicles appeared to be more suitable for incorporating phenolic molecules and less for sesquiterpene tetracyclic endoperoxylactone, which is not as much polar and has specific steric conformation [118]. Its characteristics drastically affected the intercalation inside the nutriosome bilayer thus reducing the entrapment efficiency. Results are in agreement with previous ones, in which the low entrapment efficiency was attributed to the size of prepared vesicles: the smallest the vesicles, the lowest the entrapment [117,119,120]. Actually, artemisinin loaded nutriosomes were the smallest (~95 nm), clearly the addition of curcumin or quercetin in artemisinin loaded nutriosomes modified this ratio, because the additional phytochemicals contribute to the enlargement of the vesicles. Indeed, the size of nutriosomes loading artemisinin and curcumin or quercetin was not statistically different than that of curcumin or quercetin loaded nutriosomes. These results suggested a key role of artemisinin in modulating the assembling of the phospholipids (which led the formation of smaller vesicles) and confirmed the theory according to which its entrapment is highly affected by the mean size of the final system [120–123].

The stability of vesicle dispersions on storage was inadequate, especially that of vesicles loading artemisinin, for this reason they were freeze-dried to obtain a stable powder easily re-dispersible just before use, by gentle manual shaking, avoiding the use of physical inputs, like sonication. In this way,

freeze-dried formulations can be orally administered as capsules or tablets, or even as dispersion after their simple rehydration. The rehydrated vesicles had size and polydispersity index comparable or lower than those of the same vesicles before the freeze-drying, thanks to the presence of Nutriose® FM06, which acting as cryoprotectant avoided vesicle break and allowed their reforming [124]. In their dried state, vesicle dispersions were stable for 12 months, and after rehydration only the mean diameter and polydispersity index of nutriosomes loading curcumin, alone or in association with artemisinin, increased. The loading of such high amount (10 mg/ml) of artemisinin permits to easily reach the required dose, which is around 500 mg per day in adults [125]. It is important to note that the highest part of used drug was not actually entrapped inside the vesicles, as the entrapment efficiency was ~19% and this caused the immediate release of the drug from the vesicles (~86% at 24 hours and ~100% at 48 hours). On the contrary, as previously reported, nutriosomes are optimal carriers for polyphenol delivery, imparting a delayed release (~10% of released curcumin and ~35% of released quercetin at 24 hours and ~53% of both at 48 hours). This low entrapment efficiency and rapid release of artemisinin can negatively affect its oral delivery and systemic bioavailability. However, the vesicles were stable under the harsh conditions of the gastro-intestinal tract and their vesicle size, polydispersity index and zeta potential did not change after dilution in acidic and neutral media with high ionic strength, indicating that the destabilization phenomena are avoided [115]. Nutriosomes kept their carrier structure intact, prevented the leakage of payloads, and could facilitate the passage through the intestinal membrane of the molecules loaded, such as curcumin and quercetin, and improve their systemic efficacy, as previously confirmed by *in vivo* studies performed with curcumin and other polyphenols extracted from grape by-products [100]. This advantage is expected to improve their intestinal absorption and bioavailability as previously confirmed for curcumin [101]. The efficacy of formulations was tested *in vitro*, measuring their ability to inhibit the growth of *P. falciparum* in human B+ erythrocytes [126]. In these conditions, the performances of nutriosomes, which are oral carriers, were negligible and the effectiveness of artemisinin-loaded nutriosomes was lower than that of the drug solution while that of curcumin or quercetin nutriosomes was comparable to that of the corresponding free polyphenol solutions. Additionally, the co-loading of quercetin and curcumin with artemisinin in nutriosomes did not improve the formulation efficacy, but maintained the efficacy of artemisinin alone, probably because the effect of polyphenols was masked by that of the more potent artemisinin.

In previous works, curcumin loaded nutriosomes demonstrated to be effective on inhibiting *in vivo* growth of *P. berghei* [102,103]. Nevertheless, in the light of the obtained results, nutriosomes do not seem to be suitable for the oral delivery of artemisinin, as they did not actually entrap the drug. Nutriosomes seem to be effective carriers for polyphenols like curcumin and quercetin, especially the

latter, which were usefully loaded and their release delayed. The loading in vesicles did not affect the *in vitro* efficacy of payloads, as expected being nutriosomes tailored for oral delivery and not suitable to be directly added to erythrocytes. Indeed, in their *in vivo* fate must pass the intestinal barrier inside the carrier and are expected to arrive in the systemic circulation in the free form. Clearly, curcumin and quercetin even if loaded in nutriosomes, cannot be considered comparable to artemisinin but their oral administration can improve its effect, as previously found.

5. Conclusion

In the present work, nutriosomes incorporating 10 mg/ml of artemisinin, curcumin or quercetin, alone or in association, were successfully obtained, stored in de-hydrated form and rehydrated before the use by gentle manual shaking. Vesicles seemed to be resistant to gastro-intestinal chemical stressors but unfortunately, only entrapped and retained a low concentration of artemisinin (~19%) and did not improve its *in vitro* efficacy against *P. falciparum*. Nutriosomes better loaded and retained curcumin and quercetin and their efficacy was comparable to that of free drug, the form in which the delivered payload can reach the systemic circulation. Overall results, underline good carrier ability of nutriosomes in the delivery of polyphenols but not in that of terpenic molecules, thus, curcumin and quercetin nutriosomes can be tested as adjuvants in malaria treatment while their co-loading with artemisinin in nutriosomes is not suitable.

Chapter II

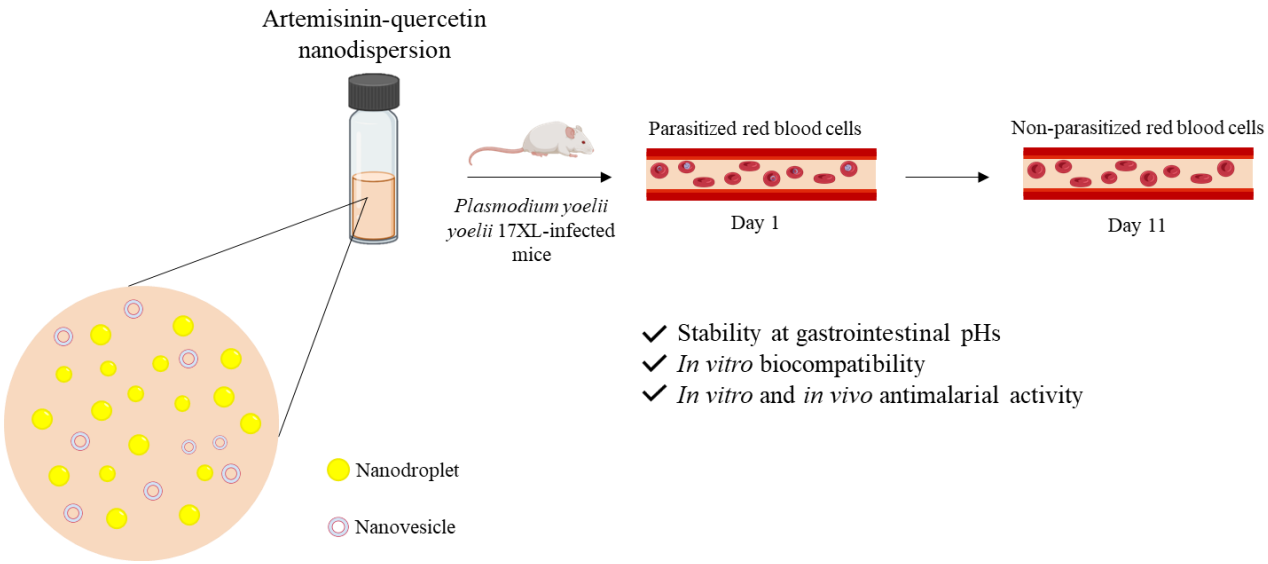
Artemisinin-quercetin nanodispersion
Plasmodium yoelii yoelii 17XL-infected mice
Parasitized red blood cells
Day 1
Non-parasitized red blood cells
Day 11
Stability at gastrointestinal pHs
In vitro biocompatibility
In vitro and in vivo antimalarial activity
Nanodroplet
Nanovesicle

Nanoemulsions loading artemisinin and quercetin as a promising nanosystem for the oral treatment of malaria: *in vitro* and *in vivo* evaluation

Federica Fulgheri[1], Miriam Ramírez[2,3], Lucía Román-Álamo[2,3], Paolo Gasco[4], Maria Manconi[1], Bianca Maria Baroli[1], Xavier Fernàndez-Busquets[2,3] and Maria Letizia Manca[1]

[1]Dept. of Life and Environmental Sciences, University of Cagliari, University Campus, S.P. Monserrato-Sestu Km 0.700, Monserrato, 09042, CA, Italy

[2]Barcelona Institute for Global Health (ISGlobal, Hospital Clínic-Universitat de Barcelona), Rosselló 149-153, ES-08036 Barcelona, Spain

[3]Nanomalaria Group, Institute for Bioengineering of Catalonia (IBEC), The Barcelona Institute of Science and Technology, Baldiri Reixac 10-12, ES-08028 Barcelona, Spain

[4]Nanovector S.r.l., Via Livorno, 60-10144 Torino, Italy

1. Introduction

During the last two decades, a significant progress has been made in malaria control, which led to a reduction of the number of cases and mortality rate, although the disease remains a major global threat in developing countries, about 247 million cases and 619 000 deaths worldwide in 2021 [1]. The current frontline treatment for uncomplicated malaria caused by *Plasmodium falciparum* (*P. falciparum*) is based on artemisinin and its derivatives [127]. Artemisinin is a sesquiterpene lactone containing an unusual peroxide bridge, which is essential for its antimalarial activity [128]. It induces a very rapid reduction of parasitaemia, starting almost immediately after administration [129]. Its ester derivative artesunate and the ether derivatives artemether and arteether are more effective since they act as pro-drugs, forming *in vivo* dihydroartemisinin, the active metabolite [130]. The oral formulations of artemisinin or its derivatives are rapidly but incompletely absorbed, reaching in 1-2 h the peak of plasma concentrations and are eliminated through hepatic metabolism with half-lives between 0.5 and 3 h [131]. Their intramuscular formulations provide lower and more variable absorption and elimination, and intravenous artesunate remains the treatment of choice for severe malaria from *P. falciparum* [132]. Due to their rapid onset of action, artemisinin derivatives are usually associated with a second antimalarial drug, which has a longer half-life and synergic activity. Artemisinin and its derivatives have been orally administered to treat uncomplicated malaria infections while parenteral administration of water-soluble artesunate or oil-soluble artemether is frequently employed for the treatment of severe malaria patients [133]. In the last 20 years, they have been extensively used for the clinical treatment of malaria caused by *P. falciparum*, but safety concerns appeared due to acute haemolytic anaemia cases [133,134].

A strategy to improve artemisinin efficacy and safety avoiding side effects consists in its delivery in affordable nanosystems and several of them have been designed and tested accordingly [135]. The choice of the most suitable nanosystem is not easy and depends on the used drug, its structure and physico-chemical properties and the administration route [136]. Nanoemulsions have emerged as optimal nanoformulations for the delivery of several antimicrobials to treat different infectious diseases and have been already used to improve the efficacy of antimalarial drugs [137]. Primaquine was loaded in nanoemulsions and, when orally administered, was more effective than a conventional oral dosage in inhibiting *Plasmodium berghei* infection in Swiss albino mice [138]. Dihydroartemisinin was loaded in surface modified lipid nanoemulsions, which were able to clear the parasitaemia in animals avoiding haemolysis [139].

According to these previous results, in this study artemisinin and quercetin have been dispersed in a mixture of oil, water and surfactants to prepare nanoemulsions tailored for oral administration [140]. Quercetin, a potent natural antioxidant with several beneficial properties, is expected to complementary improve the efficacy of artemisinin [141]. Indeed, the antiplasmodial activity of quercetin was previously confirmed *in vitro* in the 3D7/K1 *P. falciparum* line and *ex vivo* in fresh *P. falciparum* field isolates from Bangladesh [142]. The obtained formulations were fully characterized and their biocompatibility on Human colon adenocarcinoma cells (Caco-2) and Human umbilical vein endothelial cells (HUVEC) was assessed. In addition, *in vitro P. falciparum* growth inhibition assay and *in vivo* antimalarial efficacy on *Plasmodium yoelii yoelii 17XL*-infected mice were assessed.

2. Materials and methods

2.1. Materials

Soy lecithin (Lecinova®) was purchased in a local store. Artemisinin was purchased from Carbosynth Ltd (United Kingdom). Quercetin, castor oil, Kolliphor® RH40 and other reagents of analytical grade were purchased from Sigma-Aldrich (Milan, Italy). Water was purified through a Milli-Q system from Millipore (Milford, MA). Reagents and plastics for cell culture were purchased from Life Technologies Europe (Monza, Italy).

2.2. Sample preparation

Artemisinin (5 mg/mL) or quercetin (5 mg/mL) or both (5 mg/mL each), castor oil (100 mg/mL), Kolliphor® RH40 (100 mg/mL) and soy lecithin (25 mg/mL) were weighted in a glass vial, heated at 50 ± 0.5 °C in a thermostatic water bath and maintained under stirring for 20 minutes, to obtain and

homogeneous phase. Bi-distilled water (up to 1 mL) was heated at 50 ± 0.5 °C as well and gently poured over to the oil phase. The dispersions were sonicated (20 cycles, 5 sec on 2 sec off, 13 μ of probe amplitude) with a high intensity ultrasonic disintegrator (Soniprep 150, MSE Crowley, London, UK), obtaining transparent nanoemulsions.

2.3. Characterization of nanoemulsions

The morphology of nanoemulsions was observed using a cryogenic transmission electron microscope (cryo-TEM). A thin film of each sample was formed on a holey carbon grid and vitrified by plunging (kept at 100% humidity and room temperature) into ethane maintained at its melting point, using a Vitrobot (FEI Company, Eindhoven, The Netherlands). The vitreous films were transferred to a Tecnai F20 TEM (FEI Company) and the samples were observed in a low dose mode. Images were acquired at 200 kV at a temperature ~-173 °C, using low-dose imaging conditions.
Mean diameter and polydispersity index of oil droplets were measured at 25 °C by dynamic light-scattering using a Zetasizer Ultra from Malvern Instruments (Worcestershire, UK). Zeta potential was measured using the Zetasizer Ultra by the Mixed Mode Measurement-Phase Analysis Light Scattering. Before the analysis, 10 μL of each sample was diluted with 990 μL of distilled water.

2.4. Behaviour of nanoemulsions at gastrointestinal pH

Formulations' stability in gastrointestinal fluids was assessed observing their behaviour at different pH (1.2 and 7.0) simulating the gastro-intestinal environment. Each sample was diluted 100-folds with solutions at high ionic strength and pH 1.2 or 7.0. Samples at pH 1.2 were incubated at 37 °C for 2 h and that at pH 7.0 for 6 h. The solution at pH 1.2 was prepared dissolving 1.75 g of sodium chloride in 94 mL of bi-distilled water and adding 0.1 M hydrochloric acid up to 100 mL. The solution at pH 7.0 was prepared dissolving 0.726 g of disodium hydrogen phosphate, 0.356 g of sodium dihydrogen phosphate and 1.754 g of sodium chloride in bi-distilled water and adding bi-distilled water up to 100 mL. The pH was adjusted to 7.0 with a diluted solution of phosphoric acid [143]. At 2 h or 6 h, mean diameter and polydispersity index of the oil droplets were measured as an indicator of their stability.

2.5. *In vitro* cytotoxicity of nanoemulsions

Human colon adenocarcinoma cells (Caco-2) were cultured at 37 °C, 100% humidity and 5% carbon dioxide and using Dulbecco's Modified Eagle Medium (high glucose), supplemented with 10% of FBS and 1% of penicillin (10,000 units) and streptomycin (10 mg /mL) as growth medium. Human umbilical vein endothelial cells (HUVECs) were cultured at 37 °C, 100% humidity, 5% carbon

dioxide and using Medium 199 (M199) supplemented with 10% of FBS and 1% of penicillin (10,000 units) and streptomycin (10 mg /mL) as growth medium. The medium was changed every two days. Caco-2 cells were seeded at density of 10000 cells/well and HUVECs at density 5000 cells/well in a 96-well plate and incubated at 37 °C for 24 h. Cells were treated for 48 h with artemisinin or quercetin or both in combination, solubilized in dimethyl sulfoxide (10 mg/mL) or loaded in nanoemulsions. Before the experiments, samples were diluted to reach different concentrations of artemisinin and quercetin (40, 20, 10, 5, 2.5 μg/mL). Cell viability was evaluated using the resazurin assay, a fast and simple fluorometric test [108]. 10 μL of resazurin solution (0.125 mg/mL) was added to each well and, at 24 h, fluorescent signal of samples containing in the wells was measured at 530 nm excitation wavelength and 590 nm emission wavelength using a Tecan Infinity M Plex microplate reader (Tecan Group Ltd., Switzerland). Three independent experiments were performed in different times, each time in triplicate. The viability (%) was reported in comparison with the untreated control cells (100% viability).

2.6. *In vitro P. falciparum* growth inhibition

P. falciparum 3D7 culture was maintained at 1% parasitemia and 3% haematocrit in a hypoxia incubator (cell culture carbon dioxide incubator, ESCO, Singapore) with a gas mixture containing 92.5% nitrogen, 5.5% carbon dioxide, and 2.0% oxygen. The parasites were cultured in B+ red blood cells in complete Roswell Park Memorial Institute (RPMI) 1640 medium, supplemented with 2 mM L-glutamine, 50 μM hypoxanthine, 5 g/L albumax II, 25 mM HEPES, pH 7.2. Prior to the assay, parasites were synchronized to ring stage through 5% (w/v) sorbitol lysis [109].

Serial dilutions of artemisinin or quercetin or both in combination, solubilized in dimethyl sulfoxide (10 mg/mL) or loaded in nanoemulsions, were done using the complete medium. The concentrations of artemisinin solution, artemisinin nanoemulsions, artemisinin-quercetin nanoemulsions ranged from 0.500 to 0.004 μg/mL; that of quercetin solution from 50 to 2.39 μg/mL; that of quercetin nanoemulsions from 20 to 0.156 μg/mL. Each diluted sample (75 μL) was added to at least three wells of 96-well plates, each containing 75 μL of *P. falciparum* 3D7 culture at 1.5% parasitemia and 6% haematocrit. Three additional wells contained 75 μL of complete medium and 75 μL of the culture were prepared. The wells were incubated for 48 h and after dilution to 0.03% parasitemia with phosphate buffered saline (PBS) containing 0.1 μM Syto11 (Thermo Fisher Scientific, Inc.). Parasitemia percentage was determined by flow cytometry, using LSRFortesa (4 laser) cytometers (BD Biosciences, San Jose, CA, USA) and recorded using a software BD FACSDiva (BD Biosciences). Three independent experiments were performed in different times, each time in triplicate. Growth inhibition was calculated as the percentage of parasitemia measured after treatment

with samples versus the parasitemia measured in untreated control. IC50 and IC90 (expressed in μg/mL) was calculated using the GraphPad Prism 8 software (GraphPad Software, San Diego, CA, USA) by the dose-response curve of the triplicate mean for each sample.

2.7. *In vivo* antimalarial effect of nanoemulsions

The *in vivo* antimalarial activity of artemisinin or quercetin or both in combination, dispersed in PBS or loaded in nanoemulsions, was assessed using a 4-day blood suppressive test as described previously [144]. Briefly, BALB/c mice (three animals per group) were inoculated with 2×10^7 red blood cells (100 μL) from *Plasmodium yoelii yoelii* 17XL-infected mice by intraperitoneal injection. Each nanoemulsion was diluted in PBS to obtain the IC50 and IC90 previously found by *in vitro* growth inhibition assay on *P. falciparum* (Table 3). The PBS dispersions of artemisinin or quercetin or both together were diluted to reach the IC90. At 4 h (day 0), 28 h (day 1), 52 h (day 2), 76 h (day 3) from the inoculation, 100 μL of each sample were orally administered to the mice. Each day for 11 days, Giemsa-stained blood smears were used to monitor the parasitemia. At the end of the experiment, one animal treated with artemisinin-quercetin nanoemulsion at IC50 was reinfected with 2×10^7 red blood cells (100 μL) from *Plasmodium yoelii yoelii* 17XL-infected mice by intraperitoneal injection and weight, temperature, physical activity and parasitemia were observed for three weeks.

2.8. Ethical issues

The human blood used in this work was from voluntary donors and commercially obtained from the Banc de Sang i Teixits (www.bancsang.net). Blood was not collected specifically for this research; the purchased units had been discarded for transfusion, usually because of an excess of blood relative to anticoagulant solution. Prior to their use, blood units underwent the analytical checks specified in the current legislation. Before being delivered, unit data were anonymized and irreversibly dissociated, and any identification tag or label had been removed in order to guarantee the non-identification of the blood donor. No blood data were or will be supplied, in accordance with the current Spanish Ley Orgánica de Protección de Datos and Ley de Investigación Biomédica. The blood samples will not be used for studies other than those made explicit in this research.

Mice (18–20 g) were maintained under standard environmental conditions: 20–24 °C and 12/12 h light/dark cycle, with ad libitum access to a semi-solid diet and water during the duration of the experiments. In the presence of toxic effects including, among others, >20% reduction in animal weight, aggressive and unexpected animal behaviour or the presence of blood in faeces, animals were immediately anesthetized using a 100 mg/kg Ketolar plus 5 mg/kg Midazolan mixture and sacrificed by cervical dislocation. The animal care and use protocols followed adhered to the specific national

and international guidelines specified in the Spanish Royal Decree 53/2013, which is based on the European regulation 2010/63/UE. The studies reported here were performed under protocols reviewed and approved by the Ethical Committee on Clinical Research from the Hospital Clínic de Barcelona (Reg. HCB/2018/1223, January 23, 2019).

2.9. Statistical analysis of data

Results are expressed as the means of at least 3 independent experiments ± standard deviations. Multiple comparisons of means (ANOVA) were used to substantiate statistical differences between groups, while Student's t-test was used to compare two samples. Significance was tested at the 0.05 level of probability (p). Data analysis was carried out with the software package XLStatistic for Excel.

3. Results

3.1. Preparation and characterization of nanoemulsions

A preformulation study was performed to find the more suitable oil phase capable of giving the formation of stable and effective nanoemulsions. Different oils and surfactants or cosurfactants in different ratios were tested until the more suitable combination able to solubilise artemisinin and quercetin and form a transparent and homogeneous nanoemulsion was found. Castor oil, Kolliphor® RH40 and soy lecithin were selected as main components of the lipid phase and combined in the appropriate ratio (1:1:0.4). This composition was able to load the highest amount of both artemisinin and quercetin (5 mg/mL), since using higher concentrations, the size of formed droplets significantly increased, and two separated phases were quickly detectable.

The morphology of the oil droplets was analysed by cryo-TEM (Figure 1). The analysis confirmed that the main particles of prepared nanoemulsions were oil droplets, which appeared as grey spheres not delimited by a bilayered membrane. Concurrently, they coexisted with small vesicles delimited by a single double layer composed by phosphatidylcholine molecules (indicated by arrows), suggesting the simultaneous presence of some lamellar vesicles.

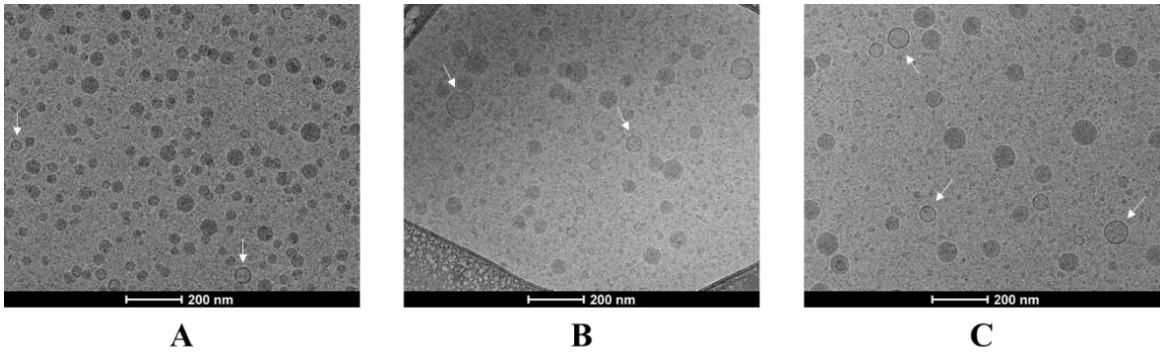

Figure 1. Representative cryo-TEM images of (A) artemisinin nanoemulsion; (B) quercetin nanoemulsion; (C) artemisinin-quercetin nanoemulsion.

Mean diameter, polydispersity index and zeta potential of oil droplets, were measured immediately after sonication and after 30 days of storage at 4 ± 1 °C. After preparation, the size of empty nanoemulsion (prepared without artemisinin and quercetin) was ~65 nm ($p>0.05$ versus other values), the polydispersity index was ~0.189 (indicating monodispersed samples) and the zeta potential was ~-45 mV ($p>0.05$ versus the zeta potential of droplets and vesicles of artemisinin nanoemulsion; $p<0.05$ versus other values). The addition of artemisinin or quercetin or even their combination did not bring changes in mean size and polydispersity index, only a slight decrease of the zeta potential was detected when quercetin was loaded alone or in association with artemisinin. Results corroborate the solubilization of bioactive molecules in the nanodroplets.

After 30 days, no changes regarding mean diameter (~65 nm, $p>0.05$ versus the starting values) and polydispersity index (~191, $p>0.05$ versus the starting values) were detected, confirming the good stability of the prepared nanoemulsions.

Table 4. Mean diameter (MD), polydispersity index (PI) and zeta potential (ZP) of empty nanoemulsion, artemisinin nanoemulsion, quercetin nanoemulsion and artemisinin-quercetin nanoemulsion. The same symbol (*, °) indicates values that are not statistically different ($p>0.05$).

Sample	MD (nm)	PI	ZP (mV)
Empty nanoemulsion	65* ± 2	0.189	-45 ± 1
Artemisinin nanoemulsion	62* ± 1	0.192	-42 ± 3
Quercetin nanoemulsion	58* ± 1	0.199	-51° ± 3
Artemisinin-quercetin nanoemulsion	60* ± 3	0.176	-49° ± 3

Table 5. Mean diameter (MD) and polydispersity index (PI) of nanoemulsions after 2 h incubation at pH 1.2 or 6 h incubation at pH 7.0. The symbol * indicates values that are not statistically different from those of nanoemulsions after preparation (Table 1; p>0.05)

Sample	**MD (nm)**		**PI**	
	2 h	**6 h**	**2 h**	**6 h**
	pH 1.2	**pH 7.0**	**pH 1.2**	**pH 7.0**
Artemisinin nanoemulsion	61* ± 2	63* ± 3	0.122	0.116
Quercetin nanoemulsion	57* ± 1	59* ± 1	0.104	0.115
Artemisinin-quercetin nanoemulsion	53* ± 4	56* ± 3	0.109	0.105

3.2. Stability at gastrointestinal pHs

At 2 h of incubation under high ionic strength and pH 1.2 or at 6 h and pH 7.0, the mean diameter and polydispersity index of the nanoemulsions tested, remained unvaried (p>0.05 versus the initial values reported in Table 1; p>0.05 versus the values at 2 h or 6 h), confirming their ability to keep the structure and the loaded molecules even under the harsh conditions of the gastrointestinal fluids (Table 2).

3.3. Cell viability assay

The biocompatibility of artemisinin or quercetin (alone or in combination) solubilized in dimethyl sulfoxide or loaded in nanoemulsions, was evaluated using Caco-2 and HUVEC cells (Figure 2). When Caco-2 cells were treated with 40 μg/mL of artemisinin solution, the viability was ~96% (p<0.05 versus the viability obtained using artemisinin solution at higher dilutions, or nanoemulsions at all dilutions). Using higher dilutions (20, 10, 5 and 2.5 μg/mL) of the same solution or all dilutions (40, 20, 10, 5 and 2.5 μg/mL) of artemisinin nanoemulsion, the viability increased up to ≈125% (p>0.05 among these values). Treating the same cells with 40 μg/mL of quercetin solution, the viability was the lowest, ~68% (p<0.05 versus viability of cells treated with other samples). Using higher dilutions of quercetin solution (20, 10, 5, 2.5 μg/mL) the cell viability increased up to ≈101% (p<0.05 versus viability of cells treated with 40 μg/ml of quercetin solution), while quercetin nanoemulsion at all the used dilutions (40, 20, 10, 5 and 2.5 μg/mL,) was highly biocompatible as the viability was ≈114% (p>0.05 among the viability of cells treated with the different dilutions). When caco-2 were treated with 40 μg/mL of artemisinin-quercetin nanoemulsion, the viability was quite high ~87% (p>0.05 versus viability of cells treated with 40 μg/mL of artemisinin solution or

nanoemulsion), and significantly increased up to ~112% using the highest dilution (2.5 μg/mL, $p<0.05$ versus viability of cells treated with 40 μg/mL of artemisinin-quercetin nanoemulsion).

The viability of HUVEC cells treated with all dilutions (40, 20, 10, 5 and 2.5 μg/mL of artemisinin solution, artemisinin nanoemulsion, and 20, 10, 5 and 2.5 μg/mL of quercetin solution, quercetin nanoemulsion and artemisinin-quercetin nanoemulsion was ≈100% ($p>0.05$ among the values), while using 40 μg/mL of artemisinin-quercetin nanoemulsion or quercetin nanoemulsion, cell viability was the lowest, ≈38% ($p>0.05$ between the two values).

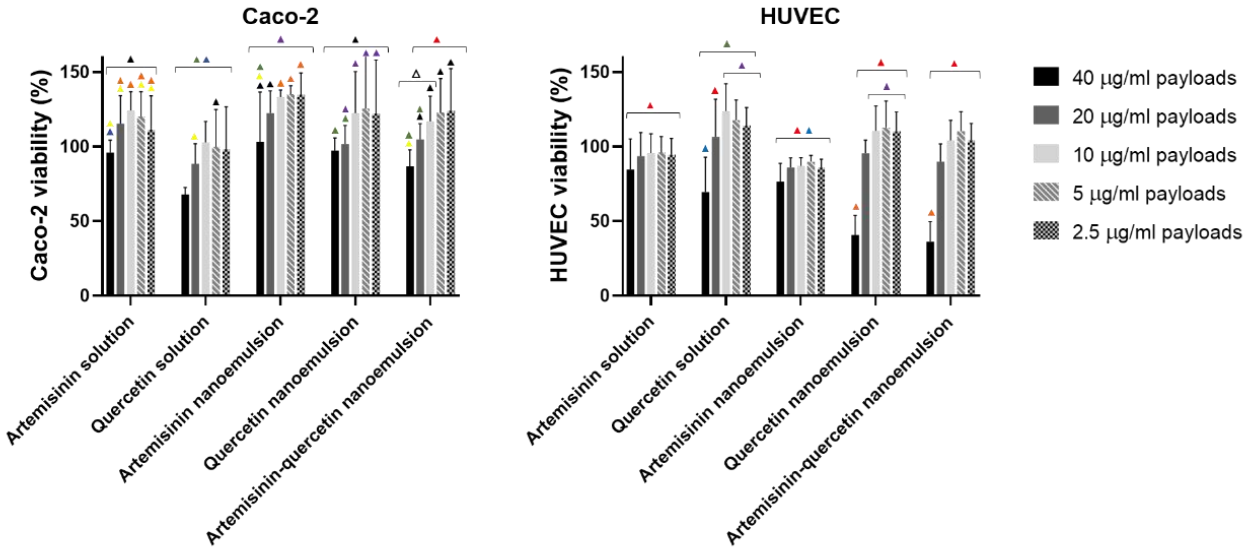

Figure 2. Viability (%) of Caco-2 (left panel) and HUVEC (right panel) cells, treated with artemisinin or quercetin in solution or loaded in nanoemulsions and properly diluted to reach 40, 20, 10, 5 and 2.5 μg/mL. Mean values (bars) ± standard deviations were reported (n=3). In each panel, the same colour indicates values that are not statistically different ($p>0.05$).

3.4. Growth inhibition assay

Growth inhibition assay of artemisinin or quercetin or their combination, in solutions and loaded in nanoemulsions of droplets and vesicles was evaluated against 3D7 strain of *P. falciparum* and the IC50 and IC90 were calculated (Table 3). The IC50 of artemisinin solution was ~0.019 μg/mL and the IC90 was ~0.065 μg/mL. The values did not statistically change following its loading in nanoemulsions as the IC50 was ~0.018 μg/mL ($p>0.05$ between the two IC50) and the IC90 was ~0.061 μg/mL ($p>0.05$ between the two IC90), suggesting that the efficacy of artemisinin as antimalarial drug was not affected by its loading in nanoemulsions. On the contrary, the IC50 and the IC90 of quercetin solution was higher if compared to that of artemisinin, as the IC50 was ~4.301

μg/mL ($p<0.05$ versus other IC50) and the IC90 ~17.847 μg/mL ($p<0.05$ versus other IC90), probably because of the lower specificity of quercetin against the parasite. Interestingly, the loading of quercetin in the nanoemulsions led to a decrease of IC50, that was not statistically different from that of artemisinin in solution or loaded in nanoemulsions, ~1.004 μg/mL ($p>0.05$ versus the IC50 of artemisinin solution or nanoemulsion). Similarly, the IC90 of quercetin nanoemulsion also decreased but in a lesser extent as it was still higher than that of artemisinin solution or nanoemulsion, ~4.545 μg/mL ($p<0.05$ versus the IC90 of artemisinin solution or nanoemulsion). The co-loading of quercetin and artemisinin did not modify the values obtained when artemisinin was tested alone, as the IC50 was ~0.009 μg/mL ($p>0.05$ versus the IC50 of artemisinin solution and artemisinin nanoemulsion) and the IC90 was ~0.041 μg/mL ($p>0.05$ versus the IC50 of artemisinin solution and artemisinin nanoemulsion). Probably, the antimalarial effect of quercetin was masked by that of artemisinin, which is well known to be one of the most potent drugs for the treatment of malaria infections.

Table 6. IC50 and IC90 (μg/mL) of artemisinin or quercetin in solution or loaded in nanoemulsions measured against 3D7 strain of *P. falciparum*. The same symbol (*, °) indicates values that are not statistically different ($p>0.05$).

Sample	**IC50 (μg/mL)**	**IC90 (μg/mL)**
Artemisinin solution	0.019* ± 0.002	0.065* ± 0.003
Quercetin solution	4.301° ± 0.078	17.847 ± 1.439
Artemisinin nanoemulsion	0.018* ± 0.012	0.061* ± 0.030
Quercetin nanoemulsion	1.004* ± 0.162	4.545° ± 0.136
Artemisinin-quercetin nanoemulsion	0.009* ± 0.001	0.041* ± 0.002

3.5. *In vivo* antimalarial assay

In vivo antimalarial efficacy of nanoemulsions was assessed through oral administration of formulations at two different concentrations (IC50 and IC90) on mice infected with *P. yoelii yoelii 17XL* (Figure 3). The survival of the infected and untreated control animals was 5 days. The treatment with the IC90 of artemisinin or quercetin solution enhanced the survival of animals until day 9, while their combination in solution achieved a reduced survival only up to day 6. The treatment with the IC50 and IC90 of artemisinin nanoemulsion and quercetin nanoemulsion addressed the death of animals at day 6 as well. Differently, the co-loading of artemisinin and quercetin in nanoemulsions led to an increased animal survival up to day 11, with one animal of each group alive at the end of the experiment (day 11), irrespective of the concentration tested. In particular, the animal treated with IC50 of artemisinin-quercetin nanoemulsion, at the end of the experiment, did not have any parasite

in the blood, suggesting a complete recovery from the infection. One month later, the same animal was reinfected with 2×10^7 red blood cells (100 µL) from *Plasmodium yoelii yoelii* 17XL-infected mice by intraperitoneal injection. The mouse did not have any malaria symptoms nor change in weight, temperature, or physical activity and parasitemia remained at 0% for three weeks, suggesting a possible immunization following the treatment.

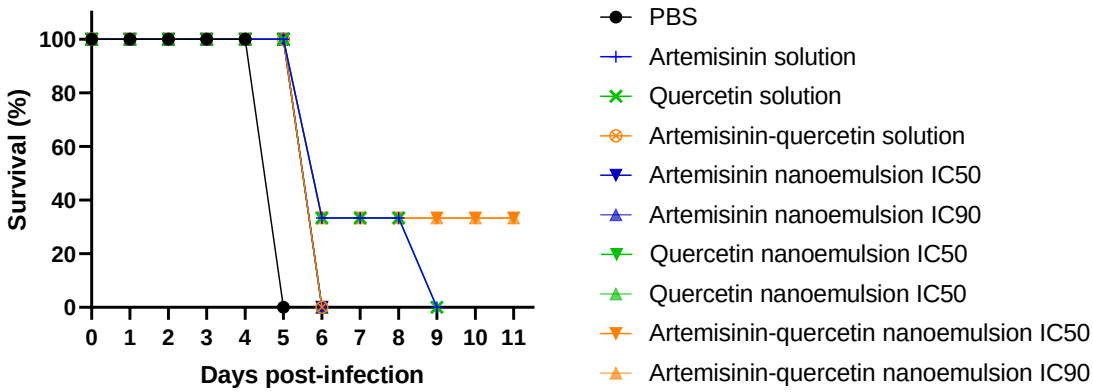

Figure 3. Kaplan-Meier plot for the *in vivo* assay of the effect of artemisinin, quercetin and their combination in solution or loaded in nanoemulsions orally administered on *P. yoelii yoelii*-infected mice.

4. Discussion

Quercetin (3,3′,4′,5,7-pentahydroxyflavone) is a natural flavonoid abundantly occurring in edible vegetables and fruits, and its daily intake is associated to several beneficial effects related to the antioxidant and anti-inflammatory activities [145]. It is also effective against a variety of viruses since it modulates the expression of inflammation mediators [146]. In particular, it is known to be able to inhibit glycogen synthase kinase-3β, an enzyme able to modulate the inflammatory response activated by pathogenic microorganisms [147]. This key activity permits the control of imbalance of cytokine production during the malaria infection, making quercetin a potential therapeutic for this pathology [148]. Indeed, the endogenous control of malaria infection and the appearance of symptoms depend on a delicate balance between inflammatory mediators and high levels of proinflammatory and anti-inflammatory cytokines, which differently affect the endogenous susceptibility to infection, clinical disease, and anaemia [149]. In this respect, quercetin contributes to decrease the malaria symptoms thus facilitating its remission thanks to the possible synergistic effect when combined with artemisinin, as confirmed by previous studies [150].

In the present study, it was disclosed that the co-loading of artemisinin and quercetin in nanoemulsions effectively increased the oral bioavailability and effectiveness of both phytochemicals. To effectively load artemisinin and quercetin, alone or in combination at high

concentrations, a preformulation study was performed testing different oils, surfactants, cosurfactants and different combinations of them, until a stable, transparent, homogeneous and nano-sized nanoemulsion was obtained [151]. The selection of castor oil, Kolliphor® RH40 as surfactants, and soy lecithin as cosurfactant was critical as it was important to load high amount of artemisinin and quercetin in stable systems [152]. Their combination in the selected amount, permitted the formation of nanometric, monodispersed and stable nanoemulsions, mainly formed by small oil droplets associated with some unilamellar vesicles, related to the soy lecithin, which was used as cosurfactant but in water spontaneously forms bilayered vesicles as well [153]. The mean diameter and polydispersity index of the prepared nanoemulsions did not undergo any significant variation, due to possible fusion phenomena, upon dilution and incubation for 2 h at pH 1.2 or 6 h at pH 7.0 and high ionic strength, disclosing their good stability in these solutions mimicking the harsh conditions of the gastro-intestinal tract, and their suitability for oral administration. All tested nanoemulsions were highly biocompatible against Caco-2 and HUVEC cells, especially at higher dilutions corresponding to the lower concentrations (10, 5, 2.5 μg/mL). The *in vitro* antimalarial activity was assessed using the same range of dilutions and the obtained results highlighted the key role played by the nanoemulsions in improving the quercetin efficacy, probably due its double loading in the oily core of droplets and in the bilayer of vesicles. Differently, the effect of artemisinin alone or artemisinin in association with quercetin was not significantly improved by the loading in nanosystems, indeed, the IC50 and IC90 were non statistically different from that of the artemisinin nanoemulsion and artemisinin-quercetin nanoemulsion and the effect of quercetin was masked by that of artemisinin, which is more effective against the parasite.

The optimal performances of the combined nanoemulsions were confirmed *in vivo*, especially when artemisinin and quercetin were co-loaded as this formulation increased animal survival up to day 11, ensured the complete recovery of one animal and even prevented its re-infection. On the contrary, the survival of animal treated with the association of artemisinin and quercetin in solution was only 6 days and those of animal treated with artemisinin in solution or quercetin in solution was 9 days. Results confirmed that only the co-loading of the two phytochemicals in nanoemulsions was effective against malaria infection and the effectiveness seem to be related to the simultaneous presence of two complementary phytochemicals and two delivery systems. The quercetin reinforced the effect of artemisinin but only when delivered in nanoemulsions probably because the oil nanodroplets acting as penetration enhancer increased its bioavailability and favoured its rapid onset while lamellar vesicles acting as carrier prolonged the bioavailability of both phytochemicals and the interaction with cells and parasites.

5. Conclusion

In this work, a biocompatible nanoemulsion loading artemisinin and quercetin was prepared using an easy and highly reproducible method. Overall, results suggest that, despite being only preliminary data, the simultaneous loading of artemisinin and quercetin in this nanoemulsion seems to be a promising system to simplify the therapeutic protocols of malaria and especially the oral treatment.

Chapter III

Improvement of oral therapy of malaria by designing an advanced natural adjuvant based on apigenin loaded in silica doped nutriosomes

Federica Fulgheri[1], Miriam Ramírez[2,3,4], Maria Letizia Manca[1*], Alessandra Scano[5], Guido Ennas[5], Francesca Marongiu[1], Ines Castangia[1], Matteo Aroffu[1], José Esteban Peris[6], Iris Usach[6], Xavier Fernàndez-Busquets[2,3,4], Maria Manconi[1]

[1]Dept. of Life and Environmental Sciences, University of Cagliari, University Campus, S.P. Monserrato-Sestu Km 0.700, Monserrato, 09042, CA, Italy

[2]Barcelona Institute for Global Health (ISGlobal), Hospital Clínic-Universitat de Barcelona, Rosselló 149-153, 08036 Barcelona, Spain

[3]Nanomalaria Group, Institute for Bioengineering of Catalonia (IBEC), The Barcelona Institute of Science and Technology, Baldiri Reixac 10-12, 08028 Barcelona, Spain

[4]Nanoscience and Nanotechnology Institute (IN2UB), University of Barcelona, Martí i Franquès 1, 08028 Barcelona, Spain

[5]Department of Chemical and Geological Sciences, University of Cagliari and INSTM Unit, SS 554 Bivio per Sestu, 09042 Monserrato, CA, Italy

[6]Department of Pharmacy and Pharmaceutical Technology and Parasitology, University of Valencia, 46100 Valencia, Spain

1. Introduction

2021 accounted for about 247 million cases and 619 000 deaths due to malaria infections, and most of them were reported in Africa [1]. The pathology is caused by unicellular protozoan parasites belonging to the genus Plasmodium. Only five Plasmodia cause malaria in humans: *Plasmodium falciparum (P. falciparum)*, *Plasmodium vivax*, *Plasmodium malariae*, *Plasmodium ovale* and *Plasmodium knowlesi* [154]. While the firsts only infect humans, the last, *Plasmodium knowlesi,* is a specific parasite of monkeys of southeast Asia that is transmitted by mosquitoes of the *Anopheles leucosphyrus* group also to humans [155]. The complex biology of *Plasmodium* and its remarkable genetic flexibility permits its adaptations to changed environmental conditions making the malaria vaccination more difficult than that against the viruses and bacteria, since it requires multiple stages of development in the human host, each stage expressing hundreds of unique antigens [156]. At the moment, a malaria vaccine has been developed but the pharmacological therapies remain crucial to avoid morbidity and mortality, especially in the endemic areas [157]. Unfortunately, drug treatment has faced set back due to the growing problem of resistance of the malarial parasites toward the conventional drugs. Currently, artemisinin-based combination therapy is the recommended treatment for malaria caused by *P. falciparum* and consists of the simultaneous administration of a fast-acting artemisinin derivative with a second antimalarial drug belonging to a different class [12,158]. A

partial resistance to artemisinin derivatives associated with partner drugs like lumefantrine, piperaquine or amodiaquine has recently emerged; this risk, combined with the poor health sector performances and lack of financial resources in endemic areas, makes eradication of the disease very hard [159]. Since the pathway to obtain new drugs could be very long and challenging, the improvement and simplification of current therapies along with the implementation and enhancement of the peripheral health service will be of paramount importance to control malaria and reduce morbidity and mortality [160]. To design alternative combination therapies, Bilia et al. reported that the antiplasmodial activities of quercetin, rutin, eriodictyol, eriodictyolchalcone and catechin is moderate at the tested concentrations but, considered their safety and abundance in nature, they can be considered potential adjuvants to safely improve the efficacy of artemisinin, indeed, when used in association significantly potentiate its antimalarial effect [150]. Fallatah et el. demonstrated that the *in vitro* inhibition of *P. falciparum* by artemisinin improved in the presence of 25 µM of apigenin, as the IC50 decreased from ~7.09 nM to ~2.8 nM. The antimalarial activity of apigenin seems to be related to a reduction of glutathione levels in erythrocytes, which in turn leads to an increase in reactive oxygen species, cause of cell death and stopping of parasite proliferation [161]. The association of artemisinin derivate with quercetin or luteolin co-loading in nanocarriers has been proposed as an advanced and economic strategy to improve the effectiveness of artemisinin [83]. However, to the best of our knowledge, the studies reporting the co-loading of artemisinin with other phytochemical in nanosystems are very limited. Just, Isacchi et al. co-loaded artemisinin with curcumin in liposomes, being curcumin an adjuvant to improve the efficacy of artemisinin [162]. The prepared formulation was more effective than free artemisinin in counteracting the parasitaemia *in vivo*. Actually, nanocarriers are successfully used to deliver artemisinin alone or in combination with other antimalarials. Fulgheri et al. simultaneously loaded artemisinin and curcumin or quercetin in nutriosomes to develop an oral drug for malaria treatment [163]. The formers are special phospholipid vesicles modified with Nutriose® FM06, a soluble non-viscous dietary fibre, which affect the arrangement of the vesicles, increasing their lamellarity, rigidity and stability, especially in the gastro-intestinal environmental [101,164]. Thank to these effects, nutriosomes are optimal delivery systems for oral administration of phytochemicals [165,166]. Considering their promising performances, they were also tested as oral formulation by Coma-Cros et al., which loaded curcumin in hyalurosomes or nutriosomes enriched with the anionic copolymer Eudragit® S100 [72]. They found that curcumin, when incorporated in eudragit-nutriosomes and orally administered, improved the survival of mice infected with *Plasmodium yoelii*. Similarly, recent findings underlined the potential of silica as additive to form a shell around phospholipid vesicles thus increasing the oral bioavailability [167]. The lipid bilayer of vesicles and the solid surface of inorganic material interacted by Van der Waals,

hydrophilic and hydrophobic forces [168]. Silica based nanomaterials seem to be ideal partners to be associated with liposomes due to their complementary properties: controllable porosity and high thermal resistance [169–172].

Taking into account these previous findings, in the present study nutriosomes, phospholipid vesicles tailored for oral administration, were combined with mesoporous silica to simultaneously load artemisinin and apigenin [173]. The prepared silica doped nutriosomes were fully characterized by evaluating the morphology and measuring average diameter, polydispersity index, zeta potential, entrapment efficiency, stability under storage and conditions mimicking the gastrointestinal environment, and release. The *in vitro* biocompatibility using Caco-2 cells and antimalarial efficacy on 3D7 strain of *P. falciparum* were tested.

2. Material and methods

2.1. Materials

Soy phosphatidylcholine (Lipoid S75, S75) was purchased from Lipoid GmbH (Ludwigshafen, Germany). Artemisinin was purchased from Biosynth Ltd (United Kingdom). Nutriose® FM06, a soluble dextrin obtained from maize, was gently provided by Roquette (Lestrem, France). Apigenin, fumed silica (99.8%), Cetyl Trimethyl Ammonium Bromide (CTAB, > 98%), ammonia solution (NH_3, 28–30%) and hydrochloric acid (HCl, 37%), were purchased from Sigma-Aldrich (Milan, Italy). Ethanol (96%) and methanol (> 99.8%) were purchased by J. T. Baker. Tetramethyl ammonium hydroxide (TMAOH) pentahydrate was purchased by Fluka. All the reagents were used as received without further purification. Water was purified through a Milli-Q system from Millipore (Milford, MA). All plastics and reagents for cells have been purchased from Sigma-Aldrich (Milan, Italy).

2.2. Synthesis of the mesoporous silica

MCM41 like mesoporous silica was prepared by using the liquid crystal templating method, according to a new composition set up [174]. In a typical preparation, cetyltrimethylammonium bromide (3.65 g) was dissolved in 18 mL of Milli-Q water. The obtained template solution was stirred and heated at 35 °C for 2 h until a clear solution was obtained, and then 1.3 mL of ammonia (28% water solution) was added. The resulting mixture was stirred for 30 min and then, mixed with a fumed silica dispersion (3.6 g of fumed silica, 6 mL of Milli-Q water and 7.1 mL of tetramethylammonium hydroxide 25%aqueous solution). After stirring, 1 h at 55 °C, a gel was obtained subsequently transferred into a Teflon-line stainless-steel autoclave and aged in the oven at 100 ° C for 96 h. An

aqueous solution of methanol (190 mL), water (8.0 mL) and hydrochloric acid (37%, 2 mL) was used to wash the obtained precipitate after cooling it to room temperature. The former was then dried in air for 12 h, separated by Soxhlet extraction (12 h) in ethanol and finally, dried in air for 12 h.

The obtainment of the ordered hexagonal pore arrangement typical of a MCM-41 material was verified by (i) x-ray powder diffraction (Seifert X3000 apparatus in the Bragg–Brentano geometry and monochromatized CuK_a radiation, performed at low angle range of 1–6 2J degrees with a step size of 0.025 2J degrees, collecting enough counts for each step to optimize the signal and noise ratio); (ii) transmission electron microscopy (Jeol JEM 1400 Plus, operating at 120 kV); (iii) nitrogen sorption (ASAP2020 apparatus operated at 77 K, calculating the specific surface area from the adsorption data by Brunauer-Emmett-Teller equation according to consistency criteria, and the total pore volume by the Barrett, Joyner, and Halenda method, considering the single point adsorption at $p/p_0 = 0.99$ [175].

2.3. Preparation and characterization of silica doped nutriosomes

A carbonate-bicarbonate buffer was prepared dissolving 1.43 g of sodium carbonate and 3.78 g of sodium bicarbonate in water, adjusting pH to 9 with hydrochloric acid or sodium hydroxide and adding water until 500 mL. Artemisinin, apigenin, mesoporous silica (5 mg/mL each) and Nutriose® FM06 (0, 300, 600 and 900 mg/mL) were dispersed in the buffer at pH 9 and the dispersion was sonicated (99 cycles, 5 s on and 3 s off, 13 μ of probe amplitude) with a high intensity ultrasonic disintegrator (Soniprep 150, MSE Crowley, London, UK). Phospholipid S75 (150 mg/mL) was finally added, and dispersions were sonicated one last time (10 cycles, 5 s on and 3 s off, 13 μ of probe amplitude) and silica doped liposomes (without Nutriose® FM06), silica doped 300nutriosomes (with 300 mg/mL of Nutriose® FM06), silica doped 600nutriosomes (with 600 mg/mL of Nutriose® FM06), and silica doped 900nutriosomes (with 900 mg/mL of Nutriose® FM06) were obtained.

Silica doped vesicles were observed using a cryogenic transmission electron microscope (cryo-TEM). A thin film of each sample was formed on a holey carbon grid and vitrified by plunging (kept at 100% humidity and room temperature) in ethane maintained at its melting point, using a Vitrobot (FEI Company, Eindhoven, The Netherlands). The vitreous films were transferred to a Tecnai F20 TEM (FEI Company) and the samples were observed in a low dose mode. Images were acquired at 200 kV at a temperature ~-173 °C, using low-dose imaging conditions.

Mean diameter and polydispersity index of vesicles were estimated by dynamic light-scattering measurements with a Zetasizer Ultra from Malvern Instruments (Worcestershire, UK). Samples were backscattered by a helium-neon laser (633 nm) at an angle of 173° and a constant temperature of 25 °C. Zeta potential was determined using the Zetasizer Ultra and analysing the data by the mixed mode

measurement-phase analysis light scattering (M3-PALS). Before the analysis, each sample was diluted 100-folds with Milli-Q water to be optically clear and avoid the attenuation of the laser beam by the particles along with the reduction of the scattered light that can be detected.

Silica doped vesicles were stored at 4 °C and their mean diameter, polydispersity index and zeta potential were measured every month until there were no visible changes, like phase separation. Silica doped nutriosomes were frozen at -80 °C and freeze-dried for 48 h, at -80 °C and 0.08 mbar, using a FDU-8606 freeze-dryer (Operon, Gimpo, South Korea). Freeze-dried samples were then rehydrated with Milli-Q water up to the initial volume (2 mL) by manually shaking.

Unentrapped phytochemicals were removed by dialysis using water (2 L) as dialysing medium. Each dispersion (1 mL) was transferred to a Spectra/Por® dialysis tube (12-14 kDa MW cut-off, 3 nm pore size; Spectrum Laboratories Inc., DG Breda, The Netherlands). The purification process was carried out for 2 h at 25 °C under constant stirring, refreshing the medium after 1 h, aiming at ensuring the complete removal of unentrapped molecules. The entrapment efficiency of payloads was calculated as the percentage of their concentration found after dialysis versus that initially measured.

Apigenin quantification was carried out measuring absorbance at 340 nm through a microplate reader (Synergy 4, BioTEK). Artemisinin quantification was performed using an ultra-performance liquid chromatograph (UPLC, ACQUITY H-class Plus system, Waters Corporation, Milan, Italy) equipped with a UV photodiode array detector and a C18 reverse-phase column (Waters Corporation, 1.7 mm, 2.1 mm x 50 mm). Analysis was carried out at 25 °C, at 216 nm, with water and acetonitrile (40:60 v/v) as a mobile phase eluted at 1 mL/min and with an injection volume of 25 µL. Stock solution (5 mg/mL) of artemisinin was prepared using the mobile phase as solvent. From these, other working solutions at different concentrations (from 5 to 500 µg/mL) were prepared by dilution. The calibration curve was obtained plotting peak areas versus concentrations. The regression analysis gave a correlation coefficient value (R^2) of 1.

2.4. Behaviour of silica doped nutriosomes at gastrointestinal pH

A solution at pH 1.2 and high ionic strength was prepared dissolving 1.75 g of sodium chloride in 94 mL of bi-distilled water and adding hydrochloric acid (0.1 M) up to 100 mL. A solution at pH 7.0 and high ionic strength was prepared dissolving 0.726 g of disodium hydrogen phosphate, 0.356 g of sodium dihydrogen phosphate and 1.754 g of sodium chloride in Milli-Q water and bringing the volume up to 100 mL. The pH was adjusted to 7.0 with a diluted solution of phosphoric acid. Silica doped nutriosomes were diluted 100-folds with the solution at pH 1.2 and incubated for 2 h or diluted 100-folds with the solution at pH 7.0 and incubated 6 h. At the end of the incubation, mean diameter, polydispersity index and zeta potential of samples were measured at 37 °C.

2.5. *In vitro* release of phytochemicals from silica doped nutriosomes

The *in vitro* release profile of artemisinin and apigenin in dispersion or loaded silica doped vesicles was measured. Artemisinin and apigenin were dispersed in a mixture of water and ethanol (50/50 v/v, 10 mg/mL each). A Spectra/Por® dialysis membrane (12-14 kDa MW cut-off, 3 nm pore size; Spectrum Laboratories Inc) was placed between the donor and receptor compartments of Franz cells. 100 µL of each sample (artemisinin dispersion, apigenin dispersion, artemisinin and apigenin loaded in silica doped 300nutriosomes, silica doped 600nutriosomes and silica doped 900nutriosomes) were placed on the donor compartment while the receptor compartment was filled with PBS (5 mL) and kept at 37 °C and 350 rpm. Every 12 h and up to 48 h, the receptor compartment's solution was replaced with an equal volume of a fresh solution. At the end of the experiment (24 h or 48 h), the dialysis membrane was washed with 2 mL of methanol to recover the total amount of phytochemicals and to break the vesicles and release the payload still entrapped. Subsequently, the content of artemisinin at 216 nm using the UPLC and that of apigenin was analysed at 340 nm using a plate reader.

2.6. Biocompatibility of silica doped nutriosomes

The human epithelial cells (Caco-2) were cultured in high glucose Dulbecco's Modified Eagle's Medium, supplemented with 10% of foetal bovine serum and 1% of penicillin and streptomycin (10000 cells/well) and subcultured every two days. For the biocompatibility assay, Caco-2 (10000 cells/well) were plated in 96-well plates and grown at 37 °C in 5% carbon dioxide. After 24 h, the medium was substituted with medium containing the samples at different dilutions (1:25, 1:50, 1:250 and 1:500). Apigenin and artemisinin, alone or in association, solubilized in dimethyl sulfoxide (5 mg/mL), and artemisinin and apigenin-loaded silica doped nutriosomes were tested. After 48 h incubation, medium was substituted with a solution of methyl thiazolyl tetrazolium (MTT, 0.5 mg/mL), which was removed 3 h later, replaced with dimethyl sulfoxide, and the absorbance of the solubilized dye was read at 570 nm with a microplate reader. The viability was calculated as percentage of living cells in comparison to the untreated control cells (100% viability).

2.7. *In vitro* inhibition of P. falciparum growth addressed by silica doped nutriosomes

The antimalarial efficacy of formulations was assessed through an *in vitro* growth inhibition assay using the 3D7 strain of *P. falciparum*, cultured in human B+ erythrocytes at 37 °C under a gas mixture of 92.5% nitrogen, 5.5% carbon dioxide, and 2% oxygen, using complete Roswell Park Memorial Institute (RPMI) 1640 medium (supplemented with 2 mM l-glutamine, 50 µM hypoxanthine, 5 g/l

Albumax II, 25 mM HEPES, pH 7.2). For the assay, culture was synchronized at ring stage using sorbitol at 5%, parasitaemia adjusted to 1% and haematocrit to 4%, and plated in 96-well plates with 75 µL of the artemisinin or apigenin in solution or loaded silica doped nutriosomes at different concentrations obtained by serial 1:2 dilutions (apigenin and artemisinin ranging from 0.500 to 0.002 µg/mL). Plates were incubated for 48 h and the percentage of parasitaemia was calculated as the value found in erythrocytes treated with formulations compared to that of untreated control erythrocytes. The IC50 and IC90 values of tested samples were calculated through sigmoidal fitting of growth data at different drug concentrations, analysed with the GraphPad Prism 8 software (GraphPad Software, San Diego, CA, USA).

2.8. *In vivo* antimalarial efficacy of silica doped nutriosomes

The *in vivo* antimalarial activity of artemisinin solubilized in dimethyl sulfoxide (5 mg/mL) or apigenin loaded in silica doped nutriosomes was assessed using a 4-day blood suppressive test as described previously. Briefly, BALB/c mice (three animals per group) were inoculated with 2×10^7 red blood cells (100 mL) from *Plasmodium yoelii yoelii* 17XL-infected mice by intraperitoneal injection. Artemisinin in solution or apigenin loaded in silica doped nutriosomes was diluted in PBS at pH 7.4 to obtain the IC50 and IC90 previously obtained by *in vitro* growth inhibition assay on *P. falciparum* (Table 3). At 4 h (day 0), 28 h (day 1), 52 h (day 2), 76 h (day 3) from the inoculation, 100 mL of each sample, or PBS as a control, were orally administered to the mice. Each day for 8 days, Giemsa-stained blood smears were used to monitor the parasitaemia.

2.9. Ethical issues

The human blood used in this work was from voluntary donors and commercially obtained from the Banc de Sang i Teixits (www.bancsang.net). Blood was not collected specifically for this research; the purchased units had been discarded for transfusion, usually because of an excess of blood relative to anticoagulant solution. Prior to their use, blood units underwent the analytical checks specified in the current legislation. Before being delivered, unit data were anonymized and irreversibly dissociated, and any identification tag or label had been removed in order to guarantee the non-identification of the blood donor. No blood data were or will be supplied, in accordance with the current Spanish Ley Orgánica de Protección de Datos and Ley de Investigación Biomédica. The blood samples will not be used for studies other than those made explicit in this research.

Mice (18–20 g) were maintained under standard environmental conditions: 20–24 °C and 12/12 h light/dark cycle, with ad libitum access to a semi-solid diet and water during the duration of the experiments. In the presence of toxic effects including, among others, >20% reduction in animal

weight, aggressive and unexpected animal behaviour or the presence of blood in faeces, animals were immediately anesthetized using a 100 mg/kg Ketolar plus 5 mg/kg Midazolan mixture and sacrificed by cervical dislocation. The animal care and protocols followed adhered to the specific national and international guidelines specified in the Spanish Royal Decree 53/2013, which is based on the European regulation 2010/63/UE. The studies reported here were performed under protocols reviewed and approved by the Ethical Committee on Clinical Research from the Hospital Clínic de Barcelona (Reg. HCB/2018/1223, January 23, 2019).

2.10. Statistical analysis of data

Results are expressed as the means ± standard deviations. Multiple comparisons of means (ANOVA) were used to substantiate statistical differences between groups, while Student's t-test was used to compare two samples. Significance was tested at the 0.05 level of probability (p). Data analysis was carried out with the software package XLStatistic for Excel.

3. Results

3.1. Physico-chemical characterization of the mesoporous silica

X-ray powder diffraction pattern had the reflection hkl lines (100, 110 and 200), typical of a MCM41 like material (Figure 1A). The first diffraction peak at 2.17 2J degrees related to the (100) plane is due to a long-range order of the hexagonal lattice symmetry. The higher angle signals from (110) and (200) Bragg peaks confirm the presence of the symmetrical hexagonal pore structure [176,177]. The formation of an ordered porous structure was also confirmed by the TEM images (Figure 1B) and the N_2 sorption analysis. In fact, the sample had a characteristic IV type N_2 sorption isotherm typical of an ordered MCM-41 material. A sharp mesopore filling step in the range 0.35–0.40 relative pressure (p/p0) was observed (Figure 1C) [178]. A high surface area value (798 m^2/g), a quite high pore volume (0.76 cm^3/g) with an average pore diameter of 3.79 nm, were observed (Figure 1C).

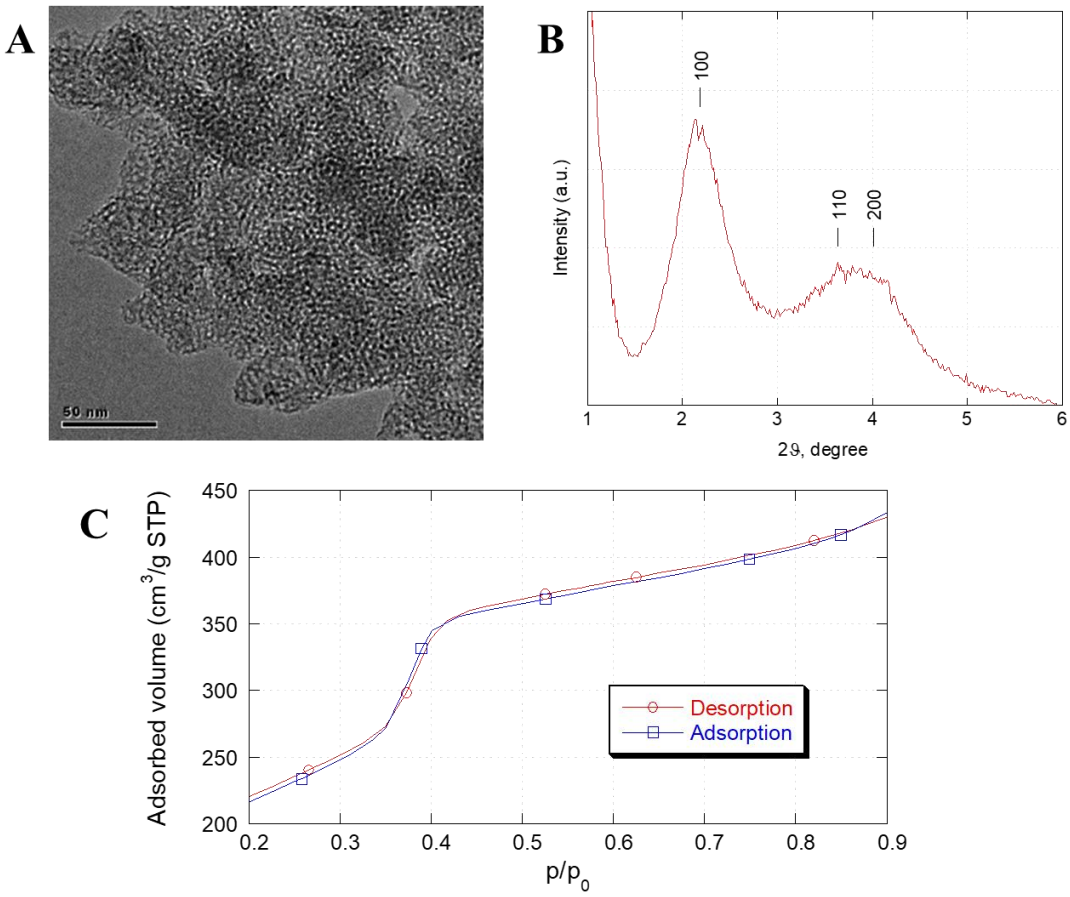

Figure 1. Transmission electron micrograph (A), low angle -X-ray powder diffraction pattern (B) and isotherm plot and pore size distribution (C) of the MCM41 like mesoporous silica.

3.2. Preparation and characterization of silica doped nutriosomes

The silica doped nutriosomes were prepared using 150 mg/mL of phospholipid, Nutriose® FM06 at increasing concentrations (0, 150, 300, 450, 600, 750, 900 mg/mL) and 5 mg/mL of silica. It was not possible to use higher amount of the former since the obtained dispersions were not stable and a precipitate appeared quickly [101]. The simultaneous loading of artemisinin and apigenin in the vesicle bilayer was very hard, since the payloads, especially apigenin, precipitated after the preparation of dispersions (Figure 2). In order to achieve the most suitable formulation, a preformulation study was performed using different concentrations of the components and hydrating solutions that permitted their simultaneous loading in the vesicles. Only using the carbonate-bicarbonate buffer solution at pH 9 as hydrating medium, apigenin was finally loaded in association with artemisinin (5 mg/mL each).

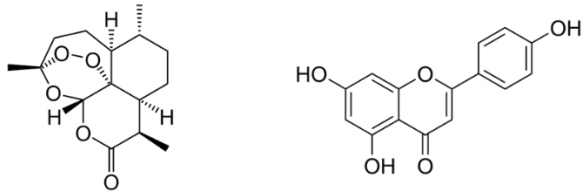

Figure 2. Chemical structure of artemisinin and apigenin.

The formation and morphology of the silica doped nutriosomes was firstly confirmed using a cryo-TEM (Figure 3). In all the dispersions, bilayered vesicles formed by the phospholipid were observed while mesoporous silica was not visible due to its very low concentration. The silica doped liposomes, 300nutriosomes and 600nutriosomes were mostly unilamellar or sometimes bilamellar, while using the highest concentration of Nutriose® FM06 (900nutriosomes) oligolamellar and multicompartment vesicles were formed, as previously reported for other modified phospholipid vesicles [143].

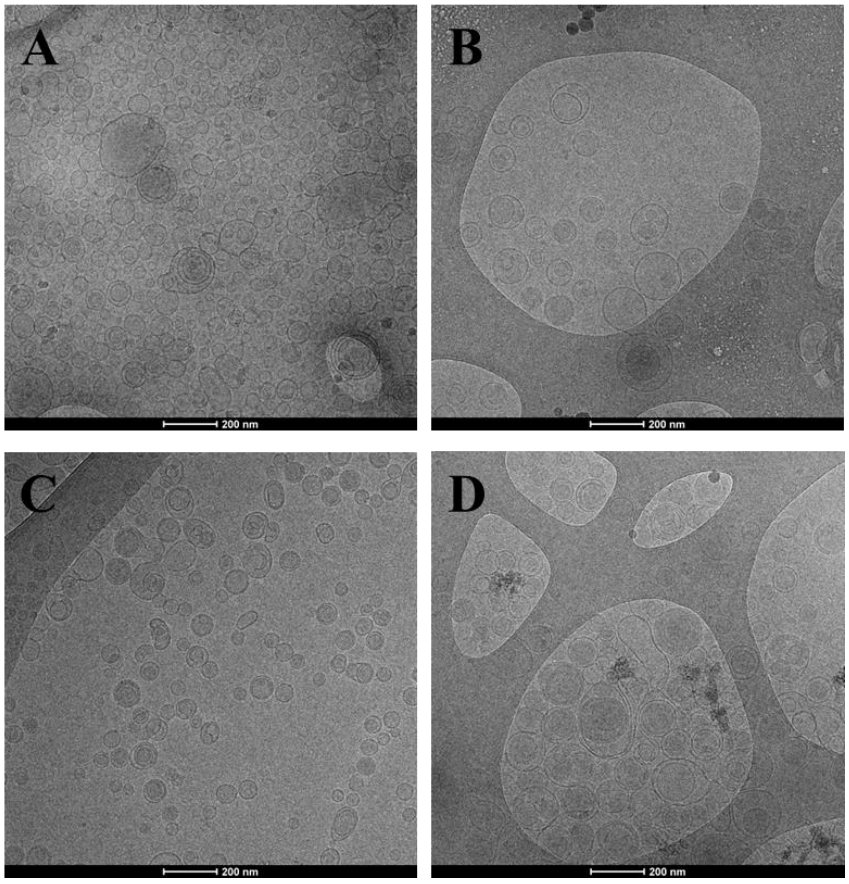

Figure 3. Representative cryo-TEM images of silica doped liposomes (A), silica doped 300nutriosomes (B), silica doped 600nutriosomes (C) and silica doped 900nutriosomes (D).

The mean diameter, polydispersity index and zeta potential of prepared silica doped nutriosomes were measured confirming their nanometric size (Table 1). The mean diameter of silica doped liposomes was the highest, ~183 nm ($p<0.05$ versus the values of other samples) and the polydispersity index as well (0.452). The addition of Nutriose® FM06 facilitated the assembling in nanometric particles as the mean diameter of silica doped 300nutriosomes was ~118 nm ($p<0.05$ versus the values of other samples) and the polydispersity index was 0.278 and those of silica doped 600nutriosomes and silica doped 900nutriosomes was ~135 nm ($p>0.05$ between the two values) and the polydispersity index was ~0.148.

Table 1. Mean diameter (MD), polydispersity index (PI), zeta potential (ZP) and apigenin entrapment efficiency of silica doped liposomes, 300nutriosomes, 600nutriosomes and 900nutriosomes. Mean values ± standard deviations (n = at least 3) are reported. The same symbol (°, ”, $^{\#}$, $^{\$}$) indicates values that are not statistically different each other ($p>0.05$) and are statistically different from values indicated with different symbols.

Sample	MD (nm)	PI	ZP (mV)	EE (%) Apigenin
Liposomes	183” ± 11	0.452	-51$^{\#}$ ± 2	
300nutriosomes	118 ± 10	0.278	-50$^{\#}$ ± 2	29$^{\$}$ ± 5
600nutriosomes	130° ± 14	0.163	-49$^{\#}$ ± 3	34$^{\$}$ ± 17
900nutriosomes	141° ± 2	0.133	-52$^{\#}$ ± 4	43$^{\$}$ ± 8

The apigenin entrapment efficiency of all the silica doped vesicles was ~35% ($p>0.05$ among the values) irrespective to the used composition while the artemisinin content of nutriosomes prepared at pH 9 was very low, ~0.6 mg/mL, due to its degradation at this pH as previous reported for its *in vivo* analogue dihydroartemisinin [179]. Indeed, basic pH caused the reduction of artemisinin and the formation of nonperoxidic analogues like deoxyartemisinin [180]. To confirm the result, a stability study of artemisinin was performed diluting it in the buffer solution at pH 9 and measuring the concentration at time 0, 30 min and 1 h (Figure 4). The peak of artemisinin appeared at = 7.26 min and decreased as a function of the time; simultaneously new small peaks were observed at 2.48, 4.62 and 6.23 min related to the formation of degradation products.

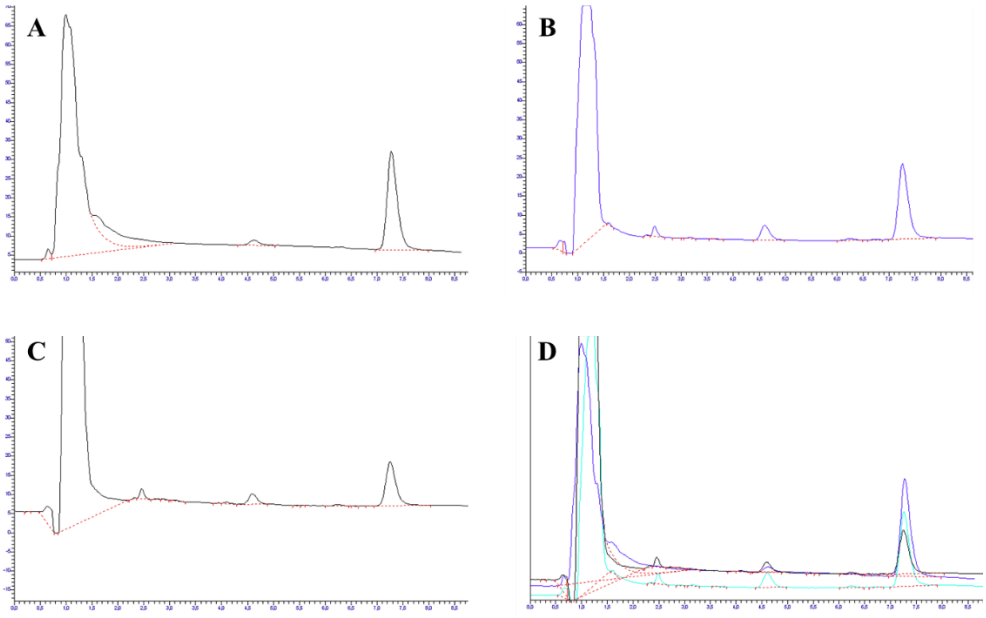

Figure 4. Representative chromatograms of artemisinin diluted in carbonate-bicarbonate buffer solution at pH 9 at time 0, after 30 min, after 1 h.

To evaluate the stability on storage of prepared silica doped vesicles, the mean diameter, polydispersity index and zeta potential were measured (Figure 5). Liposomes were not stable during storage, at 1 month their diameter increased up to ~375 ($p>0.05$ versus the value at 2 months), at 3 months was ~622 nm ($p<0.05$ versus the values at 1 and 2 months), and at 3 months the dispersion underwent phase separation, and a precipitate was observed. The size of 300nutriosomes increased less than the former but at 3 months was also separated denoting a poor stability. 600nutriosomes and 900nutriosomes were the most stable as the mean diameter of 600nutriosomes remained unchanged during the first 4 months (~139 nm; $p>0.05$ between the values at 0, 1, 2, 3, and 4 months), and slightly increased in the next 4 months, up to ~178 nm ($p>0.05$ between the values at 5, 6, 7, and 8 months; $p<0.05$ versus the values at 0, 1, 2, 3, and 4 months); the mean diameter of 900nutriosomes remained stable over 8 months, ~144 nm ($p>0.05$ between the values at different times).

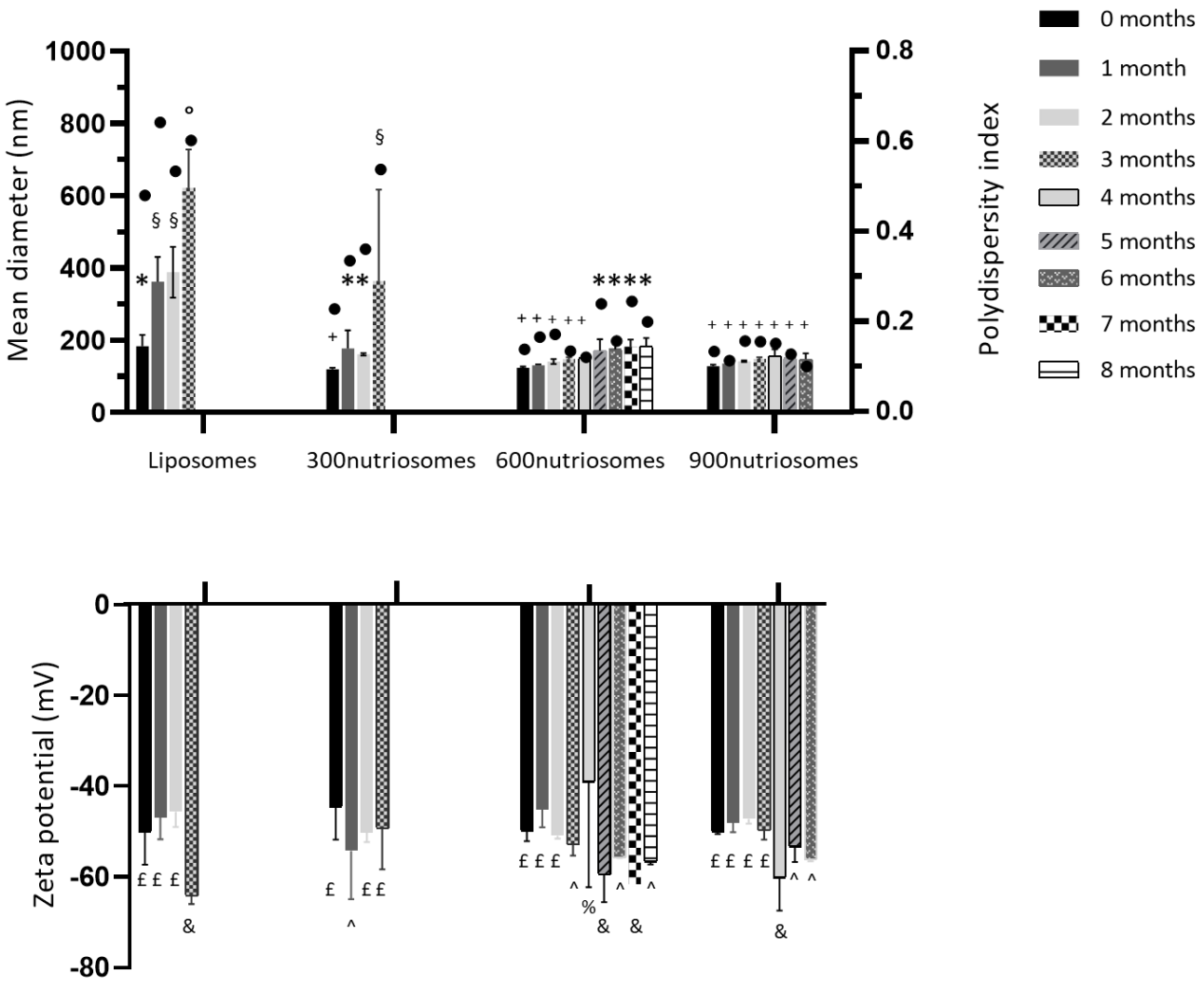

Figure 5. Mean diameter, polydispersity index and zeta potential of silica doped liposomes, 300nutriosomes, 600nutriosomes and 900nutriosomes stored over a period of 8 months at 25 °C. Mean values (bars) ± standard deviations were reported (n = 3). The same symbols (*, §, °, +, £, &, ^ and %), indicate values that are not statistically different each other (p>0.05) and are statistically different from values indicated with different symbols.

Considering the low stability of silica doped liposomes, further studies were performed using only nutriosomes. To ensure a better stability, vesicle dispersions were freeze-dried and re-hydrated. After re-hydration the size of 300nutriosomes increased from ~118 to ~185 nm ($p<0.05$ between the two values) those of 600nutriosomes and 900nutriosomes did not undergo a statistically significant enlargement, the first increased from ~130 to ~150 nm ($p>0.05$ between the two values) and the second from ~141 to ~161 nm ($p>0.05$ between the two values). Probably the higher concentration of Nutriose® FM06 was enough to avoid the break of the vesicles during the freeze-drying. In none of the samples the zeta potential changed significantly after re-hydration.

Table 2. Mean diameter (MD), polydispersity index (PI) and zeta potential (ZP) of silica doped 300nutriosomes, 600nutriosomes and 900nutriosomes after freeze-drying and re-hydration. Mean values ± standard deviations obtained from at least 3 samples are reported. The same symbols (§, $^{\#}$) indicate values that are not statistically different each other ($p>0.05$) and are statistically different from values indicated with different symbols.

Sample	MD (nm)	PI	ZP (mV)
300nutriosomes	185 ± 7	0.322	$-55^{\#@}$ ± 8
600nutriosomes	$150^{\S}$ ± 3	0.187	$-59^{\#@}$ ± 5
900nutriosomes	$161^{\S}$ ± 7	0.203	$-61^{@}$ ± 1

3.2. Stability of silica doped nutriosomes at pH 1.2 and 7.0

At 2 h of incubation at pH 1.2, the mean diameter of 300nutriosomes increased up to ~153 nm, that of 600nutriosomes up to ~155 nm and that of 900nutriosomes up to ~136 nm ($p<0.05$ between the value at 2 h and that of the corresponding fresh sample). At 6 h of incubation at pH 7.0, the mean diameter of 300nutriosomes and 600nutriosomes increased up to ~153 ($p<0.05$ between the value at 2 h and that of the corresponding fresh sample), while size of 900 nutriosomes did not change statistically (~144 nm, $p>0.05$ between value at 2 h and that of the corresponding fresh sample). The results confirmed the key role played by Nutriose® FM06 in ensuring vesicle stability also at acidic pH.

Table 3. Mean diameter (MD), polydispersity index (PI) and zeta potential (ZP) of 300nutriosomes, 600nutriosomes and 900nutriosomes incubated for 2 h at pH 1.2 or 6 h at pH 7.0. Mean values ± standard deviations are reported (n = 3. The same symbols (°, $^{\#}$, $^{@}$) indicate values that are not statistically different each other ($p>0.05$) and are statistically different from values indicated with different symbols.

Sample	Time	MD (nm)		PI		ZP (mV)	
		pH 1.2	pH 7	pH 1.2	pH 7	pH 1.2	pH 7
300nutriosomes	$t_{2h/6h}$	153° ± 8	148° ± 9	0.273	0.297	$1^{\#}$ ± 2	$-7^{@}$ ± 2
600nutriosomes	$t_{2h/6h}$	155° ± 9	159° ± 26	0.243	0.232	$2^{\#}$ ± 1	$-7^{@}$ ± 1
900nutriosomes	$t_{2h/6h}$	136° ± 3	144° ± 15	0.139	0.178	$2^{\#}$ ± 2	$-7^{@}$ ± 1

3.3. *In vitro* release assay

The apigenin release from nutriosomes was measured at pH 7.0 while it was not possible to measure that of artemisinin due to its almost complete degradation, ~88%. The release of apigenin and artemisinin dispersed in PBS at pH 7.4 was used as reference, indeed at this pH the artemisinin was stable and could be quantify. Using the artemisinin dispersion, the drug was completely released (~99%) at 48 h and almost completely at 24 (~82%, $p<0.05$ between the two values), confirming the suitability of the used experimental conditions. Release of apigenin in dispersion was similar, as the percentage at 24 was ~80% and at 48 h was ~100% ($p<0.05$ between the values). The release of apigenin from nutriosomes was comparable to that from dispersion: at 24 h ~88% ($p>0.05$ versus the apigenin release from dispersion at 24 h) and at 48 h ~93% ($p>0.05$ versus the apigenin release from dispersion at 48 h). The amount of apigenin released from 600nutriosomes was slightly lower than that released from the dispersion but not statistically different. Only using 900nutriosomes the apigenin released was statistically lower than that released using the dispersion: ~69% at 24 h and 88% at 48 h ($p<0.05$ versus the apigenin released using the dispersion). Once more results corroborate the role of Nutriose® FM06 in the performances of silica doped nutriosomes.

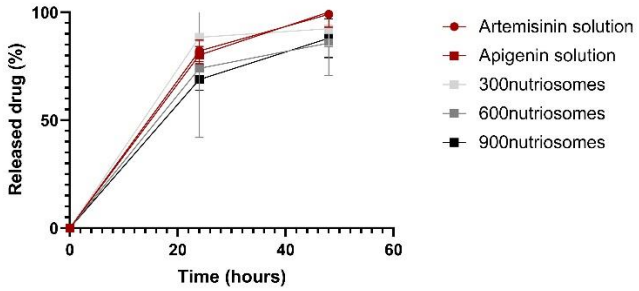

Figure 6. Artemisinin and apigenin released (%) at 24 h and 48 h through a dialysis membrane filled with their aqueous dispersions or vesicle dispersions. Mean values ± standard deviations are reported (n = 3).

3.4. Cell viability assay

Before evaluating the formulation efficacy against *Plasmodium*, their biocompatibility was screened using Caco-2 cells as model of intestinal epithelium, which they meet after oral administration. Formulations were used at 4 different dilutions. The viability of cells incubated with artemisinin in solution, regardless of the concentration used, was ≈110% ($p>0.05$ among the values obtained using different dilutions). The viability of cells incubated with apigenin or artemisinin and apigenin in solution was dilution depending: at the lowest dilution (1:25) was the lowest, ≈57% ($p<0.05$ versus the viability obtained using higher dilutions of the same samples and all the dilutions of other

samples), using higher dilutions (1:50, 1:250) it increased up to ≈82% ($p<0.05$ versus the viability obtained using 1:50 and 1:250 of apigenin or artemisinin and apigenin solution; $p<0.05$ versus the viability obtained using all the dilutions of other samples) and further increased (≈105%) using the highest dilution (1:500). Incubating the cells with artemisinin and apigenin loaded nutriosomes (600nutriosomes), the cell viability was ≈112%, irrespective of the used dilution ($p>0.05$ among the viability measured using different dilutions).

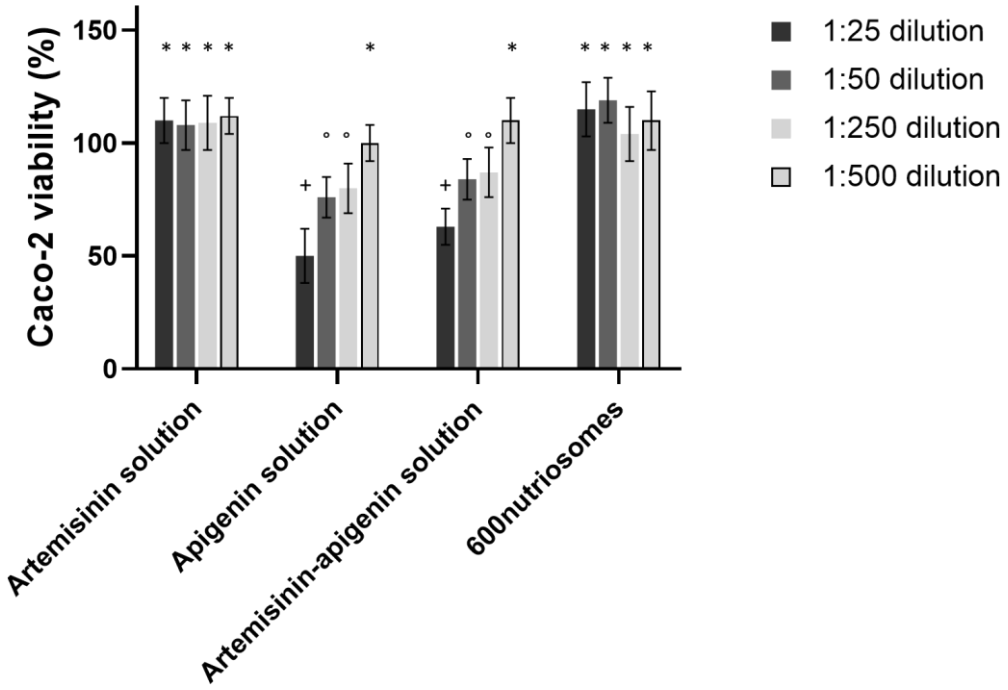

Figure 7. Viability of Caco-2 cells, incubated with artemisinin solution, apigenin solution, artemisinin and apigenin solution, 600nutriosomes at different dilutions (1:25, 1:50, 1:250 and 1:500). Mean values (bars) ± standard deviations are reported. The same symbols (*, +, °) indicate values that are not statistically different each other ($p>0.05$) and are statistically different from values indicated with different symbols.

3.5. *In vitro P. falciparum* growth inhibition assay

Considering the biocompatibility of artemisinin and apigenin loaded silica doped 600nutriosomes at all the tested dilutions, the *in vitro* ability to inhibit the growth of *P. falciparum* was evaluated using different concentrations ranging from 0.500 to 0.002 µg/mL of apigenin and artemisinin. The measured IC50 of artemisinin in solution was ~0.019 µg/mL and that of apigenin was the highest ~4.129 µg/mL ($p>0.05$ between the two values), however the value was not statistically different from that of artemisinin solution. When the two phytochemicals were loaded in silica doped

300nutriosomes the IC50 was~0.031 µg/mL, that of 600 nutriosomes was ~0.106 µg/mL and that of 900nutriosomes was ~0.035 µg/mL, then the values were comparable and not statistically different versus the IC50 of artemisinin solution ($p>0.05$ among all the IC50 values). The IC90 had a similar behavior, the value of apigenin solution was the highest but it was statistically different versus the other one.

Table 4. IC50 and IC90 (µg/mL) of artemisinin and apigenin in solution or loaded in silica doped nutriosomes against *in vitro P. falciparum* 3D7 cultures. Mean values ± standard deviations are reported (n = 3). The same symbol (*) indicate values that are not statistically different each other ($p>0.05$) and are statistically different from values indicated with different symbols.

Samples	IC50 (µg/mL)	IC90 (µg/mL)
Artemisinin solution	0.019* ± 0.002	0.065* ± 0.003
Apigenin solution	4.129* ± 4.507	24.611 ± 12.875
300nutriosomes	0.031*± 0.002	0.117* ± 0.008
600nutriosomes	0.106* ± 0.025	0.847* ± 0.377
900nutriosomes	0.035* ± 0.005	0.153* ± 0.003

3.6. *In vivo* antimalarial efficacy

The *in vivo* antimalarial efficacy of silica doped nutriosomes was tested as a function of the survival period of animals. Considering that nutriosomes prepared with different concentrations of Nutriose® FM06 had comparable physico-chemical properties and IC50, but 600nutriosomes and 900nutriosomes were more stable than 300nutriosomes, only 600nutriosomes were selected to be used for *in vivo* study thus reducing the number of animals. For the same reason, only artemisinin solution was used as reference drug since the IC50 and IC90 of apigenin in solution was very high and not comparable to that of artemisinin solution and nutriosomes. Control animals (infected and untreated) survived until day 5, while those treated with artemisinin solution had the highest survival up to the day 9. The animals treated with IC50 of 600nutriosomes survived up to day 6, more than the control. The animal survival increased up to day 8 when 600nutriosomes were used at IC90, being the dose higher, ~0.106 µg/mL versus ~0.847 µg/mL.

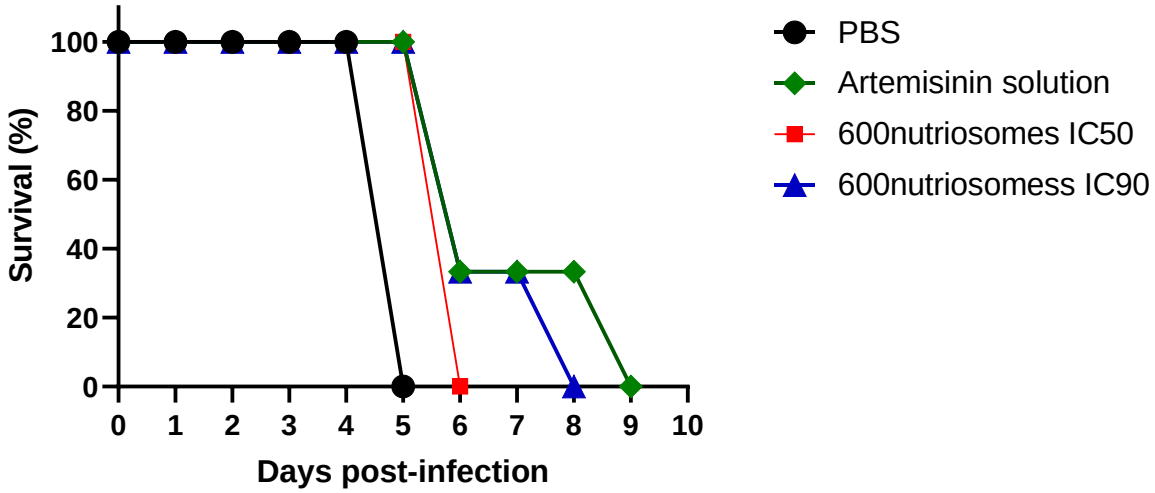

Figure 8. Survival of animals (%) at different post-infection days, untreated (control) or treated with artemisinin solution and 600nutriosomes orally administered at IC50 and IC90 on *P. yoelii yoelii*-infected mice.

4. Discussion

During the preformulation study (data not shown), different concentrations of phospholipid, Nutriose® FM06, artemisinin, apigenin and mesoporous silica were used to select the most stable and homogeneous formulation. Using water or phosphate buffer at pH 7.4 as hydrating medium, all the obtained dispersions quickly separated forming a precipitate. Vesicles loading only artemisinin and only apigenin were prepared and it was found that artemisinin was stably loaded while apigenin always precipitated. The co-loading of artemisinin and apigenin in stable and homogeneous dispersions was allowed only when a carbonate-bicarbonate buffer at pH 9 was used and the preparation was performed in two steps. Firstly, the homogenous dispersion of artemisinin, apigenin, mesoporous silica (5 mg/mL of each) and Nutriose® FM06 (at increasing concentrations) by sonication was performed. It was followed by the addition of phospholipid S75 (150 mg/mL) and a further sonication. In this way and using these concentrations of components the two phytochemicals seemed to be stably loaded. Unfortunately, the used buffer at pH 9 facilitated the loading of apigenin (avoiding its precipitation) but caused a rapid degradation of artemisinin, as its concentration was reduced up to ~0.6 mg/mL. Indeed, artemisinin is a sesquiterpene lactone containing an unusual endoperoxide bridge that makes it unique for malaria effect but susceptible to the external environmental since the lactone ring undergoes electrochemical reduction at high temperatures and basic pH [180]. The derivatives formed upon thermal or chemical degradation have identical structure but lack the peroxide bond, which is responsible of the antimalarial effect thanks to its peculiar

structure [181]. The endoperoxide bridge generates free radicals through iron-mediated catalysis, which reacts with or incapacitates target proteins, thus killing the *Plasmodium* parasite [182].

Anyway, the prepared silica doped nutriosomes containing 300, 600 and 900 mg/mL of Nutriose® FM06 were fully characterized from the physico-chemical and technological point of view. The concentrations of 600 and 900 mg/mL of Nutriose® FM06 (600nutriosomes and 900nutriosomes) were the most promising as the obtained vesicles were stable up to 8 months of storage at 4 °C and controlled the release of apigenin. All the prepared silica doped nutriosomes were stable in solutions mimicking gastrointestinal environmental and seemed to be proper for the oral administration. *In vitro* study with Caco-2 cells, used as a model of intestine epithelium, confirmed the high biocompatibility of nutriosomes, which added to the cell medium for 48 h did not caused reduction of cell viability.

The results of *in vitro* growth inhibition assay were interesting, because confirmed the effectiveness of apigenin against *P. falciparum* and the optimal carrier performance of silica loaded nutriosomes. Indeed, in artemisinin and apigenin loaded silica doped nutriosomes the concentration of artemisinin was very low (~0.6 mg/mL), 36 folds lower than the used one (5 mg/mL) due to its degradation at the basic pH (9), despite it, the formulation had an inhibitory effect comparable to that addressed by the artemisinin solution (actual 5 mg/mL). More specifically, the IC50 and IC90 of artemisinin in solution were the lowest (IC50 = ~0.019 µg/mL) although the values were not statistically different from the others. In this case the artemisinin was dissolved in dimethyl sulfoxide and extemporaneously diluted with buffer solution at pH 7.4 and at this pH the drug is more stable, and its activity is mostly preserved [179]. As expected, the IC50 and IC90 of apigenin in solution were the highest (IC50 = ~4.129 µg/mL), although the values were not statistically different from the others since it is not a potent antimalarial drug like artemisinin. It is interesting to note that the IC50 and IC90 of artemisinin and apigenin loaded silica doped nutriosomes had the same magnitude order of the artemisinin solution (IC50 300nutriosomess = ~0.031 µg/mL, IC50 600nutriosomess = ~0.106 µg/mL and IC50 900nutriosomess = ~0.035 µg/mL) then 400-folds lower than that of apigenin in solution. The inhibitory effect could not be related to the artemisinin, that was almost completely degraded, and to the free apigenin, that was less effective, than it underlines the effectiveness of apigenin loaded in nutriosomes.

Considering the high IC50 founded for apigenin solution indicating a low efficacy and aiming at reducing the number of animals, in the *in vivo* study, the apigenin solution was not used, artemisinin solution, being the most potent drug, was used as reference and only 600nutriosomes, seeming the most promising, were tested. When 600nutriosomes at IC50 were orally administered to *Plasmodium yoelii yoelii*-infected mice, animal survived until day 6, one day more compared to control animals. While using the same formulation, 600nutriosomes at IC90, survival increased up to 8 days, like in

the case of artemisinin in solution, which at IC90 addressed the higher survival rate (9 days). Considering that during the preparation of the formulation, artemisinin was probably almost completely inactivated, the increase in animal survival was most likely due to the apigenin activity and its suitable delivery in silica doped 600nutriosomes.

5. Conclusion

Overall results of this study point out two important findings: a) apigenin if properly load in silica doped nutriosomes can improve the malaria-infected mice survival upon oral administration, acting as adjuvant to reinforce the effect of the therapy of artemisinin derivatives; b) artemisinin is very susceptible to pH changes and cannot be used at basic pHs since its endoperoxide bridge responsible of its antimalarial activity is reduced and its therapeutic activity as well.

Further studies are needed to better evaluate the *in vivo* effectiveness of apigenin and the suitability of the tested delivery system, but also to better understand the fate of artemisinin at basic pH.

References

1. World Health Organization *World Malaria Report 2022*; 2022;
2. Tizifa, T.A.; Kabaghe, A.N.; McCann, R.S.; van den Berg, H.; Van Vugt, M.; Phiri, K.S. Prevention Efforts for Malaria. *Curr Trop Med Rep* **2018**, *5*, 41–50, doi:10.1007/s40475-018-0133-y.
3. Centers for Disease Control and Prevention Where Malaria Occurs.
4. Liu, Q.; Jing, W.; Kang, L.; Liu, J.; Liu, M. Trends of the Global, Regional and National Incidence of Malaria in 204 Countries from 1990 to 2019 and Implications for Malaria Prevention. *J Travel Med* **2021**, *28*, doi:10.1093/jtm/taab046.
5. Wongsrichanalai, C.; Kurdova-Mintcheva, R.; Palmer, K. Current Malaria Situation in Asia-Oceania. In; 2019; pp. 45–56.
6. Nissan, H.; Ukawuba, I.; Thomson, M. Climate-Proofing a Malaria Eradication Strategy. *Malar J* **2021**, *20*, 190, doi:10.1186/s12936-021-03718-x.
7. Matuschewski, K. Getting Infectious: Formation and Maturation of Plasmodium Sporozoites in the Anopheles Vector. *Cell Microbiol* **2006**, *8*, 1547–1556, doi:10.1111/j.1462-5822.2006.00778.x.
8. Rossati, A.; Bargiacchi, O.; Kroumova, V.; Zaramella, M.; Caputo, A.; Garavelli, P.L. Climate, Environment and Transmission of Malaria.
9. Memvanga, P.B.; Nkanga, C.I. Liposomes for Malaria Management: The Evolution from 1980 to 2020. *Malar J* 2021, *20*.
10. Balaji, S.N.; Deshmukh, R.; Trivedi, V. *Severe Malaria: Biology, Clinical Manifestation, Pathogenesis and Consequences*; 2020; Vol. 57;.
11. Cowman, A.F.; Healer, J.; Marapana, D.; Marsh, K. Malaria: Biology and Disease. *Cell* 2016, *167*, 610–624.
12. Health Organization, W. *Guideline WHO Guidelines for Malaria - 3 June 2022*; 2022;
13. Permin, H.; Norn, S.; Kruse, E.; Kruse, P.R. On the History of Cinchona Bark in the Treatment of Malaria. *Dan Medicinhist Arbog* **2016**, *44*, 9–30.
14. Thomas, K.; Ying, W. Artemisinin — an Innovative Cornerstone for Anti-Malaria Therapy. In *Natural Compounds as Drugs*; Birkhäuser Basel: Basel; pp. 383–422.
15. World Health Organization *Guidelines for the Treatment of Malaria*; ISBN 9789241549127.
16. Hiben, M.G.; Sibhat, G.G.; Fanta, B.S.; Gebrezgi, H.D.; Tesema, S.B. Evaluation of Senna Singueana Leaf Extract as an Alternative or Adjuvant Therapy for Malaria. *J Tradit Complement Med* **2016**, *6*, 112–117, doi:10.1016/j.jtcme.2014.11.014.
17. El-Missiry, M.A.; Fekri, A.; Kesar, L.A.; Othman, A.I. Polyphenols Are Potential Nutritional Adjuvants for Targeting <scp>COVID</Scp> -19. *Phytotherapy Research* **2021**, *35*, 2879–2889, doi:10.1002/ptr.6992.
18. Licciardi, P. V; Underwood, J.R. Plant-Derived Medicines: A Novel Class of Immunological Adjuvants. *Int Immunopharmacol* **2011**, *11*, 390–398, doi:10.1016/j.intimp.2010.10.014.
19. Kirira, P.G.; Rukunga, G.M.; Wanyonyi, A.W.; Muregi, F.M.; Gathirwa, J.W.; Muthaura, C.N.; Omar, S.A.; Tolo, F.; Mungai, G.M.; Ndiege, I.O. Anti-Plasmodial Activity and Toxicity of Extracts of Plants Used in Traditional Malaria Therapy in Meru and Kilifi Districts of Kenya. *J Ethnopharmacol* **2006**, *106*, 403–407, doi:10.1016/j.jep.2006.01.017.
20. Zhao, Z.; Ukidve, A.; Krishnan, V.; Mitragotri, S. Effect of Physicochemical and Surface Properties on in Vivo Fate of Drug Nanocarriers. *Adv Drug Deliv Rev* **2019**, *143*, 3–21, doi:10.1016/j.addr.2019.01.002.
21. Berbel Manaia, E.; Paiva Abuçafy, M.; Chiari-Andréo, B.G.; Lallo Silva, B.; Oshiro-Júnior, J.A.; Chiavacci, L. Physicochemical Characterization of Drug Nanocarriers. *Int J Nanomedicine* **2017**, *Volume 12*, 4991–5011, doi:10.2147/IJN.S133832.

22. Greenwood, D. The Quinine Connection. *Journal of Antimicrobial Chemotherapy* **1992**, *30*, 417–427, doi:10.1093/jac/30.4.417.
23. Johnston, W. The Discovery of Aniline and the Origin of the Term “Aniline Dye.” *Biotechnic & Histochemistry* **2008**, *83*, 83–87, doi:10.1080/10520290802136793.
24. Kaufman, T.S.; Rúveda, E.A. The Quest for Quinine: Those Who Won the Battles and Those Who Won the War. *Angewandte Chemie International Edition* **2005**, *44*, 854–885, doi:10.1002/anie.200400663.
25. Nosten, F.; Richard-Lenoble, D.; Danis, M. A Brief History of Malaria. *Presse Med* **2022**, *51*, 104130, doi:10.1016/j.lpm.2022.104130.
26. Tu, Y. The Discovery of Artemisinin (Qinghaosu) and Gifts from Chinese Medicine. *Nat Med* **2011**, *17*, 1217–1220, doi:10.1038/nm.2471.
27. Ma, N.; Zhang, Z.; Liao, F.; Jiang, T.; Tu, Y. The Birth of Artemisinin. *Pharmacol Ther* **2020**, *216*, 107658, doi:10.1016/j.pharmthera.2020.107658.
28. Cui, L.; Su, X. Discovery, Mechanisms of Action and Combination Therapy of Artemisinin. *Expert Rev Anti Infect Ther* **2009**, *7*, 999–1013, doi:10.1586/eri.09.68.
29. Wang, J.; Xu, C.; Lun, Z.-R.; Meshnick, S.R. Unpacking ‘Artemisinin Resistance.’ *Trends Pharmacol Sci* **2017**, *38*, 506–511, doi:10.1016/j.tips.2017.03.007.
30. Nsanzabana, C. Resistance to Artemisinin Combination Therapies (ACTs): Do Not Forget the Partner Drug! *Trop Med Infect Dis* **2019**, *4*, 26, doi:10.3390/tropicalmed4010026.
31. Tougher, S.; Ye, Y.; Amuasi, J.H.; Kourgueni, I.A.; Thomson, R.; Goodman, C.; Mann, A.G.; Ren, R.; Willey, B.A.; Adegoke, C.A.; et al. Effect of the Affordable Medicines Facility—Malaria (AMFm) on the Availability, Price, and Market Share of Quality-Assured Artemisinin-Based Combination Therapies in Seven Countries: A before-and-after Analysis of Outlet Survey Data. *The Lancet* **2012**, *380*, 1916–1926, doi:10.1016/S0140-6736(12)61732-2.
32. Moussa, A.Y.; Xu, B. A Narrative Review on Inhibitory Effects of Edible Mushrooms against Malaria and Tuberculosis-the World’s Deadliest Diseases. *Food Science and Human Wellness* **2023**, *12*, 942–958, doi:10.1016/j.fshw.2022.10.017.
33. Bamgbose, T.; Anvikar, A.R.; Alberdi, P.; Abdullahi, I.O.; Inabo, H.I.; Bello, M.; Cabezas-Cruz, A.; de la Fuente, J. Functional Food for the Stimulation of the Immune System Against Malaria. *Probiotics Antimicrob Proteins* **2021**, *13*, 1254–1266, doi:10.1007/s12602-021-09780-w.
34. Isaka, M.; Srisanoh, U.; Choowong, W.; Boonpratuang, T. Sterostreins A–E, New Terpenoids from Cultures of the Basidiomycete *Stereum Ostrea* BCC 22955. *Org Lett* **2011**, *13*, 4886–4889, doi:10.1021/ol2019778.
35. Samchai, S.; Seephonkai, P.; Sangdee, A.; Puntumchai, A.; Klinhom, U. Antioxidant, Cytotoxic and Antimalarial Activities from Crude Extracts of Mushroom Phellinus Linteus. *Journal of Biological Sciences* **2009**, *9*, 778–783, doi:10.3923/jbs.2009.778.783.
36. Muregi, F.W.; Chhabra, S.C.; Njagi, E.N.M.; Lang’at-Thoruwa, C.C.; Njue, W.M.; Orago, A.S.S.; Omar, S.A.; Ndiege, I.O. In Vitro Antiplasmodial Activity of Some Plants Used in Kisii, Kenya against Malaria and Their Chloroquine Potentiation Effects. *J Ethnopharmacol* **2003**, *84*, 235–239, doi:10.1016/S0378-8741(02)00327-6.
37. Rashidzadeh, H.; Mosavi, F.S.; Shafiee, T.; Adyani, S.M.; Eghlima, G.; Sanikhani, M.; Kheiry, A.; Amiri, M.; Tavakolizadeh, M.; Ramazani, A. Anti-Plasmodial Effects of Different Ecotypes of Glycyrrhiza Glabra Traditionally Used for Malaria in Iran. *Revista Brasileira de Farmacognosia* **2023**, doi:10.1007/s43450-022-00353-8.
38. Bankole, A.E.; Adekunle, A.A.; Sowemimo, A.A.; Umebese, C.E.; Abiodun, O.; Gbotosho, G.O. Phytochemical Screening and in Vivo Antimalarial Activity of Extracts from Three Medicinal Plants Used in Malaria Treatment in Nigeria. *Parasitol Res* **2016**, *115*, 299–305, doi:10.1007/s00436-015-4747-x.

39. Adams, L.; Afiadenyo, M.; Kwofie, S.K.; Wilson, M.D.; Kusi, K.A.; Obiri-Yeboah, D.; Moane, S.; McKeon-Bennett, M. In Silico Screening of Phytochemicals from Dissotis Rotundifolia against Plasmodium Falciparum Dihydrofolate Reductase. *Phytomedicine Plus* **2023**, *3*, 100447, doi:10.1016/j.phyplu.2023.100447.
40. Sharma, G.; Rana, D.; Sundriyal, S.; Sharma, A.; Panwar, P.; Mahindroo, N. Plants from Annonaceae Family as Antimalarials: An Ethnopharmacology and Phytochemistry Review to Identify Potential Lead Molecules. *South African Journal of Botany* **2023**, *155*, 154–170, doi:10.1016/j.sajb.2023.02.015.
41. Singh, A.; Mukhtar, H.M.; Kaur, H.; Kaur, L. Investigation of Antiplasmodial Efficacy of Lupeol and Ursolic Acid Isolated from *Ficus Benjamina* Leaves Extract. *Nat Prod Res* **2020**, *34*, 2514–2517, doi:10.1080/14786419.2018.1540476.
42. Hemasa, A.L.; Mack, M.; Saliba, K.J. Roseoflavin, a Natural Riboflavin Analogue, Possesses *In Vitro* and *In Vivo* Antiplasmodial Activity. *Antimicrob Agents Chemother* **2022**, *66*, doi:10.1128/aac.00540-22.
43. Annang, F.; Pérez-Moreno, G.; González-Menéndez, V.; Lacret, R.; Pérez-Victoria, I.; Martín, J.; Cantizani, J.; de Pedro, N.; Choquesillo-Lazarte, D.; Ruiz-Pérez, L.M.; et al. Strasseriolides A–D, A Family of Antiplasmodial Macrolides Isolated from the Fungus *Strasseria Geniculata* CF-247251. *Org Lett* **2020**, *22*, 6709–6713, doi:10.1021/acs.orglett.0c01665.
44. Ezenyi, I.C.; Salawu, O.A.; Kulkarni, R.; Emeje, M. Antiplasmodial Activity-Aided Isolation and Identification of Quercetin-4'-Methyl Ether in Chromolaena Odorata Leaf Fraction with High Activity against Chloroquine-Resistant Plasmodium Falciparum. *Parasitol Res* **2014**, *113*, 4415–4422, doi:10.1007/s00436-014-4119-y.
45. Ganesh, D.; Fuehrer, H.-P.; Starzengrüber, P.; Swoboda, P.; Khan, W.A.; Reismann, J.A.B.; Mueller, M.S.K.; Chiba, P.; Noedl, H. Antiplasmodial Activity of Flavonol Quercetin and Its Analogues in Plasmodium Falciparum: Evidence from Clinical Isolates in Bangladesh and Standardized Parasite Clones. *Parasitol Res* **2012**, *110*, 2289–2295, doi:10.1007/s00436-011-2763-z.
46. Gogoi, M. Recent Advances in Nanomedicine for Antimalarial Drug Delivery. *Biomedical Research Journal* **2017**, *4*, 151, doi:10.4103/2349-3666.240598.
47. Neves Borgheti-Cardoso, L.; San Anselmo, M.; Lantero, E.; Lancelot, A.; Serrano, J.L.; Hernández-Ainsa, S.; Fernàndez-Busquets, X.; Sierra, T. Promising Nanomaterials in the Fight against Malaria. *J Mater Chem B* **2020**, *8*, 9428–9448, doi:10.1039/D0TB01398F.
48. Urban, P.; Fernandez-Busquets, X. Nanomedicine Against Malaria. *Curr Med Chem* **2014**, *21*, 605–629, doi:10.2174/09298673113206660292.
49. Movellan, J.; Urbán, P.; Moles, E.; de la Fuente, J.M.; Sierra, T.; Serrano, J.L.; Fernàndez-Busquets, X. Amphiphilic Dendritic Derivatives as Nanocarriers for the Targeted Delivery of Antimalarial Drugs. *Biomaterials* **2014**, *35*, 7940–7950, doi:10.1016/j.biomaterials.2014.05.061.
50. Izaguirry, A.P.; Pavin, N.F.; Soares, M.B.; Spiazzi, C.C.; Araújo, F.A.; Michels, L.R.; Leivas, F.G.; Brum, D. dos S.; Haas, S.E.; Santos, F.W. Effect of Quinine-Loaded Polysorbate-Coated Nanocapsules on Male and Female Reproductive Systems of Rats. *Toxicol Res (Camb)* **2016**, *5*, 1561–1572, doi:10.1039/C6TX00203J.
51. Velasques, K.; Maciel, T.R.; de Castro Dal Forno, A.H.; Teixeira, F.E.G.; da Fonseca, A.L.; Varotti, F. de P.; Fajardo, A.R.; Ávila, D.S. de; Haas, S.E. Co-Nanoencapsulation of Antimalarial Drugs Increases Their in Vitro Efficacy against Plasmodium Falciparum and Decreases Their Toxicity to Caenorhabditis Elegans. *European Journal of Pharmaceutical Sciences* **2018**, *118*, 1–12, doi:10.1016/j.ejps.2018.03.014.
52. Bajerski, L.; Maciel, T.R.; Haas, S.E. Simultaneous Determination of Curcumin and Quinine Co-Encapsulated in Nanoemulsion by Stability-Indicating LC Method. *Curr Pharm Anal* **2018**, *14*, 255–261, doi:10.2174/1573412913666170330151347.

53. Amolegbe, S.A.; Hirano, Y.; Adebayo, J.O.; Ademowo, O.G.; Balogun, E.A.; Obaleye, J.A.; Krettli, A.U.; Yu, C.; Hayami, S. Mesoporous Silica Nanocarriers Encapsulated Antimalarials with High Therapeutic Performance. *Sci Rep* **2018**, *8*, 3078, doi:10.1038/s41598-018-21351-8.
54. Gomes, G.S.; Maciel, T.R.; Piegas, E.M.; Michels, L.R.; Colomé, L.M.; Freddo, R.J.; Ávila, D.S. de; Gundel, A.; Haas, S.E. Optimization of Curcuma Oil/Quinine-Loaded Nanocapsules for Malaria Treatment. *AAPS PharmSciTech* **2018**, *19*, 551–564, doi:10.1208/s12249-017-0854-6.
55. Michels, L.R.; Maciel, T.R.; Nakama, K.A.; Teixeira, F.E.G.; Carvalho, F.B. de; Gundel, A.; Araújo, B.V. de; Haas, S.E. <p>Effects of Surface Characteristics of Polymeric Nanocapsules on the Pharmacokinetics and Efficacy of Antimalarial Quinine</P>. *Int J Nanomedicine* **2019**, *Volume 14*, 10165–10178, doi:10.2147/IJN.S227914.
56. Urbán, P.; Estelrich, J.; Adeva, A.; Cortés, A.; Fernàndez-Busquets, X. Study of the Efficacy of Antimalarial Drugs Delivered inside Targeted Immunoliposomal Nanovectors. *Nanoscale Res Lett* **2011**, *6*, 620, doi:10.1186/1556-276X-6-620.
57. Khanmohammadi, A.; Sadighian, S.; Ramazani, A. Anti-Plasmodial Effects of Quinine-Loaded Magnetic Nanocomposite Coated with Heparin. *Int J Pharm* **2022**, *628*, 122260, doi:10.1016/j.ijpharm.2022.122260.
58. Haas, S.E.; Bettoni, C.C.; de Oliveira, L.K.; Guterres, S.S.; Dalla Costa, T. Nanoencapsulation Increases Quinine Antimalarial Efficacy against Plasmodium Berghei in Vivo. *Int J Antimicrob Agents* **2009**, *34*, 156–161, doi:10.1016/j.ijantimicag.2009.02.024.
59. Okell, L.C.; Cairns, M.; Griffin, J.T.; Ferguson, N.M.; Tarning, J.; Jagoe, G.; Hugo, P.; Baker, M.; D'Alessandro, U.; Bousema, T.; et al. Contrasting Benefits of Different Artemisinin Combination Therapies as First-Line Malaria Treatments Using Model-Based Cost-Effectiveness Analysis. *Nat Commun* **2014**, *5*, 5606, doi:10.1038/ncomms6606.
60. Isacchi, B.; Arrigucci, S.; Marca, G. la; Bergonzi, M.C.; Vannucchi, M.G.; Novelli, A.; Bilia, A.R. Conventional and Long-Circulating Liposomes of Artemisinin: Preparation, Characterization, and Pharmacokinetic Profile in Mice. *J Liposome Res* **2011**, *21*, 237–244, doi:10.3109/08982104.2010.539185.
61. Wang, X.; Xie, Y.; Jiang, N.; Wang, J.; Liang, H.; Liu, D.; Yang, N.; Sang, X.; Feng, Y.; Chen, R.; et al. Enhanced Antimalarial Efficacy Obtained by Targeted Delivery of Artemisinin in Heparin-Coated Magnetic Hollow Mesoporous Nanoparticles. *ACS Appl Mater Interfaces* **2021**, *13*, 287–297, doi:10.1021/acsami.0c20070.
62. Ismail, M.; Ling, L.; Du, Y.; Yao, C.; Li, X. Liposomes of Dimeric Artesunate Phospholipid: A Combination of Dimerization and Self-Assembly to Combat Malaria. *Biomaterials* **2018**, *163*, 76–87, doi:10.1016/j.biomaterials.2018.02.026.
63. He, W.; Du, Y.; Li, C.; Wang, J.; Wang, Y.; Dogovski, C.; Hu, R.; Tao, Z.; Yao, C.; Li, X. Dimeric Artesunate-Choline Conjugate Micelles Coated with Hyaluronic Acid as a Stable, Safe and Potent Alternative Anti-Malarial Injection of Artesunate. *Int J Pharm* **2021**, *609*, 121138, doi:10.1016/j.ijpharm.2021.121138.
64. Aditya, N.P.; Patankar, S.; Madhusudhan, B.; Murthy, R.S.R.; Souto, E.B. Arthemeter-Loaded Lipid Nanoparticles Produced by Modified Thin-Film Hydration: Pharmacokinetics, Toxicological and in Vivo Anti-Malarial Activity. *European Journal of Pharmaceutical Sciences* **2010**, *40*, 448–455, doi:10.1016/j.ejps.2010.05.007.
65. Dwivedi, P.; Khatik, R.; Chaturvedi, P.; Khandelwal, K.; Taneja, I.; Raju, K.S.R.; Dwivedi, H.; Singh, S. kumar; Gupta, P.K.; Shukla, P.; et al. Arteether Nanoemulsion for Enhanced Efficacy against Plasmodium Yoelii Nigeriensis Malaria: An Approach by Enhanced Bioavailability. *Colloids Surf B Biointerfaces* **2015**, *126*, 467–475, doi:10.1016/j.colsurfb.2014.12.052.

66. Boateng-Marfo, Y.; Dong, Y.; Ng, W.K.; Lin, H.-S. Artemether-Loaded Zein Nanoparticles: An Innovative Intravenous Dosage Form for the Management of Severe Malaria. *Int J Mol Sci* **2021**, *22*, 1141, doi:10.3390/ijms22031141.
67. Umeyor, C.E.; Obachie, O.; Chukwuka, R.; Attama, A. Development Insights of Surface Modified Lipid Nanoemulsions of Dihydroartemisinin for Malaria Chemotherapy: Characterization, and in Vivo Antimalarial Evaluation. *Recent Pat Biotechnol* **2019**, *13*, 149–165, doi:10.2174/1872208313666181204095314.
68. Kalaskar, M.G.; Duraiswami, B.; Surana, S.J.; Shirkhedkar, A.A. Herbs Used in Parasitic Infection—Malaria. In *Herbal Drugs for the Management of Infectious Diseases*; Wiley, 2022; pp. 443–517.
69. Al-Kassas, R.; Bansal, M.; Shaw, J. Nanosizing Techniques for Improving Bioavailability of Drugs. *Journal of Controlled Release* **2017**, *260*, 202–212, doi:10.1016/j.jconrel.2017.06.003.
70. Balducci, A.G.; Magosso, E.; Colombo, G.; Sonvico, F. From Tablets to Pharmaceutical Nanotechnologies: Innovation in Drug Delivery Strategies for the Administration of Antimalarial Drugs. *J Drug Deliv Sci Technol* **2016**, *32*, 167–173, doi:10.1016/j.jddst.2015.06.003.
71. Hanif, H.; Abdollahi, V.; Javani Jouni, F.; Nikoukar, M.; Rahimi Esboei, B.; Shams, E.; vazini, H. Quercetin Nano Phytosome: As a Novel Anti-Leishmania and Anti-Malarial Natural Product. *Journal of Parasitic Diseases* **2023**, doi:10.1007/s12639-022-01561-8.
72. Martí Coma-Cros, E.; Biosca, A.; Lantero, E.; Manca, M.; Caddeo, C.; Gutiérrez, L.; Ramírez, M.; Borgheti-Cardoso, L.; Manconi, M.; Fernàndez-Busquets, X. Antimalarial Activity of Orally Administered Curcumin Incorporated in Eudragit®-Containing Liposomes. *Int J Mol Sci* **2018**, *19*, 1361, doi:10.3390/ijms19051361.
73. Manconi, M.; Manca, M.L.; Escribano-Ferrer, E.; Coma-Cros, E.M.; Biosca, A.; Lantero, E.; Fernàndez-Busquets, X.; Fadda, A.M.; Caddeo, C. Nanoformulation of Curcumin-Loaded Eudragit-Nutriosomes to Counteract Malaria Infection by a Dual Strategy: Improving Antioxidant Intestinal Activity and Systemic Efficacy. *Int J Pharm* **2019**, *556*, 82–88, doi:10.1016/j.ijpharm.2018.11.073.
74. Rashidzadeh, H.; Salimi, M.; Sadighian, S.; Rostamizadeh, K.; Ramazani, A. In Vivo Antiplasmodial Activity of Curcumin-Loaded Nanostructured Lipid Carriers. *Curr Drug Deliv* **2019**, *16*, 923–930, doi:10.2174/1567201816666191029121036.
75. Nayak, A.P.; Tiyaboonchai, W.; Patankar, S.; Madhusudhan, B.; Souto, E.B. Curcuminoids-Loaded Lipid Nanoparticles: Novel Approach towards Malaria Treatment. *Colloids Surf B Biointerfaces* **2010**, *81*, 263–273, doi:10.1016/j.colsurfb.2010.07.020.
76. Biosca, A.; Cabanach, P.; Abdulkarim, M.; Gumbleton, M.; Gómez-Canela, C.; Ramírez, M.; Bouzón-Arnáiz, I.; Avalos-Padilla, Y.; Borros, S.; Fernàndez-Busquets, X. Zwitterionic Self-Assembled Nanoparticles as Carriers for Plasmodium Targeting in Malaria Oral Treatment. *Journal of Controlled Release* **2021**, *331*, 364–375, doi:10.1016/j.jconrel.2021.01.028.
77. Dandekar, P.P.; Jain, R.; Patil, S.; Dhumal, R.; Tiwari, D.; Sharma, S.; Vanage, G.; Patravale, V. Curcumin-Loaded Hydrogel Nanoparticles: Application in Anti-Malarial Therapy and Toxicological Evaluation. *J Pharm Sci* **2010**, *99*, 4992–5010, doi:10.1002/jps.22191.
78. Rajendran, V.; Rohra, S.; Raza, M.; Hasan, G.M.; Dutt, S.; Ghosh, P.C. Stearylamine Liposomal Delivery of Monensin in Combination with Free Artemisinin Eliminates Blood Stages of Plasmodium Falciparum in Culture and P. Berghei Infection in Murine Malaria. *Antimicrob Agents Chemother* **2016**, *60*, 1304–1318, doi:10.1128/AAC.01796-15.
79. Jyotshna; Chand Gupta, A.; Bawankule, D.U.; Verma, A.K.; Shanker, K. Nanoemulsion Preconcentrate of a Pentacyclic Triterpene for Improved Oral Efficacy: Formulation Design and in-Vivo Antimalarial Activity. *J Drug Deliv Sci Technol* **2020**, *57*, 101734, doi:10.1016/j.jddst.2020.101734.

80. World Health Organization Malaria Eradication: Benefits, Future Scenarios & Feasibility.
81. Habibi, P.; Shi, Y.; Fatima Grossi-de-Sa, M.; Khan, I. Plants as Sources of Natural and Recombinant Antimalaria Agents. *Mol Biotechnol* **2022**, *64*, 1177–1197, doi:10.1007/s12033-022-00499-9.
82. Santos-Magalhães, N.S.; Mosqueira, V.C.F. Nanotechnology Applied to the Treatment of Malaria. *Adv Drug Deliv Rev* **2010**, *62*, 560–575, doi:10.1016/j.addr.2009.11.024.
83. Puttappa, N.; Kumar, R.S.; Yamjala, K. Artesunate-Quercetin/Luteolin Dual Drug Nanofacilitated Synergistic Treatment for Malaria: A Plausible Approach to Overcome Artemisinin Combination Therapy Resistance. *Med Hypotheses* **2017**, *109*, 176–180, doi:10.1016/j.mehy.2017.10.016.
84. Badmos, A.O.; Alaran, A.J.; Adebisi, Y.A.; Bouaddi, O.; Onibon, Z.; Dada, A.; Lin, X.; Lucero-Prisno, D.E. What Sub-Saharan African Countries Can Learn from Malaria Elimination in China. *Trop Med Health* **2021**, *49*, doi:10.1186/s41182-021-00379-z.
85. Ricci, F. SOCIAL IMPLICATIONS OF MALARIA AND THEIR RELATIONSHIPS WITH POVERTY. *Mediterr J Hematol Infect Dis* **2012**, *4*, e2012048, doi:10.4084/mjhid.2012.048.
86. Geleta, G.; Ketema, T. Severe Malaria Associated with *Plasmodium Falciparum* and *P. Vivax* among Children in Pawe Hospital, Northwest Ethiopia. *Malar Res Treat* **2016**, *2016*, 1–7, doi:10.1155/2016/1240962.
87. Krafts, K.; Hempelmann, E.; Skórska-Stania, A. From Methylene Blue to Chloroquine: A Brief Review of the Development of an Antimalarial Therapy. *Parasitol Res* **2012**, *111*, 1–6, doi:10.1007/s00436-012-2886-x.
88. Arya, A.; Kojom Foko, L.P.; Chaudhry, S.; Sharma, A.; Singh, V. Artemisinin-Based Combination Therapy (ACT) and Drug Resistance Molecular Markers: A Systematic Review of Clinical Studies from Two Malaria Endemic Regions – India and Sub-Saharan Africa. *Int J Parasitol Drugs Drug Resist* **2021**, *15*, 43–56, doi:10.1016/j.ijpddr.2020.11.006.
89. White, N.J. Qinghaosu (Artemisinin): The Price of Success. *Science (1979)* **2008**, *320*, 330–334, doi:10.1126/science.1155165.
90. Alven, S.; Aderibigbe, B. Combination Therapy Strategies for the Treatment of Malaria. *Molecules* **2019**, *24*, 3601, doi:10.3390/molecules24193601.
91. Banek, K.; Lalani, M.; Staedke, S.G.; Chandramohan, D. Adherence to Artemisinin-Based Combination Therapy for the Treatment of Malaria: A Systematic Review of the Evidence. *Malar J* **2014**, *13*, 7, doi:10.1186/1475-2875-13-7.
92. Isacchi, B.; Bergonzi, M.C.; Grazioso, M.; Righeschi, C.; Pietretti, A.; Severini, C.; Bilia, A.R. Artemisinin and Artemisinin plus Curcumin Liposomal Formulations: Enhanced Antimalarial Efficacy against Plasmodium Berghei-Infected Mice. *European Journal of Pharmaceutics and Biopharmaceutics* **2012**, *80*, 528–534, doi:10.1016/j.ejpb.2011.11.015.
93. Mehanny, M.; Hathout, R.M.; Geneidi, A.S.; Mansour, S. Exploring the Use of Nanocarrier Systems to Deliver the Magical Molecule; Curcumin and Its Derivatives. *Journal of Controlled Release* **2016**, *225*, 1–30, doi:10.1016/j.jconrel.2016.01.018.
94. Reddy, R.C.; Vatsala, P.G.; Keshamouni, V.G.; Padmanaban, G.; Rangarajan, P.N. Curcumin for Malaria Therapy. *Biochem Biophys Res Commun* **2005**, *326*, 472–474, doi:10.1016/j.bbrc.2004.11.051.
95. NOSE, M.; KOIDE, T.; OGIHARA, Y.; YABU, Y.; OHTA, N. Trypanocidal Effects of Curcumin in Vitro. *Biol Pharm Bull* **1998**, *21*, 643–645, doi:10.1248/bpb.21.643.
96. Koide, T.; Nose, M.; Ogihara, Y.; Yabu, Y.; Ohta, N. Leishmanicidal Effect of Curcumin in Vitro. *Biol Pharm Bull* **2002**, *25*, 131–133, doi:10.1248/bpb.25.131.
97. D'Andrea, G. Quercetin: A Flavonol with Multifaceted Therapeutic Applications? *Fitoterapia* **2015**, *106*, 256–271, doi:10.1016/j.fitote.2015.09.018.
98. Ganesh, D.; Fuehrer, H.P.; Starzengrüber, P.; Swoboda, P.; Khan, W.A.; Reismann, J.A.B.; Mueller, M.S.K.; Chiba, P.; Noedl, H. Antiplasmodial Activity of Flavonol Quercetin and Its Analogues in Plasmodium Falciparum: Evidence from Clinical Isolates in Bangladesh and

Standardized Parasite Clones. *Parasitol Res* **2012**, *110*, 2289–2295, doi:10.1007/s00436-011-2763-z.

99. Rajwar, T.K.; Pradhan, D.; Halder, J.; Rai, V.K.; Kar, B.; Ghosh, G.; Rath, G. Opportunity in Nanomedicine to Counter the Challenges of Current Drug Delivery Approaches Used for the Treatment of Malaria: A Review. *J Drug Target* **2023**, *31*, 354–368, doi:10.1080/1061186X.2022.2164290.
100. Parekh, P.; Serra, M.; Allaw, M.; Perra, M.; Marongiu, J.; Tolle, G.; Pinna, A.; Casu, M.A.; Manconi, M.; Caboni, P.; et al. Characterization of Nasco Grape Pomace-Loaded Nutriosomes and Their Neuroprotective Effects in the MPTP Mouse Model of Parkinson's Disease. *Front Pharmacol* **2022**, *13*, doi:10.3389/fphar.2022.935784.
101. Catalán-Latorre, A.; Pleguezuelos-Villa, M.; Castangia, I.; Manca, M.L.; Caddeo, C.; Nácher, A.; Díez-Sales, O.; Peris, J.E.; Pons, R.; Escribano-Ferrer, E.; et al. Nutriosomes: Prebiotic Delivery Systems Combining Phospholipids, a Soluble Dextrin and Curcumin to Counteract Intestinal Oxidative Stress and Inflammation. *Nanoscale* **2018**, *10*, 1957–1969, doi:10.1039/c7nr05929a.
102. Coma-Cros, E.M.; Biosca, A.; Lantero, E.; Manca, M.L.; Caddeo, C.; Gutiérrez, L.; Ramírez, M.; Borgheti-Cardoso, L.N.; Manconi, M.; Fernàndez-Busquets, X. Antimalarial Activity of Orally Administered Curcumin Incorporated in Eudragit®-Containing Liposomes. *Int J Mol Sci* **2018**, *19*, doi:10.3390/ijms19051361.
103. Manconi, M.; Manca, M.L.; Escribano-Ferrer, E.; Coma-Cros, E.M.; Biosca, A.; Lantero, E.; Fernàndez-Busquets, X.; Fadda, A.M.; Caddeo, C. Nanoformulation of Curcumin-Loaded Eudragit-Nutriosomes to Counteract Malaria Infection by a Dual Strategy: Improving Antioxidant Intestinal Activity and Systemic Efficacy. *Int J Pharm* **2019**, *556*, 82–88, doi:10.1016/j.ijpharm.2018.11.073.
104. Allaw, M.; Manca, M.L.; Caddeo, C.; Recio, M.C.; Pérez-Brocal, V.; Moya, A.; Fernàndez-Busquets, X.; Manconi, M. Advanced Strategy to Exploit Wine-Making Waste by Manufacturing Antioxidant and Prebiotic Fibre-Enriched Vesicles for Intestinal Health. *Colloids Surf B Biointerfaces* **2020**, *193*, doi:10.1016/j.colsurfb.2020.111146.
105. Manconi, M.; Manca, M.L.; Valenti, D.; Escribano, E.; Hillaireau, H.; Fadda, A.M.; Fattal, E. Chitosan and Hyaluronan Coated Liposomes for Pulmonary Administration of Curcumin. *Int J Pharm* **2017**, *525*, 203–210, doi:10.1016/j.ijpharm.2017.04.044.
106. Manca, M.L.; Lattuada, D.; Valenti, D.; Marelli, O.; Corradini, C.; Fernàndez-Busquets, X.; Zaru, M.; Maccioni, A.M.; Fadda, A.M.; Manconi, M. Potential Therapeutic Effect of Curcumin Loaded Hyalurosomes against Inflammatory and Oxidative Processes Involved in the Pathogenesis of Rheumatoid Arthritis: The Use of Fibroblast-like Synovial Cells Cultured in Synovial Fluid. *European Journal of Pharmaceutics and Biopharmaceutics* **2019**, *136*, 84–92, doi:10.1016/j.ejpb.2019.01.012.
107. Allaw, M.; Manca, M.L.; Gómez-Fernández, J.C.; Pedraz, J.L.; Terencio, M.C.; Sales, O.D.; Nacher, A.; Manconi, M. Oleuropein Multicompartment Nanovesicles Enriched with Collagen as a Natural Strategy for the Treatment of Skin Wounds Connected with Oxidative Stress. *Nanomedicine* **2021**, *16*, 2363–2376, doi:10.2217/nnm-2021-0197.
108. Rodríguez-Corrales, J.; Josan, J.S. Resazurin Live Cell Assay: Setup and Fine-Tuning for Reliable Cytotoxicity Results. In *Methods in Molecular Biology*; Humana Press Inc., 2017; Vol. 1647, pp. 207–219.
109. Lambros, C.; Vanderberg, J.P. *Synchronization of Plasmodium Falciparum Erythrocytic Stages in Culture*; 1979; Vol. 65;.
110. Rezvani, M.; Manca, M.L.; Caddeo, C.; Escribano-Ferrer, E.; Carbone, C.; Peris, J.E.; Usach, I.; Diez-Sales, O.; Fadda, A.M.; Manconi, M. Co-Loading of Ascorbic Acid and Tocopherol in Eudragit-Nutriosomes to Counteract Intestinal Oxidative Stress. *Pharmaceutics* **2019**, *11*, doi:10.3390/pharmaceutics11010013.

111. Taylor, T.M.; Gaysinsky, S.; Davidson, P.M.; Bruce, B.D.; Weiss, J. Characterization of Antimicrobial-Bearing Liposomes by ζ-Potential, Vesicle Size, and Encapsulation Efficiency. *Food Biophys* **2007**, *2*, 1–9, doi:10.1007/s11483-007-9023-x.
112. Obata, Y.; Tajima, S.; Takeoka, S. Evaluation of PH-Responsive Liposomes Containing Amino Acid-Based Zwitterionic Lipids for Improving Intracellular Drug Delivery in Vitro and in Vivo. *Journal of Controlled Release* **2010**, *142*, 267–276, doi:10.1016/j.jconrel.2009.10.023.
113. Marinho, S.; Illanes, M.; Ávila-Román, J.; Motilva, V.; Talero, E. Anti-Inflammatory Effects of Rosmarinic Acid-Loaded Nanovesicles in Acute Colitis through Modulation of NLRP3 Inflammasome. *Biomolecules* **2021**, *11*, 1–17, doi:10.3390/biom11020162.
114. Schmitt, C.; Lechanteur, A.; Cossais, F.; Bellefroid, C.; Arnold, P.; Lucius, R.; Held-Feindt, J.; Piel, G.; Hattermann, K. Liposomal Encapsulated Curcumin Effectively Attenuates Neuroinflammatory and Reactive Astrogliosis Reactions in Glia Cells and Organotypic Brain Slices. *Int J Nanomedicine* **2020**, *15*, 3649–3667, doi:10.2147/IJN.S245300.
115. Wang, C.; Han, Z.; Wu, Y.; Lu, X.; Tang, X.; Xiao, J.; Li, N. Enhancing Stability and Anti-Inflammatory Properties of Curcumin in Ulcerative Colitis Therapy Using Liposomes Mediated Colon-Specific Drug Delivery System. *Food and Chemical Toxicology* **2021**, *151*, 112123, doi:10.1016/j.fct.2021.112123.
116. Valissery, P.; Thapa, R.; Singh, J.; Gaur, D.; Bhattacharya, J.; Singh, A.P.; Dhar, S.K. Potent *in Vivo* Antimalarial Activity of Water-Soluble Artemisinin Nano-Preparations. *RSC Adv* **2020**, *10*, 36201–36211, doi:10.1039/D0RA05597B.
117. Isacchi, B.; Arrigucci, S.; Marca, G. La; Bergonzi, M.C.; Vannucchi, M.G.; Novelli, A.; Bilia, A.R. Conventional and Long-Circulating Liposomes of Artemisinin: Preparation, Characterization, and Pharmacokinetic Profile in Mice. *J Liposome Res* **2011**, *21*, 237–244, doi:10.3109/08982104.2010.539185.
118. Jahan, M.; Leon, F.; Fronczek, F.R.; Elokely, K.M.; Rimoldi, J.; Khan, S.I.; Avery, M.A. Structure–Activity Relationships of the Antimalarial Agent Artemisinin 10. Synthesis and Antimalarial Activity of Enantiomers of Rac-5β-Hydroxy-d-Secoartemisinin and Analogs: Implications Regarding the Mechanism of Action. *Molecules* **2021**, *26*, 4163, doi:10.3390/molecules26144163.
119. Righeschi, C.; Coronnello, M.; Mastrantoni, A.; Isacchi, B.; Bergonzi, M.C.; Mini, E.; Bilia, A.R. Strategy to Provide a Useful Solution to Effective Delivery of Dihydroartemisinin: Development, Characterization and in Vitro Studies of Liposomal Formulations. *Colloids Surf B Biointerfaces* **2014**, *116*, 121–127, doi:10.1016/j.colsurfb.2013.12.019.
120. Dadgar, N.; Alavi, S.E.; Esfahani, M.K.M.; Akbarzadeh, A. Study of Toxicity Effect of Pegylated Nanoliposomal Artemisinin on Breast Cancer Cell Line. *Indian Journal of Clinical Biochemistry* **2013**, *28*, 410–412, doi:10.1007/s12291-013-0306-3.
121. Jin, M.; Shen, X.; Zhao, C.; Qin, X.; Liu, H.; Huang, L.; Qiu, Z.; Liu, Y. *In Vivo* Study of Effects of Artesunate Nanoliposomes on Human Hepatocellular Carcinoma Xenografts in Nude Mice. *Drug Deliv* **2013**, *20*, 127–133, doi:10.3109/10717544.2013.801047.
122. Dwivedi, A.; Mazumder, A.; du Plessis, L.; du Preez, J.L.; Haynes, R.K.; du Plessis, J. In Vitro Anti-Cancer Effects of Artemisone Nano-Vesicular Formulations on Melanoma Cells. *Nanomedicine* **2015**, *11*, 2041–2050, doi:10.1016/j.nano.2015.07.010.
123. Chen, H.-J.; Huang, X.-R.; Zhou, X.-B.; Zheng, B.-Y.; Huang, J.-D. Potential Sonodynamic Anticancer Activities of Artemether and Liposome-Encapsulated Artemether. *Chemical Communications* **2015**, *51*, 4681–4684, doi:10.1039/C5CC00927H.
124. Karinawatie S; Kusnadi J; Martati dan E Effectiveness of Whey Protein Consentrates and Dextrins to Maintain Viability of Lactic Acid Bacteria in Frozen Dried Starter Yoghurt. *Jurnal Teknologi Pertanian* **2008**, 121–130.

125. Ashton, M.; Ngoc Hai, T.; Duy, N.S.; Xuan Huong, D.; van Huong, N.; Thi Niêu, N.; Dinh Công, L. *ARTEMISININ PHARMACOKINETICS IS TIME-DEPENDENT DURING REPEATED ORAL ADMINISTRATION IN HEALTHY MALE ADULTS*; 1998; Vol. 26;.
126. Bouzón-Arnáiz, I.; Avalos-Padilla, Y.; Biosca, A.; Caño-Prades, O.; Román-Álamo, L.; Valle, J.; Andreu, D.; Moita, D.; Prudêncio, M.; Arce, E.M.; et al. The Protein Aggregation Inhibitor YAT2150 Has Potent Antimalarial Activity in Plasmodium Falciparum in Vitro Cultures. *BMC Biol* **2022**, *20*, 197, doi:10.1186/s12915-022-01374-4.
127. World Health Organization *Guidelines for the Treatment of Malaria*; ISBN 9789241549127.
128. Yang, J.; He, Y.; Li, Y.; Zhang, X.; Wong, Y.-K.; Shen, S.; Zhong, T.; Zhang, J.; Liu, Q.; Wang, J. Advances in the Research on the Targets of Anti-Malaria Actions of Artemisinin. *Pharmacol Ther* **2020**, *216*, 107697, doi:10.1016/j.pharmthera.2020.107697.
129. Balint, G.A. Artemisinin and Its Derivatives: An Important New Class of Antimalarial Agents. *Pharmacol Ther* **2001**, *90*, 261–265, doi:10.1016/S0163-7258(01)00140-1.
130. Price, R.N. Artemisinin Drugs: Novel Antimalarial Agents. *Expert Opin Investig Drugs* **2000**, *9*, 1815–1827, doi:10.1517/13543784.9.8.1815.
131. Navaratnam, V.; Mansor, S.M.; Sit, N.-W.; Grace, J.; Li, Q.; Olliaro, P. Pharmacokinetics of Artemisinin-Type Compounds. *Clin Pharmacokinet* **2000**, *39*, 255–270, doi:10.2165/00003088-200039040-00002.
132. van Agtmael, M. Artemisinin Drugs in the Treatment of Malaria: From Medicinal Herb to Registered Medication. *Trends Pharmacol Sci* **1999**, *20*, 199–205, doi:10.1016/S0165-6147(99)01302-4.
133. Gordi, T.; Lepist, E.-I. Artemisinin Derivatives: Toxic for Laboratory Animals, Safe for Humans? *Toxicol Lett* **2004**, *147*, 99–107, doi:10.1016/j.toxlet.2003.12.009.
134. Rehman, K.; Lötsch, F.; Kremsner, P.G.; Ramharter, M. Haemolysis Associated with the Treatment of Malaria with Artemisinin Derivatives: A Systematic Review of Current Evidence. *International Journal of Infectious Diseases* **2014**, *29*, 268–273, doi:10.1016/j.ijid.2014.09.007.
135. Urban, P.; Fernandez-Busquets, X. Nanomedicine Against Malaria. *Curr Med Chem* **2014**, *21*, 605–629, doi:10.2174/09298673113206660292.
136. Charlie-Silva, I.; Fraceto, L.F.; de Melo, N.F.S. Progress in Nano-Drug Delivery of Artemisinin and Its Derivatives: Towards to Use in Immunomodulatory Approaches. *Artif Cells Nanomed Biotechnol* **2018**, *46*, 611–620, doi:10.1080/21691401.2018.1505739.
137. Juneja, M.; Suthar, T.; Pardhi, V.P.; Ahmad, J.; Jain, K. Emerging Trends and Promises of Nanoemulsions in Therapeutics of Infectious Diseases. *Nanomedicine* **2022**, *17*, 793–812, doi:10.2217/nnm-2022-0006.
138. Singh, K.K.; Vingkar, S.K. Formulation, Antimalarial Activity and Biodistribution of Oral Lipid Nanoemulsion of Primaquine. *Int J Pharm* **2008**, *347*, 136–143, doi:10.1016/j.ijpharm.2007.06.035.
139. Umeyor, C.E.; Obachie, O.; Chukwuka, R.; Attama, A. Development Insights of Surface Modified Lipid Nanoemulsions of Dihydroartemisinin for Malaria Chemotherapy: Characterization, and in Vivo Antimalarial Evaluation. *Recent Pat Biotechnol* **2019**, *13*, 149–165, doi:10.2174/1872208313666181204095314.
140. Wilson, R.J.; Li, Y.; Yang, G.; Zhao, C.X. Nanoemulsions for Drug Delivery. *Particuology* **2022**, *64*, 85–97, doi:10.1016/j.partic.2021.05.009.
141. Boots, A.W.; Haenen, G.R.M.M.; Bast, A. Health Effects of Quercetin: From Antioxidant to Nutraceutical. *Eur J Pharmacol* **2008**, *585*, 325–337, doi:10.1016/j.ejphar.2008.03.008.
142. Ganesh, D.; Fuehrer, H.-P.; Starzengrüber, P.; Swoboda, P.; Khan, W.A.; Reismann, J.A.B.; Mueller, M.S.K.; Chiba, P.; Noedl, H. Antiplasmodial Activity of Flavonol Quercetin and Its Analogues in Plasmodium Falciparum: Evidence from Clinical Isolates in Bangladesh and Standardized Parasite Clones. *Parasitol Res* **2012**, *110*, 2289–2295, doi:10.1007/s00436-011-2763-z.

143. Catalan-Latorre, A.; Ravaghi, M.; Manca, M.L.; Caddeo, C.; Marongiu, F.; Ennas, G.; Escribano-Ferrer, E.; Peris, J.E.; Diez-Sales, O.; Fadda, A.M.; et al. Freeze-Dried Eudragit-Hyaluronan Multicompartment Liposomes to Improve the Intestinal Bioavailability of Curcumin. *European Journal of Pharmaceutics and Biopharmaceutics* **2016**, *107*, 49–55, doi:10.1016/j.ejpb.2016.06.016.
144. Fidock, D.A.; Rosenthal, P.J.; Croft, S.L.; Brun, R.; Nwaka, S. Antimalarial Drug Discovery: Efficacy Models for Compound Screening. *Nat Rev Drug Discov* **2004**, *3*, 509–520, doi:10.1038/nrd1416.
145. Lesjak, M.; Beara, I.; Simin, N.; Pintać, D.; Majkić, T.; Bekvalac, K.; Orčić, D.; Mimica-Dukić, N. Antioxidant and Anti-Inflammatory Activities of Quercetin and Its Derivatives. *J Funct Foods* **2018**, *40*, 68–75, doi:10.1016/j.jff.2017.10.047.
146. Shorobi, F.M.; Nisa, F.Y.; Saha, S.; Chowdhury, M.A.H.; Srisuphanunt, M.; Hossain, K.H.; Rahman, Md.A. Quercetin: A Functional Food-Flavonoid Incredibly Attenuates Emerging and Re-Emerging Viral Infections through Immunomodulatory Actions. *Molecules* **2023**, *28*, 938, doi:10.3390/molecules28030938.
147. Abdou, H.M.; Abd Elkader, H.-T.A.E. The Potential Therapeutic Effects of Trifolium Alexandrinum Extract, Hesperetin and Quercetin against Diabetic Nephropathy via Attenuation of Oxidative Stress, Inflammation, GSK-3β and Apoptosis in Male Rats. *Chem Biol Interact* **2022**, *352*, 109781, doi:10.1016/j.cbi.2021.109781.
148. Ali, A.H.; Sudi, S.; Shi-Jing, N.; Hassan, W.R.M.; Basir, R.; Agustar, H.K.; Embi, N.; Sidek, H.M.; Latip, J. Dual Anti-Malarial and GSK3β-Mediated Cytokine-Modulating Activities of Quercetin Are Requisite of Its Potential as a Plant-Derived Therapeutic in Malaria. *Pharmaceuticals* **2021**, *14*, 248, doi:10.3390/ph14030248.
149. Dodoo, D.; Omer, F.M.; Todd, J.; Akanmori, B.D.; Koram, K.A.; Riley, E.M. Absolute Levels and Ratios of Proinflammatory and Anti-inflammatory Cytokine Production In Vitro Predict Clinical Immunity to *Plasmodium Falciparum* Malaria. *J Infect Dis* **2002**, *185*, 971–979, doi:10.1086/339408.
150. Rita Bilia, A.; Rosa Sannella, A.; Francesco Vincieri, F.; Messori, L.; Casini, A.; Gabbiani, C.; Severini, C.; Majori, G. *Antiplasmodial Effects of a Few Selected Natural Flavonoids and Their Modulation of Artemisinin Activity*;
151. Borhade, V.; Pathak, S.; Sharma, S.; Patravale, V. Clotrimazole Nanoemulsion for Malaria Chemotherapy. Part I: Preformulation Studies, Formulation Design and Physicochemical Evaluation. *Int J Pharm* **2012**, *431*, 138–148, doi:10.1016/j.ijpharm.2011.12.040.
152. Jaiswal, M.; Dudhe, R.; Sharma, P.K. Nanoemulsion: An Advanced Mode of Drug Delivery System. *3 Biotech* **2015**, *5*, 123–127, doi:10.1007/s13205-014-0214-0.
153. Chang, Y.; McClements, D.J. Optimization of Orange Oil Nanoemulsion Formation by Isothermal Low-Energy Methods: Influence of the Oil Phase, Surfactant, and Temperature. *J Agric Food Chem* **2014**, *62*, 2306–2312, doi:10.1021/jf500160y.
154. Sato, S. Plasmodium—a Brief Introduction to the Parasites Causing Human Malaria and Their Basic Biology. *J Physiol Anthropol* **2021**, *40*, 1, doi:10.1186/s40101-020-00251-9.
155. Collins, W.E. *Plasmodium Knowlesi* : A Malaria Parasite of Monkeys and Humans. *Annu Rev Entomol* **2012**, *57*, 107–121, doi:10.1146/annurev-ento-121510-133540.
156. Hoffman, S.L.; Vekemans, J.; Richie, T.L.; Duffy, P.E. The March toward Malaria Vaccines. *Vaccine* **2015**, *33*, D13–D23, doi:10.1016/j.vaccine.2015.07.091.
157. Casares, S.; Brumeanu, T.-D.; Richie, T.L. The RTS,S Malaria Vaccine. *Vaccine* **2010**, *28*, 4880–4894, doi:10.1016/j.vaccine.2010.05.033.
158. Efferth, T.; R. Romero, M.; Rita Bilia, A.; Galal Osman, A.; ElSohly, M.; Wink, M.; Bauer, R.; Khan, I.; Camilla Bergonzi, M.; J.G. Marin, J. Expanding the Therapeutic Spectrum of Artemisinin: Activity Against Infectious Diseases Beyond Malaria and Novel Pharmaceutical Developments. *World J Tradit Chin Med* **2016**, *2*, 1–23, doi:10.15806/j.issn.2311-8571.2016.0002.

159. Hemingway, J.; Shretta, R.; Wells, T.N.C.; Bell, D.; Djimdé, A.A.; Achee, N.; Qi, G. Tools and Strategies for Malaria Control and Elimination: What Do We Need to Achieve a Grand Convergence in Malaria? *PLoS Biol* **2016**, *14*, e1002380, doi:10.1371/journal.pbio.1002380.
160. Kager, P.A. Malaria Control: Constraints and Opportunities. *Tropical Medicine and International Health* **2002**, *7*, 1042–1046, doi:10.1046/j.1365-3156.2002.00981.x.
161. Fallatah, O.; Georges, E. Apigenin-Induced ABCC1-Mediated Efflux of Glutathione from Mature Erythrocytes Inhibits the Proliferation of Plasmodium Falciparum. *Int J Antimicrob Agents* **2017**, *50*, 673–677, doi:10.1016/J.IJANTIMICAG.2017.08.014.
162. Artemisinin and Artemisinin plus Curcumin Liposomal Formulations_ Enhanced Antimalarial Efficacy against Plasmodium Berghei-Infected Mice _ Elsevier Enhanced Reader.
163. Fulgheri, F.; Aroffu, M.; Ramírez, M.; Román-Álamo, L.; Peris, J.E.; Usach, I.; Nacher, A.; Manconi, M.; Fernàndez-Busquets, X.; Manca, M.L. Formulation of Nutriosomes Loading Curcumin or Quercetin, Alone or in Association with Artemisinin, as a Potential Adjunctive Oral Treatment of Malaria Infections (under Review) . *Int J Pharm* **2023**.
164. Guerin-Deremaux, L.; Li, S.; Pochat, M.; Wils, D.; Mubasher, M.; Reifer, C.; Miller, L.E. Effects of NUTRIOSE® Dietary Fiber Supplementation on Body Weight, Body Composition, Energy Intake, and Hunger in Overweight Men. *Int J Food Sci Nutr* **2011**, *62*, 628–635, doi:10.3109/09637486.2011.569492.
165. Liu, D.; Yang, F.; Xiong, F.; Gu, N. The Smart Drug Delivery System and Its Clinical Potential. *Theranostics* **2016**, *6*, 1306–1323, doi:10.7150/thno.14858.
166. Manconi, M.; Caddeo, C.; Manca, M.L.; Fadda, A.M. Oral Delivery of Natural Compounds by Phospholipid Vesicles. *Nanomedicine* **2020**, *15*, 1795–1803, doi:10.2217/nnm-2020-0085.
167. Li, C.; Zhang; Su; Feng; Long; Chen Silica-Coated Flexible Liposomes as a Nanohybrid Delivery System for Enhanced Oral Bioavailability of Curcumin. *Int J Nanomedicine* **2012**, 5995, doi:10.2147/IJN.S38043.
168. Michel, R.; Gradzielski, M. Experimental Aspects of Colloidal Interactions in Mixed Systems of Liposome and Inorganic Nanoparticle and Their Applications. *Int J Mol Sci* **2012**, *13*, 11610–11642, doi:10.3390/ijms130911610.
169. Huang, Y.; Li, P.; Zhao, R.; Zhao, L.; Liu, J.; Peng, S.; Fu, X.; Wang, X.; Luo, R.; Wang, R.; et al. Silica Nanoparticles: Biomedical Applications and Toxicity. *Biomedicine & Pharmacotherapy* **2022**, *151*, 113053, doi:10.1016/j.biopha.2022.113053.
170. Ebau, F.; Scano, A.; Manca, M.L.; Manconi, M.; Cabras, V.; Pilloni, M.; Ennas, G. *Centella Asiatica* <scp> Extract-SiO $_2$ </Scp> Nanocomposite: More than a Drug-delivery System for Skin Protection from Oxidative Damage. *J Biomed Mater Res A* **2023**, *111*, 300–308, doi:10.1002/jbm.a.37462.
171. Pilloni, M.; Ennas, G.; Casu, M.; Fadda, A.M.; Frongia, F.; Marongiu, F.; Sanna, R.; Scano, A.; Valenti, D.; Sinico, C. Drug Silica Nanocomposite: Preparation, Characterization and Skin Permeation Studies. *Pharm Dev Technol* **2013**, *18*, 626–633, doi:10.3109/10837450.2011.653821.
172. Scano, A.; Ebau, F.; Manca, M.L.; Cabras, V.; Cesare Marincola, F.; Manconi, M.; Pilloni, M.; Fadda, A.M.; Ennas, G. Novel Drug Delivery Systems for Natural Extracts: The Case Study of Vitis Vinifera Extract-SiO2 Nanocomposites. *Int J Pharm* **2018**, *551*, 84–96, doi:10.1016/j.ijpharm.2018.08.057.
173. Amiri, M.; Nourian, A.; Khoshkam, M.; Ramazani, A. Apigenin Inhibits Growth of the *Plasmodium Berghei* and Disrupts Some Metabolic Pathways in Mice. *Phytotherapy Research* **2018**, *32*, 1795–1802, doi:10.1002/ptr.6113.
174. Scano, A.; Ebau, F.; Cabras, V.; Sini, F.; Ennas, G. Alternative Silica Sources in the Synthesis of Ordered Mesoporous Silica. *J Nanosci Nanotechnol* **2021**, *21*, 2847–2854, doi:10.1166/jnn.2021.19059.

175. Barrett, E.P.; Joyner, L.G.; Halenda, P.P. The Determination of Pore Volume and Area Distributions in Porous Substances. I. Computations from Nitrogen Isotherms. *J Am Chem Soc* **1951**, *73*, 373–380, doi:10.1021/ja01145a126.
176. Beck, J.S.; Vartuli, J.C.; Roth, W.J.; Leonowicz, M.E.; Kresge, C.T.; Schmitt, K.D.; Chu, C.T.W.; Olson, D.H.; Sheppard, E.W.; McCullen, S.B.; et al. A New Family of Mesoporous Molecular Sieves Prepared with Liquid Crystal Templates. *J Am Chem Soc* **1992**, *114*, 10834–10843, doi:10.1021/ja00053a020.
177. Kresge, C.T.; Leonowicz, M.E.; Roth, W.J.; Vartuli, J.C.; Beck, J.S. Ordered Mesoporous Molecular Sieves Synthesized by a Liquid-Crystal Template Mechanism. *Nature* **1992**, *359*, 710–712, doi:10.1038/359710a0.
178. Sing, K.S.W. Reporting Physisorption Data for Gas/Solid Systems with Special Reference to the Determination of Surface Area and Porosity (Recommendations 1984). *Pure and Applied Chemistry* **1985**, *57*, 603–619, doi:10.1351/pac198557040603.
179. Parapini, S.; Olliaro, P.; Navaratnam, V.; Taramelli, D.; Basilico, N. Stability of the Antimalarial Drug Dihydroartemisinin under Physiologically Relevant Conditions: Implications for Clinical Treatment and Pharmacokinetic and *In Vitro* Assays. *Antimicrob Agents Chemother* **2015**, *59*, 4046–4052, doi:10.1128/AAC.00183-15.
180. Kulkarni, C.; Kelly, A.L.; Gough, T.; Jadhav, V.; Singh, K.K.; Paradkar, A. Application of Hot Melt Extrusion for Improving Bioavailability of Artemisinin a Thermolabile Drug. *Drug Dev Ind Pharm* **2018**, *44*, 206–214, doi:10.1080/03639045.2017.1386200.
181. Kaiser, M.; Wittlin, S.; Nehrbass-Stuedli, A.; Dong, Y.; Wang, X.; Hemphill, A.; Matile, H.; Brun, R.; Vennerstrom, J.L. Peroxide Bond-Dependent Antiplasmodial Specificity of Artemisinin and OZ277 (RBx11160). *Antimicrob Agents Chemother* **2007**, *51*, 2991–2993, doi:10.1128/AAC.00225-07.
182. Li, J.; Zhou, B. Biological Actions of Artemisinin: Insights from Medicinal Chemistry Studies. *Molecules* **2010**, *15*, 1378–1397, doi:10.3390/molecules15031378.

La borsa di dottorato è stata cofinanziata con risorse del
Programma Operativo Nazionale Ricerca e Innovazione 2014-2020 (CCI 2014IT16M2OP005),
Fondo Sociale Europeo, Azione I.1 "Dottorati Innovativi con caratterizzazione Industriale"

UNIONE EUROPEA
Fondo Sociale Europeo